Universitat Autònoma de Barcelona

Arsenic carcinogenesis and associated mechanisms after environmentally relevant long-term (co)exposures

Irene Barguilla Moreno

Universitat Autònoma de Barcelona

Facultat de Biociències

Departament de Genètica i de Microbiologia

Grup de Mutagènesi

Arsenic carcinogenesis and associated mechanisms after environmentally relevant long-term (co)exposures

DOCTORAL DISSERTATION

Irene Barguilla Moreno

2020

Universitat Autònoma de Barcelona

Facultat de Biociències

Departament de Genètica i de Microbiologia

Grup de Mutagènesi

Arsenic carcinogenesis and associated mechanisms after environmentally relevant long-term (co)exposures

Dissertation respectfully submitted by

Irene Barguilla Moreno

To Universitat Autònoma de Barcelona in partial fulfillment of the requirements for the degree of Doctor of Philosophy, as per the Doctorate Program in Genetics

Under the supervision of Dr. Alba Hernández Bonilla

Dra. Alba Hernández Bonilla **Irene Barguilla Moreno**

ABBREVIATIONS LIST

8-OHdG	8-hydroxy-2-deoxyguanosine
AP-1	Activator protein 1
AS3MT	Arsenic 3-methyltranspherase
As^{III}	Arsenite
AsTC	Arsenic-transformed cells
As^{V}	Arsenate
ATO	Arsenic trioxide
BaP	Benzo[a]pyrene
CA	Chromosomal aberrations
CeONPs	Cerium oxide nanoparticles
CoNPs	Cobalt nanoparticles
CSC	Cigarette smoke condensate
CSCs	Cancer stem cells
CTAs	Cell transformation assays
DMA^{III}	Dymethylarsonous acid
DMA^{V}	Dimethylarsonate
DNA	Deoxyribonucleic acid
dNPTs	Deoxyribonucleotide triphosphate
EMT	Epithelial-mesenchymal transition
EMT-TFs	Epithelial-mesenchymal transition transcription factors
FRA1	*Fos*-related antigen 1
GIT	Gastrointestinal tract
GSH	Glutathione

IARC	International Agency for Research in Cancer
IL-6	Interleukin 6
MEFs	Mouse embryonic fibroblasts
MMAIII	Mnomethylarsonous acid
MMAV	Monomethylarsonate
MMPs	Matrix metalloproteinases
MN	Miconucleus
MNPLs	Micro- and nano-plastics
MTH1	Mut T Homolog 1
NF-κβ	Nuclear factor kappa-light-chain-enhancer of activated B cells
NPs	Nanoparticles
NRF2	Nuclear factor erythroid 2-related factor 2
ODD	Oxidative DNA damage
OGG1	8-Oxoguanine glycosylase
PETMPs	Polyethylene microplastics
PETNPs	Polyethylene nanoplastics
PPMPs	Polypropylene microplastics
PSMPs	Polystyrene microplastics
PSNPs	Polystyrene nanoplastics
ROS	Reactive oxygen species
RT	Respiratory tract
SAM	S-Adenosyl methionine
SCE	Sister chromatid exchange
shRNA	Short-hairpin RNA

SiO_2NPs	Silica dioxide nanoparticles
TFs	Transcription factors
TGFβ	Transforming growth factor beta 1
TiO_2NPs	Titanium dioxide nanoparticles
UV	Ultraviolet
WHO	World Health Organization
ZnONPs	Zinc oxide nanoparticles

ABSTRACT

Arsenic is a ubiquitously distributed environmental pollutant with well-known cytotoxic, genotoxic, and carcinogenic effects. Large human populations are subjected to sustained arsenic exposure mainly via the intake of contaminated water in arsenic-rich areas. Although extensive epidemiological data has linked this exposure to an increase in the incidence of skin, lung, bladder, liver, kidney and prostate cancers, the mechanisms leading to arsenic-associated carcinogenesis remain incompletely characterized. Therefore, in this Thesis we have performed extended *in vitro* studies with the aim to gain new insight into the mechanisms of action leading to arsenic-derived effects, highly valuable for an in-depth risk assessment and to support regulatory decision-making.

Several potential mechanisms of arsenic carcinogenesis are suggested in the literature, including epigenetic alterations and growth factors deregulation. Nonetheless, arsenic-induced oxidative stress and genotoxicity remains the most explored up to date. The high levels of reactive oxygen species (ROS) generated during arsenic biotransformation are proposed to play a crucial role in its transforming potential. In this sense, our first study reported in this Thesis, confirmed that oxidative and chromosomal DNA damage progressively accumulate in cells chronically exposed to arsenic. This increment was observed up to the cells' transformation point (week 20-30 of exposure), and the DNA damage decreased rapidly thereafter. In our findings, the arsenic-metabolizing enzyme AS3MT underwent expression changes concordantly to the variation of DNA damage levels and, importantly, its stable inhibition resulted in a reduction of the arsenic-induced genotoxicity. On the other hand, the stress-protective protein MTH1 was significantly stimulated after the transformation point and its knockdown remarkably increased the levels of DNA damage and decreased the aggressiveness of the oncogenic phenotype. Thus, we demonstrated that *As3mt* gene function contributes to the genotoxic effects before the arsenic-induced transformation, while *Mth1* prevents the DNA damage fixation and allows the progression of the oncogenic phenotype.

Among the other published mechanism of arsenic carcinogenesis, it has been described that arsenic induces oncogenic effects by activating stress-related signaling pathways such as Nrf2 or NF-κB. Hence, another point of interest of this Thesis was to assess the role of the stress-response FRA1 transcription factor in arsenic-induced oncogenesis. *Fra1* is frequently overexpressed in tumor tissue and, accordingly, in our second study, we described the progressive stimulation of its expression during the cell transformation process induced by the chronic arsenic exposure. The levels of upstream FRA1

activators were monitored at the same time-points and ERK, p38, and RAS were pinpointed as potential drivers of arsenic-associated FRA1 stimulation. In turn, FRA1 overexpression potentially leads to the observed altered expression in downstream target genes such as *Pten*, *Pdcd4*, *Tpm1*, *Tgfβ1*, *Tgfβ2*, *Zeb1, Zeb2,* and *Twist*. Further, we found that FRA1 stable knockdown, under chronic arsenic exposure settings, elicits a remarkable impact on the features relative to cells' oncogenic phenotype. FRA1 knockdown cells showed significantly diminished proliferation rate, migration and invasion potential, and stem-like status in the cell population. Thus, these findings demonstrate the essential role of FRA1 in the tumor development and in the aggressiveness of the *in vitro* transformed phenotype induced by long-term arsenic exposure.

The characterization of new mechanisms associated to arsenic carcinogenesis is of utmost importance to obtain accurate risk estimations; however, other aspects of the exposure must be considered as well. Chemical safety research has largely proceeded through a material-by-material approach. The result of this is an incomplete picture of contamination, human exposure and potential hazard effects. The increasingly higher number of environmental pollutants calls for a more comprehensive hazard assessment in which the effects and behavior of mixtures of contaminants are taken into account. In this context, one of the objectives of this Thesis was to evaluate the impact of the long-term co-exposure to arsenic and micro- and nanoplastics (MNPLs). MNPLs are widespread emergent pollutants gaining increasing attention due to the existent knowledge gap regarding their potential health effects. Remarkably, our third study demonstrated that 12-weeks of arsenic and polystyrene nanoparticles (PSNPs) combined exposure was able to enhance the cancer-like features of the cells' transformed phenotype induced and characterized in the previous studies. Co-exposed cells presented an increased proportion of spindle-like cells within the population, an increased capacity to grow independently of anchorage, as well as enhanced migrating and invading potentials. In addition, our data show that arsenic-induced DNA damage was also promoted after the concurrent exposure. Although the mechanisms by which the joint impact of arsenic and PSNPs are not explored in this work, we have demonstrated that both pollutants physically interact. Thus, this study brings out the need to further explore the long-term effects of contaminants of emerging concern, such as MNPLs, and to consider co-exposures and complex mixtures when assessing their potential hazardous effects.

INDEX

1. INTRODUCTION

1. INTRODUCTION

1.1. ARSENIC

1.1.1. Arsenic: a widespread environmental contaminant

Arsenic is a ubiquitous and abundant metalloid part of our natural environment. While it presents both metal and non-metal features, it is often referred to as a heavy metal in the context of toxicology, given its toxic nature and the threat that it poses to human health (Jomova et al., 2011). The risk is such that international environmental agencies including the International Agency for Research on Cancer (IARC), the World Health Organization (WHO), the European Environment Agency (EEA), and the United States Environmental Protection Agency (EPA) have recognized arsenic as a Group 1 human carcinogen (IARC, 2012; WHO, 2019).

Although in terms of human exposure there is no identifiable threshold below which arsenic exposure levels can be considered safe, the regulatory agencies have set target values to be attained, aiming to minimize the associated risks. In drinking water, the standard has been reduced from the original 50 µg/L to the current 10 µg/L (WHO, 2019); however, being naturally occurring, arsenic levels are unavoidably higher in certain geographical areas. As seen in the map (Figure 1), arsenic groundwater contamination is distributed worldwide and there is a high probability of exposure above the standards in broad areas including Bangladesh, China, Taiwan, India, Argentina, Chile, Mexico, Australia, or the United States (Podgorski & Berg, 2020).

In these highly contaminated areas, inorganic arsenic species such as arsenates (As^{V}) and arsenites (As^{III}) are the most environmentally relevant, being present in rocks and minerals. Therefore, these arsenic forms are an inherent part of the Earths' crust, while organic arsenicals derive from the biotransformation processess suffered by inorganic arsenic (further described in section 1.2.1.1).

Naturally occurring arsenic contamination of surface water and groundwater is modulated by environmental factors. The weathering of rocks and minerals releases the most volatile and soluble inorganic arsenic forms that enter the arsenic cycle and are carried by rivers, rain or groundwater (Masuda, 2018). This mobilization is favored under reducing conditions which are common in poorly flushed aquifers where the groundwater flow is slow and, thus, arsenic tends to accumulate. Given that aquifers are the main source of drinking-water worldwide, a large proportion of the population is exposed to arsenic via the intake of contaminated water (Smedley & Kinniburgh, 2002). This

situation is more dramatic in areas where an intensive exploitation of aquifers is done, since the deeper layers have higher arsenic contents. Besides, arsenic in groundwater can also be incorporated by plants, being an additional pathway for arsenic entrance in the food chain (Zhao et al., 2010).

The natural sources of arsenic are mostly responsible for the broad impact of this exposure on populations. Nonetheless, there is also a certain risk of exposure derived from anthropogenic activities that play an important role in increasing and dispersing arsenic contamination. As an example, the concentration of arsenic in rivers or lakes is usually bellow 10 µg/L but it can reach levels as high as 5 mg/L in areas near anthropogenic sources (IARC, 2012). The main anthropogenic sources of arsenic include mines exploitation and fossil fuel burning that have classically released dusts, sludges, or volatile forms of arsenic into the environment, contributing to its dissipation (Han et al., 2003). Arsenic has also been historically used as pesticide, wood preservative, cosmetic pigment, food additive, or in medical applications (Hughes et al., 2011). The arsenic released due to its use in these varied industries adds to the environmental levels derived from natural sources, greatly incrementing the exposure risk of populations worldwide (Jones, 2007).

1.1.2. Impact on human populations and health effects

In humans, the main arsenic exposure routes are ingestion of soluble forms via the intake of contaminated water or food, and inhalation of volatile forms, mainly released due to mining and related industrial activities. Only under certain occupational exposure scenarios the dermal contact is considered of high risk and, therefore, it is negligible for the general population (Ravenscroft et al., 2009). Regarding inhalation, industry workers and miners are the most vulnerable collective, while for the overall population it is estimated that this exposure route contributes to less than 1% of total arsenic exposure; even when the higher levels of arsenic in air of urban and industrial areas entail an increased uptake through respiration (Hughes et al., 2011). As introduced in section 1.1.1, the intake of contaminated water accounts for the vast majority of arsenic exposures. Therefore, it is no surprise that this route gathers most of the attention when assessing arsenic exposure risk.

Groundwater arsenic typically ranges from 1-2 µg/L, however, concentrations in the most contaminated areas can rise up to 5 mg/L, well above the 10 µg/L standard for drinking water (IARC, 2012). Globally, it is estimated that more than 200 million people are exposed to arsenic levels above the standard (WHO, 2019). Although the proportion of population affected by these high levels greatly varies depending on the regional water

sources, estimations on the extent of chronic arsenic exposure via drinking water have shown numbers as concerning as more than 1 million people affected in India, Argentina, United States, China, or Vietnam (Figure 1) (Naujokas et al., 2013). The case of Bangladesh is especially dramatic as 35-77 million people are at risk of drinking contaminated water. The scale of this environmental disaster is such that the WHO has referred to it as the largest mass poisoning of a human population in history (Smith et al., 2000).

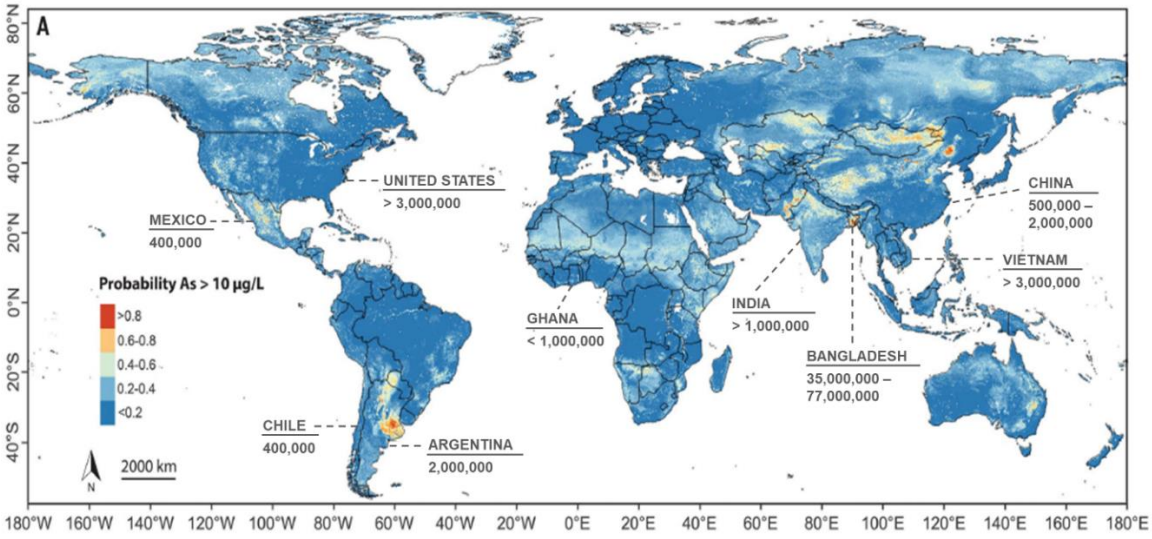

Figure 1. Probability of arsenic concentration exceeding 10 µg/L in groundwater and the estimated number of people at risk in some of the most affected areas (Adapted from Naujokas et al., 2013; Podgorski & Berg, 2020).

The severity of arsenic's impact on populations comes not only from the large number of people affected but also from its serious adverse health effects. The dose and duration of arsenic exposure greatly determines the clinical symptoms developed. Acute arsenic exposure can quicky damage internal organs and, in the most extreme cases, may be lethal (Abdul et al., 2015). In fact, arsenic has been classically used as poison over the historical times. Whereas chronic exposure to low doses can induce a wide diversity of pathologies including skin lesions, neurological alterations, gastrointestinal symptoms, diabetes, cardiac disorders, and several types of cancer (WHO, 2019).

With such diverse impact on health, and due to the great proportion of population at risk, understanding the mode of action and carcinogenesis of this natural occurring contaminant is a pressing matter. Long-term exposures are considered as the most relevant in terms of impact on the general population via environmental contamination, and are closely linked to cancer development. Therefore, extensive work (including the one presented in this Thesis dissertation) has been performed focusing on the evaluation

of effects induced by chronic exposure to inorganic arsenic species following *in vitro*, *in vivo,* and epidemiological approaches.

Regarding epidemiological studies addressing risk assessment in exposed populations, it has been described that monitoring the health effects of drinking arsenic-contaminated water for one year is not enough time to observe the onset of clinical symptoms. Nonetheless, during that time significant high concentrations of arsenicals were detected in urine, hair, and nails when comparing the exposed groups with the tap water-drinking control groups (Hong et al., 2017). When following the selected subjects for longer periods of time, prospective cohort studies have found different associations between low-moderate arsenic exposure and diverse pathologies. Thus, a 6-year study showed an increase in the prevalence of skin lesions associated with a chronic arsenic exposure in Bangladesh (Zhang et al., 2018). Neuropsychological disorders have been reported in children due to arsenic dietary exposure for 4-5 years in Spain (Signes-Pastor et al., 2019), where a 10-year study also associated this kind of exposure to a higher diabetes prevalence in adults (Grau-Perez et al., 2018). In the US, the 6-year monitoring of a population showed that low-moderate arsenic exposure contributes to the development of diabetes or metabolic syndrome (Spratlen et al., 2018), restrictive lung disease (Powers et al., 2019), and cardiac disorders (Pichler et al., 2019). Besides, chronic arsenic exposure has also been positively associated with male infertility (Wang et al., 2016) and various adverse birth outcomes after maternal exposure (Liu et al., 2018a).

Despite all the possible diseases derived from the chronic exposure arsenic is, above all, a carcinogenic compound. As introduced before, IARC and other regulatory agencies have classified arsenic as a Group 1 carcinogen for skin, bladder, and lung cancer, and as a Group 2 possible carcinogen for liver, prostate, and kidney tumors (IARC, 2012). Several cohort studies have been stablished to evaluate the carcinogenic potential of long-term arsenic exposure in different populations. As examples, monitoring a sample population from Taiwan for up to 12 years evidenced an increase in urothelial cancer development (Huang et al., 2008). In the same area, 20 years of chronic arsenic exposure resulted in a higher prevalence of liver cancer (Lin et al., 2013). Besides, meta-analyses have corroborated that environmental arsenic exposure is associated to prostate cancer development (Benbrahim-Tallaa & Waalkes, 2008), and case-control studies have also reported the association between low-moderate arsenic exposure and kidney carcinomas (Ferreccio et al., 2013), non-melanoma skin cancer (Kim et al., 2017) and squamous cell lung carcinoma (Kuo et al., 2017).

1.2. ARSENIC CARCINOGENESIS AND MODE OF ACTION

As described above, arsenic presents a well-established carcinogenic potential widely explored in epidemiological studies, but also in plenty of studies using *in vitro* and *in vivo* models.

As some representative examples of *in vivo* studies, the strain A/J mice was reported to develop lung tumors after the 18-months-long administration of sodium arsenate in drinking-water (Cui et al., 2006). Likewise, mutant *Ogg*$^{-/-}$ mice -deficient for oxidative DNA damage repair- developed this kind of tumor after a 50-week-exposure to dimethylarsonate (DMA^{V}), while no carcinogenesis was described in the wild-type strain (Kinoshita et al., 2007). The increase in other types of tumors such as bladder, liver and renal carcinomas have also been described upon the oral administration of arsenicals in rat models (Tokar et al., 2010a).

In *in vitro* studies, diverse cell lines derived from target organs have been used as models for chronic arsenic exposures ranging from 12 to 30 weeks. This long-term exposure has proven to induce the malignant transformation of human bronchial epithelial cells (Xu et al., 2013), human HaCaT keratinocytes (Pi et al., 2008; Li et al., 2010), human lung epithelial BEAS-2B cells (Stueckle et al., 2012), human small airway epithelial cells (Wen et al., 2008), rat liver epithelial TRL1215 cells (Liu et al., 2006), human prostate epithelial RWPE-1 cells (Treas et al., 2013), and breast epithelial cells (Xu et al., 2014) among others. These cellular models are all of epithelial origin as arsenic-induced tumors mainly arise from epithelial cells. Nonetheless, there is evidence that arsenic can also affect stromal cells (Shearer et al., 2016) and fibroblasts, which undergo transformation after 30 weeks of chronic As^{III} exposure (Bach et al., 2016).

Despite the great efforts to determine the underlying mode of action and carcinogenesis of arsenic, we still do not have a complete understanding of the mechanisms that induce the very diverse adverse effects of a chronic exposure. Thus, the specific link between arsenic exposure and arsenic-induced effects -with special emphasis on cancer- have not been defined yet.

Exploring the literature, several hypotheses related to the mechanisms of action of arsenic have been suggested, including the induction of oxidative stress, genotoxic damage and chromosomal aberrations, the modification of gene expression, several epigenetic mechanisms, and the alteration of growth factors (Hong et al., 2014; Zhou & Xi, 2018). These changes produce genomic damage that the cells overcome by activating different responses, eventually leading to enhanced cell proliferation, cell

death resistance and the onset of cell transformation. However, none of these mechanisms are arsenic-specific and there is still room to explore their role in arsenic-induced carcinogenesis.

The work developed during this Thesis is mainly focused on arsenic-mediated reactive oxygen species (ROS) production, genotoxicity, and signaling disruption (Figure 2). Therefore, these mechanisms will be further described in the following sections.

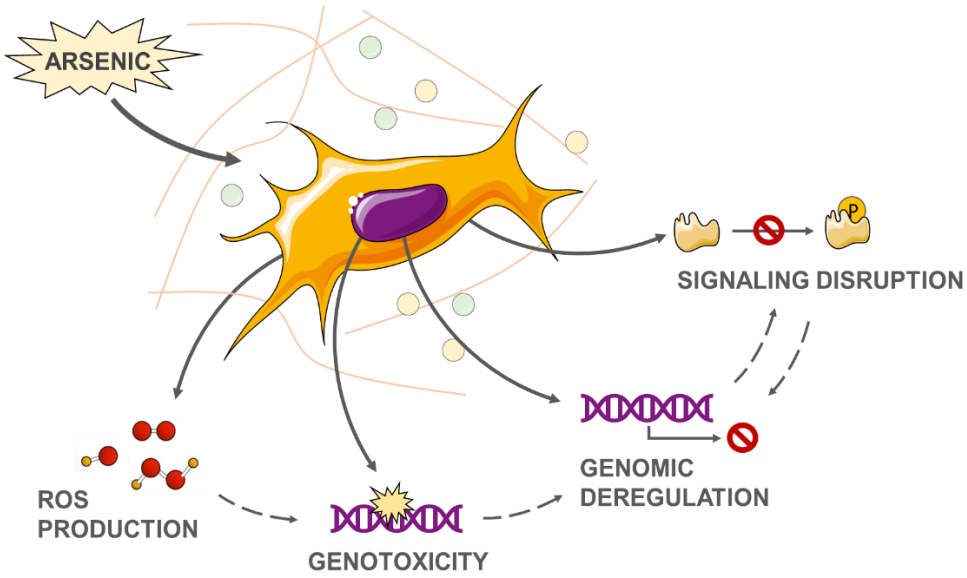

Figure 2. Arsenic mechanisms of action explored in this Thesis dissertation.

1.2.1. Oxidative DNA damage and ROS generation

Arsenic induction of oxidative stress through increased intracellular ROS production is the earliest described mechanism of arsenic cytotoxicity and carcinogenicity, and among the most studied.

Thus, arsenic-induced increase of intracellular ROS levels has long been described in very different cell lines such as mice epithelial cells (HEL30) (Corsini et al., 1999), vascular smooth muscle cells (VSMC) (Lynn et al., 2000), hematopoietic cells (U937) (Iwama et al., 2001), human-hamster hybrid cells (CHO-K1) (Liu et al., 2001), and lung bronchial epithelial cells (BEAS-2B) (Chang et al., 2010; Zhang et al., 2015).

ROS are unstable molecules that present one or more unpaired electrons in its atomic orbital. There are diverse forms of ROS but, among the ones typically produced upon arsenic exposure, we find superoxide anion ($O_2^{-\bullet}$), hydroxyl radical ($OH^{\bullet}$), and hydrogen peroxide (H_2O_2). Multiple mechanisms have been suggested as responsible for the arsenic-induced persistent ROS production. The arsenic-mediated alteration of the

mitochondrial integrity causes a rapid decline of mitochondrial membrane potential, leading to the uncontrolled and random ROS formation. The oxidation and reduction steps within the metabolism of arsenic process generate intracellular ROS under physiological conditions (further described in section 1.2.1.1). Also, arsenic exposure promotes Fenton-type reactions, directly releasing ROS (Jomova et al., 2011). Moreover, arsenic can indirectly increase ROS levels by affecting the cells' antioxidant defenses, such as depleting glutathione (GSH) or activating the reduced form of nicotinamide adenine dinucleotide phosphate (NADPH)-oxidase (Zhu & Costa, 2020).

High levels of intracellular ROS contribute to oxidative DNA damage (ODD) through the formation of oxidative DNA adducts, which are responsible for a large proportion of arsenic-induced DNA strand breaks. The most typical lesion is the production of 8-hydroxy-2-deoxyguanosine (8-OHdG), which can generate G>T conversions that trigger GC>TA transversions (Mandal, 2017). Interestingly, 8-OHdG can be detected in urine of arsenic-exposed individuals and its levels correlate with the development of carcinomas (Huang et al., 2012), which are characterized by high rates of T>G/A>C transversions, considering the overall low number of point mutations (Martinez et al., 2013).

Arsenic-induced cell transformation is closely linked to oxidative stress as the cells try to react to high ROS levels by overexpressing antioxidant enzymes (e.g. superoxide dismutase, catalase, and GSH), which contribute to their escape from apoptotic mechanisms. Consequently, the persistence of heavily damaged cells protected from apoptosis increase the carcinogenic potential in the cell population (Eckstein et al., 2017).

1.2.1.1. Arsenic metabolism and the role of AS3MT in ROS production

As indicated above, ROS generation has been identified as an inherent outcome to the arsenic biotransformation process, which evidences the importance of characterizing the metabolic pathways induced by environmental contaminants.

After ingestion, inorganic arsenic is mainly absorbed by the gastrointestinal tract (GIT) and, through the bloodstream, it reaches the liver, kidneys, lungs, and bladder, where it is primarily bioaccumulated (Palma-Lara et al., 2020). In humans and most mammals, inorganic arsenic biotransformation happens mainly in the liver and involves alternating reduction and oxidation steps coupled to methylation events.

During the metabolic process, inorganic arsenic is methylated with S-adenosylmethionine (SAM) acting as methyl donor, GSH as a cofactor, and arsenic

methyltransferase (AS3MT) as the main catalytic enzyme. The most accepted arsenic metabolism pathway involves the reduction of pentavalent arsenic forms to trivalent species that subsequently undergo an oxidative methylation generating intermediate metabolites. These metabolites can be further methylated and reduced in successive steps until the dimethylated arsenic metabolites are excreted into urine. Therefore, the arsenicals generated during inorganic As^{III} and As^{V} biotransformation are: monomethylarsonate (MMA^{V}), monomethylarsonous acid (MMA^{III}), dimethylarsonate (DMA^{V}), and dymethylarsonous acid (DMA^{III}) (Hughes et al., 2011) (Figure 3).

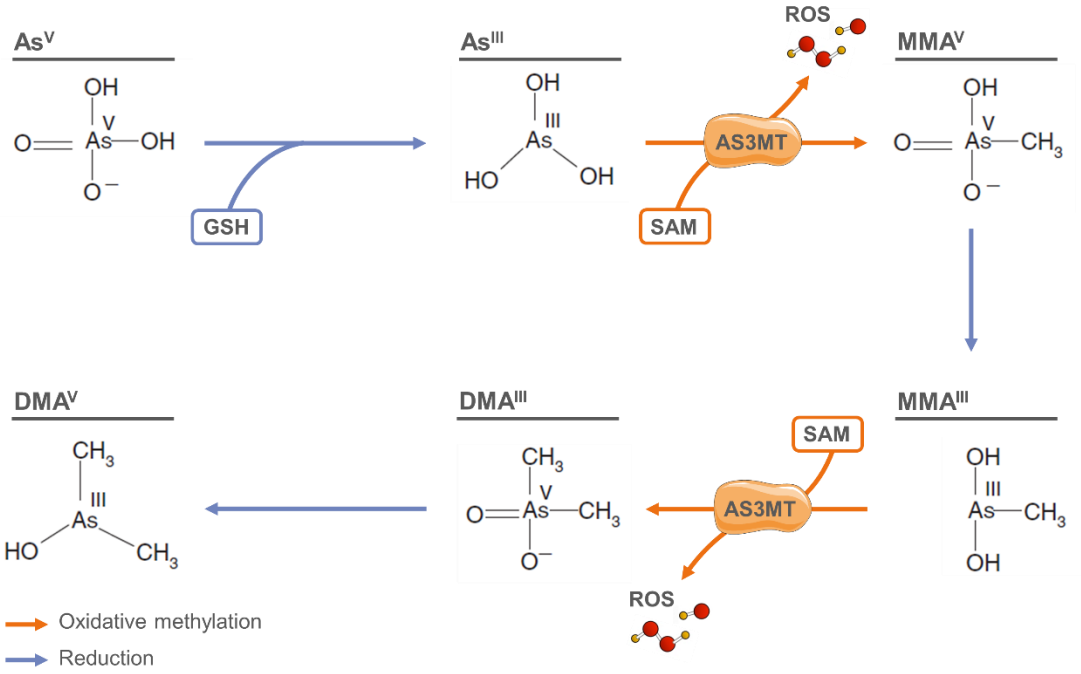

Figure 3. Arsenic metabolic process is linked to the generation of ROS and cytotoxic intermediate metabolites (Adapted from Jomova et al., 2011)

Two pathways linking the arsenic metabolic process and arsenic-associated carcinogenesis have been proposed: (1) The potential generation of ROS as a byproduct of the oxidative methylation steps within the process, and (2) the accumulation of intermediate metabolites able to efficiently induce adverse effects. Thus, these proposals are explained in the next paragraphs.

Regarding the close link between arsenic metabolism, ROS generation, oxidative DNA damage (ODD) and tumorigenesis, the work by Kojima et al. (2009) has become one of the most relevant. These authors demonstrated that the exposure to doses as low as 1 μM for 5-18 weeks was sufficient to transform methylation-competent cells, which also sustained significant ODD. However, methylation-deficient cells were not equally affected even after a 5 μM exposure for 30 weeks. In addition, the chemical inhibition of

the arsenic biomethylation capacity in methylation-competent cells reduced ODD and slowed down the development of the tumoral phenotype. Thus, this study concluded that arsenic biomethylation seems necessary for arsenic-induced ODD and the accelerated transformation process.

The second mechanism of arsenic carcinogenesis proposes that the biotransformation process is related to the accumulation of intermediate metabolites. Arsenic biotransformation has classically been considered a detoxification route. However, accumulating evidence indicates that some of the intermediate metabolites generated -especially trivalent forms- are more genotoxic and appear to stimulate ROS production more efficiently than inorganic arsenic species (Tokar et al., 2014), enhancing arsenic cytotoxicity and carcinogenicity (Khairul et al., 2017). MMA^{III} centers most of the attention in this aspect, as it has been described that can induce ROS-mediated DNA damage and lead to cell malignant transformation after long-term exposures to doses within the range of those detected in human urine after environmental exposure (Bredfeldt et al., 2006).

Therefore, there is sufficient evidence supporting that the efficiency of arsenic metabolism has an essential role in determining the adverse effects derived from arsenic exposure. Hence the relevance of exploring the potential role in arsenic-induced carcinogenesis of essential players on the biotransformation process such as AS3MT.

AS3MT is a highly conserved enzyme across species, from bacteria to higher mammals (Roy et al., 2020). Its essential role, catalyzing the transfer of a methyl group from SAM to trivalent arsenicals in arsenic biotransformation, has been fairly explored. Different AS3MT polymorphisms have been identified and correlated with variations in arsenic methylation efficiency. Higher levels of inorganic arsenic and monomethylated forms have been detected in individuals with slow metabolizing AS3MT activity (Roy et al., 2020). Moreover, certain AS3MT polymorphisms have been associated with increasing risk of bladder (Lin et al., 2018) and lung cancer development (de la Rosa et al., 2017). Specifically, the Met(287)Thr polymorphism has been associated with the metabolization efficiency (Hernández & Marcos, 2008) and with the levels of DNA damage (Sampayo-Reyes et al., 2010; Hernández et al., 2014). However, the specific role of AS3MT in arsenic-induced carcinogenesis is still poorly explored, specially in chronic arsenic exposure scenarios. Thus, within this Thesis we have evaluated the involvement of AS3MT on the arsenic-induced genotoxicity under long-term exposure settings.

1.2.1.2. dNTPs oxidation and the role of MTH1

High ROS levels not only produce direct DNA damage but can also oxidize free bases in the nucleotide pools before they are incorporated into the DNA. The presence of oxidized or otherwise damaged deoxyribonucleotides (dNTPs) in the cells' reservoirs entails a higher probability of misincorporations into the DNA during replication or repair and, thus, poses a threat to genomic integrity. As an example, the previously discussed 8-OHdG can be formed by direct oxidation of guanine bases in the DNA or by the oxidation of dGTP to 8-OHdGTP in the nucleotide pools, which seems to be a more probable event leading to G to T transversions (Markkanen, 2017).

The MutT homolog 1 (MTH1) is the main mammalian phosphorylase that catalyzes the hydrolysis of oxidized dNTPs preventing their incorporation into the DNA. MTH1 activity includes the hydrolyzation of 8-OHdGTP to 8-OHdGDP, and eventually to 8-OHdGMP, that will neither be integrated into the DNA, nor reutilized to regenerate 8-OHdGTP as the guanylate kinase is not active on this base form. While there are other enzymes involved in the sanitation of the nucleotide pools -MTH2, MTH3, and NUDT5-, MTH1 is considered the most important contributor to the mitigation of the potential mutational effects produced by oxidized nucleotides accumulation (Markkanen, 2017).

In normal tissues under physiological conditions, the generally low levels of oxidized dNTPs are solved by basal MTH1 expression, which prevents mutagenic events and protects from pathological processes such as neurodegeneration. In cancer tissues, the metabolic switch to glycolysis, and the enhanced angiogenesis and inflammatory responses are linked to a hypoxic tumor environment and high levels of oxidative stress. Thus, cancer cells present higher ROS levels and are more susceptible to undergo oxidative DNA damage than non-transformed cells (Nakabeppu et al., 2017). As shown in Figure 4, basal levels of MTH1 expression in this scenario would be linked to high genomic instability and eventual cell death (Rai & Sobol, 2019). However, together with the high oxidative stress, a correlative significant overexpression of MTH1 has been described in tumoral cells which seems essential for their survival. Tumor cells rely on MTH1 overexpression to sanitize their dNTP pools and progress towards the development of a malignant phenotype (Nakabeppu et al., 2017) (Figure 4).

Considering the essential role of MTH1 overexpression in tumor progression, great efforts have been directed towards the development of inhibitors as chemotherapeutic agents. It has been described that MTH1 inhibition by different approaches -short-interference RNA (siRNA), short-hairpin RNA (shRNA), or chemical inhibitors- results in the accumulation of DNA damage, followed by compromised cell survival and reduced

xenograft tumor formation (Gad et al., 2014; Warpman Berglund et al., 2016). However, there is a certain controversy in the suitability of MTH1 as a therapeutic target for cancer treatment due to some contradictory outcomes in the *in vitro* and *in vivo* tests of MTH1 inhibitors (Samaranayake et al., 2017), as well as the uprising of off-target effects (Rai & Sobol, 2019).

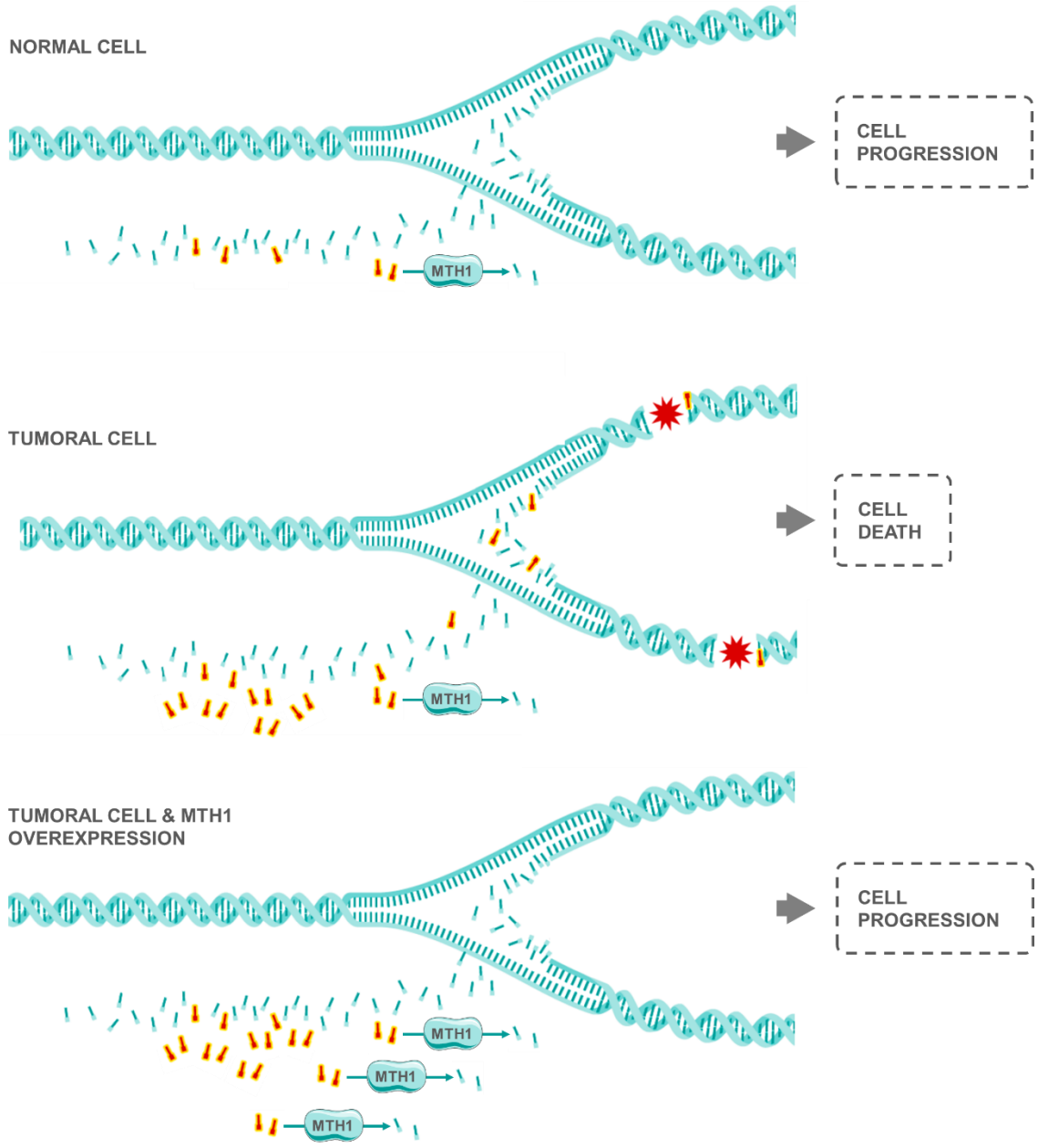

Figure 4. MTH1 protects cells from the incorporation of oxidized lesions in the DNA and their associated adverse effects (Adapted from Longás, 2014).

Given that arsenic exposure induces carcinogenesis and oxidative stress, in the context of this Thesis, we aimed to evaluate the potential role of MTH1 as an adaptative

mechanism for the cells' survival and transformation during a chronic arsenic exposure. Indeed, up-regulation of MTH1 on mRNA/protein levels, as well as its activity level, has been described after exposure of cells to different agents inducing oxidative stress, as discussed in Markkanen et al (2019).

1.2.2. Genotoxicity

Arsenic does not bind directly to DNA forming arsenic-DNA adducts, however together with the DNA damage produced by the oxidative stress, it can lead to high rates of chromosome damage. As a result of the disruption of chromosome structure and stability, mainly in the centromeres, increased incidences of chromosomal aberrations (CA), sister chromatid exchange (SCE), and micronucleus (MN) formation have been detected in arsenic-exposed populations (Sage et al., 2017). Multiple studies have quantified this genotoxicity endpoints as biomarkers of effect. As representative examples, the frequency of CA, SCE, and MN was significantly higher in urothelial cells, oral mucosa, and lymphocytes collected from a population from arsenic-contaminated districts in Wet Bengal, India (Basu et al., 2002; Mahata et al., 2003). Similar results were obtained with lymphocytes from an arsenic-exposed group in Chile (Martínez et al., 2004).

In addition to the epidemiological studies, the genotoxicity of arsenic has long been explored *in vitro*. A significant increase in CA was described in human fibroblasts upon the exposure to different arsenic species (Oya-Ohta et al., 1996); in fibroblasts, MN induction was also observed after both acute and chronic arsenic exposure (Yih & Lee, 1999); and more recently, sodium arsenite and arsenic trioxide-induced chromosomal breakage and MN formation was demonstrated in lung adenocarcinoma cells (A549) (Jiang et al., 2013a). Thus, there is sufficient evidence supporting that arsenic exposure induces genotoxicity that eventually can drive the oncogenic processes, since genotoxicity can lead to induced mutations. These mutations are particularly damaging if they inhibit the expression of genes involved in repair pathways, tumor suppressor genes such as *PTEN, p53,* and *p16* (Sage et al., 2017; Zhu & Costa, 2020), or well-known oncogenes involved in carcinogenesis initiation and promotion including *KRAS* (Merrick et al., 2019).

1.2.3. Signal transduction pathways

Cellular processes are drived and controlled by multiple signal transduction pathways. Among many others, proliferation, differentiation, and apoptosis are directly dependent on the proper activity of the many proteins involved in signaling pathways or cascades.

Arsenic exposure alters signal transduction through different mechanisms. On the one hand, arsenic-induced genomic instability can lead to the deregulation of gene expression for essential components within signaling pathways. As a representative example, gene amplification of mutated *KRAS* will eventually alter KRAS-driven proliferation pathways and lead to cell transformation (Merrick et al., 2019). Besides, arsenic can directly interact covalently with certain signaling-related proteins disrupting their activity and downstream effects. For instance, arsenic can covalently bind to the IκB kinase (IKK) catalytic site and, as a result, cellular responses that require of nuclear factor-κβ (NF-κβ) transcriptional activity will be inhibited. NF-κB is a transcription factor involved in stress response, as also are activator protein-1 (AP-1) and Nrf2. Due to the high levels of oxidative stress produced by arsenic exposure, the cascades regulating the cell homeostasis and stress factors activity are altered, causing expression changes in genes downstream (Druwe & Vaillancourt, 2010). Thus, arsenic impact on signal transduction further contributes to gene instability, alters proliferation and cell death-related cascades, and can eventually lead to the deregulation of cell fate and to probable events of cellular transformation.

1.2.3.1. AP-1/FRA1 pathway

AP-1 represents a family of dimeric stress-response transcription factors involved in the regulation of multiple cellular processes, including cell proliferation, differentiation, invasion, and apoptosis. AP-1 homo- or heterodimers are comprised of combinations of members of Jun (c-Jun, JunB, JunD), Fos (c-Fos, FosB, FRA1, FRA2), ATF (ATFa, ATF2, ATF3, ATF4), JDP (JDP-1, JDP-2), and MAF (c-MAF, MAFA, MAFB, MAFF, MAFG, MAFK) protein families (Bejjani et al., 2019). Through the basic leucine zipper (bZIP), the dimers bind to AP-1-like sites in promoters like 12-otetradecanoylphorbol-13-acetate response element (TRE), cAMP response element (CRE), or antioxidant response element (ARE), regulating the expression of numerous genes such as transforming growth factor β (*TGFβ*), epithelial-mesenchymal transition transcription factors (EMT-TFs), or interleukin 6 (*IL-6*) (Bakiri et al., 2015). Therefore, AP-1 exerts its regulatory function over very diverse targets.

Some of the AP-1 components present a context-dependent dual function and can act either as oncogenes or tumor suppressors. Under the influence of upstream oncogenic events, dysregulated signaling can alter the expression of AP-1 constituent genes, as well as shift the stabilization and activation of its subunits. This can trigger the alteration of the cells' transcriptional programs, eventually leading to tumor initiation or progression due to cell fate deregulation (Bejjani et al., 2019).

FRA1 is one of the most common components of AP-1 and it presents the oncogenic or tumor suppressor duality in its activity (Figure 5). FRA1 regulation mainly depends on the MAPKs activity; namely ERK1/2, p38, and JNK1/2/3. In response to external stimuli or stress, a cascade is activated leading to MAPKs-mediated FRA1 phosphorylation. Being a transcription factor, FRA1 is an unstable protein with a high degradation rate that relies on ubiquitin-independent proteasome action. However, FRA1 phosphorylation enhances its stability and activity (Jiang et al., 2020). The increase of active FRA1 levels in cells perpetuates its own transcription through a positive feedback loop, as FRA1-encoding gene contains an enhancer with AP-1-like sites where FRA1 itself can bind and induce its own transcription (Talotta et al., 2020).

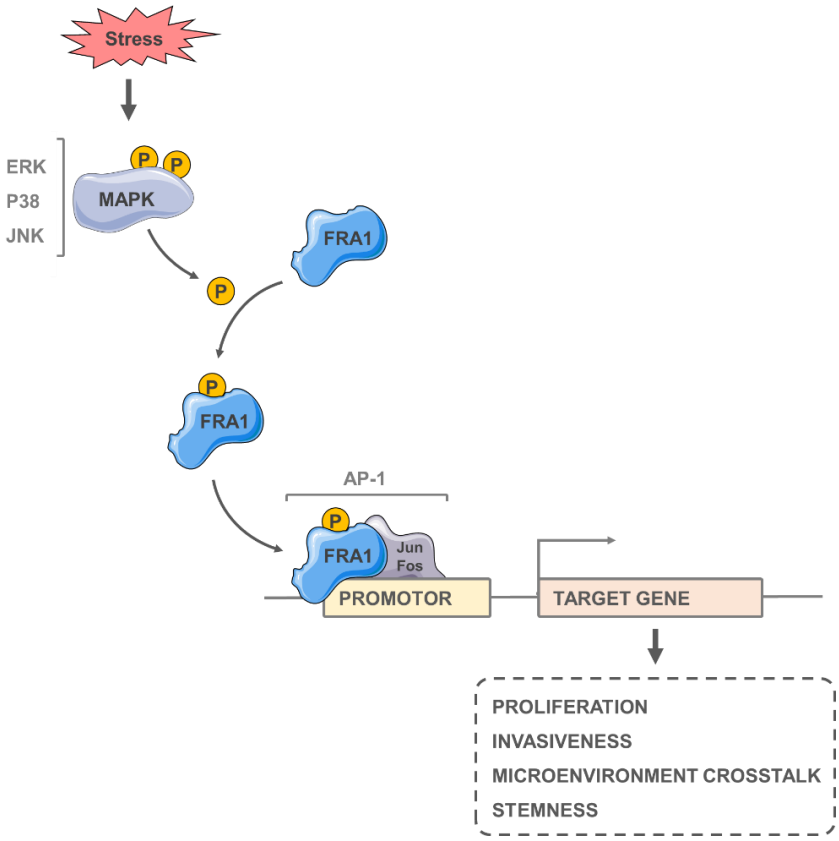

Figure 5. Stress-mediated activation of MAPKs results in FRA1 phosphorylation and stabilization, which leads to the regulation of genes involved in cell processes related to tumorigenesis.

FRA1 overexpression and accumulation has been linked with the malignant progression of tumors. Multiple studies have explored the abnormal FRA1 expression in breast, colorectal, lung, cervical, ovarian, and skin cancers, among others. Within the tumor, FRA1 plays a role in cell proliferation and survival by directly regulating the expression of cell cycle-related proteins such as cyclin-dependent kinases (CDKs) (Jiang et al.,

2020). Notably, it is considered a master switch of epithelial-to-mesenchymal transition (EMT) given its regulating activity over the expression of EMT-TFs (e.g. *ZEB1*, *ZEB2*, *TWIST1*, *SLUG,* and *SNAIL*) and matrix metalloproteinases (MMPs). Moreover, FRA1 also has a role in cell plasticity through TGFβ regulation (Dhillon & Tulchinsky, 2015), and it is involved in the tumor-microenvironment crosstalk through transcriptional targets such as *IL-6*, and can promote stemness via *NANOG* and *SOX2* regulation (Talotta et al., 2020). Thus, FRA-1 has a central role in the transcription and signaling pathways that coordinate gene expression changes during tumor promotion, contributing to the development of an aggressive transformed phenotype.

While very limited, there is some evidence of arsenic-mediated alteration of AP-1 and upstream activators. AP-1 activation and DNA binding are enhanced through the stimulation of MAPKs in human urinary bladder epithelial cells (UROtsa) after the acute exposure to inorganic arsenic and its derived methylated metabolites (Drobná et al., 2003). It has also been described that p38 MAPK activation and eventual increase in AP-1 activity, are essential in arsenic-induced cellular transformation of BALB/c 3T3 mouse embryonic fibroblasts (MEFs) when treated with low doses of arsenic for 4 weeks (Kim et al., 2016). However, and despite the important part played specifically by FRA1 in tumor promotion and aggressiveness, there is no available data on its presumed dysregulation due to arsenic-induced stress. Within the context of this Thesis, AP-1 and arsenic-related studies gave us the lead to analyze the impact of chronic arsenic exposure over FRA1, its activation and stabilization pathway, and its potential role as a mechanism of action for arsenic carcinogenesis.

1.3. *IN VITRO* HALLMARKS OF CANCER

The carcinogenic effects of arsenic or other environmental pollutants are developed due to sustained exposure throughout extended periods of time. In this context, the study of the long-term accumulative effects of the pollutants under chronic exposure settings is of utmost importance to understand their associated health risk and mechanisms of action.

The large amount of experimentation animals, as well as the high cost and time, required to meet the necessities of chronic exposure studies, make *in vivo* models practically unviable. Therefore, alternative methods based on 3-R recommendations (replacement, refinement, and reduction in animal studies) are necessary (Annys et al., 2014). In terms of standardized approaches, cell transformation assays (CTAs) are the recommended *in vitro* alternatives to predict the carcinogenic potential of chemicals, having been included

in the OECD Test Guidelines (OECD, 2013). However, regulated CTAs present certain limitations as they are based on rodent cells, they evaluate a single phenotypic carcinogenic characteristic (despite the multi-step nature of tumorigenesis), and they lack a mechanistic understanding of the transformation process (Steinberg et al., 2017).

1.3.1. Studying arsenic carcinogenesis from an *in vitro* perspective

Several *in vitro* cell models have prove to be successful for the identification of environmental carcinogens (Heeg et al., 2006). Indeed, our group and others have developed multiple cell line-based models for arsenic-induced cell transformation. As representative examples, chronic exposure to low doses of arsenic has been demonstrated to drive the transformation of prostate epithelial RWPE-1 cells (Achanzar et al., 2002), human prostate epithelial progenitor WPE-stem cell line (Tokar et al., 2010b), human lung peripheral epithelial HPL-1D cells (Person et al., 2015), human lung epithelial BEAS-2B cells (Ganapathy et al., 2019), and MEF cells (Bach et al., 2016). The latter is a well-characterized model developed in our group. In our model, after 30 weeks of chronic arsenic exposure, MEFs presented characteristic transformed features and, thus, they are the focus of this Thesis dissertation as a model to explore different mechanisms of arsenic-induced (co)carcinogenesis.

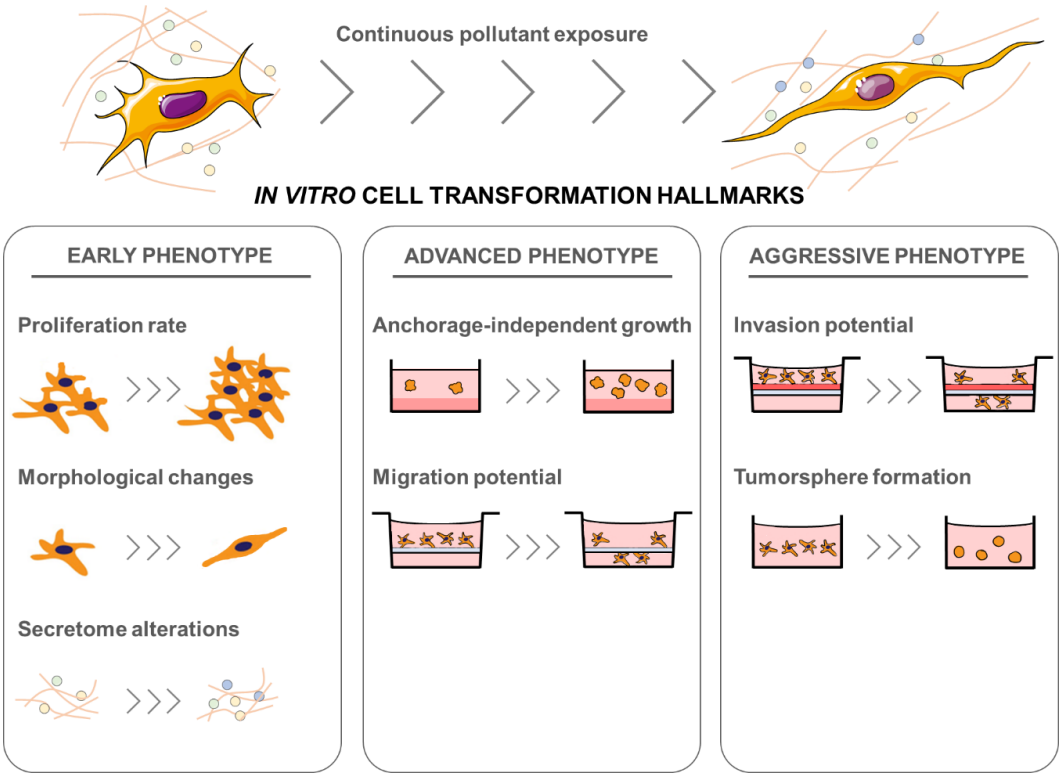

Figure 6. Cell transformation hallmarks and related assays give information on the different stages that the cells undergo during the oncogenic transformation process *in vitro*.

In vitro cell transformation is a process characterized by distinctive events that emulate important stages of *in vivo* tumorigenesis. During the transformation process well-established phenotypic alterations in the culture allow for the discrimination of transformed cells from non-transformed ones. Likewise, transformed cells present distinct features representative of different stages during the progression of the tumoral phenotype -early, advanced, or aggressive phenotype- (Figure 6). Thereby, in our group, we have established a battery of assays aiming to evaluate multiple outcomes associated with different hallmarks of carcinogenesis, including the assessment of cell morphology, cell proliferation, and secretome changes; anchorage-independent growth, migration, and invasion potential, as well as the tumorsphere formation ability.

1.3.1.1. Cell proliferation

Up to date, eight hallmarks of cancer have been identified as capabilities that the cells have to acquire to undergo transformation These include: sustained proliferative signaling, growth suppressors evasion, cell death resistance, activation of replicative immortality, angiogenesis induction, invasion and metastasis activation, energy metabolism reprogramming, and immune destruction escape. Out of these features, dysregulated sustained proliferation is arguably the most essential trait of cancer cells (Hanahan & Weinberg, 2011).

The proliferation of normal cell populations requires a balance between growth-promoting signals and growth-suppressing ones to maintain a controlled cell number that allows normal tissue architecture and function. Thus, cells in phase G1 of the division cycle respond to extracellular signals to either continue dividing or withdraw from the cycle into G0 or apoptosis (Sherr, 1996). Cancer cells acquire the capability to constitutively activate proliferative signaling through diverse mechanisms, such as autocrine signaling to their own growth factors, increased levels of mitogen receptors, ligand-independent signaling, or enhanced stroma signaling. Moreover, transformed cells can evade cycle arrest signals such as contact inhibition (Hanahan & Weinberg, 2011; Darwiche, 2020). As a result, early in the tumorigenesis process, cancer cells drive uncontrolled cell proliferation and cell cycle deregulation. Thus, the increase in cell population doubling is used as an early cell transformation marker.

1.3.1.2. Cell morphology

Normal epithelial tissues can acquire mesenchymal features through the activation of the EMT program. EMT is prominently involved in the cells ability to invade, disseminate, and escape apoptosis (Hanahan & Weinberg, 2011). EMT program is characterized by

major transcriptional alterations and eventual phenotypical changes in cells. Early in the oncogenic process, transformed cells with an active EMT program undergo morphological changes from a normal polygonal shape to spindle-like shaped cells. The modification of cell morphology also means the lost of polarity in epithelial cells (Yang & Weinberg, 2008). Regarding fibroblasts, their activation into myofibroblasts -typically found in tumor microenvironment- also entails the morphological alterations (Sahai et al., 2020). Thus, cell morphology is an early transformation marker generally associated with the conversion of stationary cells to cells able to disseminate to other tissues, or promote the invasive potential of surrounding cells.

1.3.1.3. Secretome alterations

Tumor cells are not isolated but rather subsist within a heterogenous population of both tumor and stromal cells. Fibroblast, endothelial cells, pericytes, leukocytes and other cell types contribute to the generation of a rich tumor microenvironment, which has a central role in cancer initiation, growth, and progression (Pietras & Östman, 2010). Tumor and stromal cells communicate through the secretion of soluble factors that constitute the cells' secretome. Inflammatory cytokines (e.g. IL-6, IL-8, and IL-1β), growth factors and MMPs, among others comprise the secretome that varies in composition during the oncogenic transformation (Bussard et al., 2016). Changes in the secretome composition, early in the transformation process, are related to the later promotion of tumor invasiveness; thus, these alterations are often considered early markers of tumorigenesis. MMPs are tumoral secretome-related proteins involved in the extracellular matrix degradation promoting invasiveness and angiogenesis. These proteins are upregulated in almost all types of human tumors (Egeblad & Werb, 2002) and, thus, are typically measured as a marker of *in vitro* transformation from the microenvironment perspective.

However, instead of focusing on specific proteins from the cells' secretome linked to tumorigenesis (typically MMPs), in this work we have pursued a more global analysis of the secretome at the functional level. Our approach consists in the collection of the exposed cells' conditioned media, which represents the whole set of secreted factors. When model tumoral cells are put in contact with this conditioned media, the interaction with the different factors renders them susceptible of changing their phenotype. Then, the alteration of the tumoral features, particularly of the cells' ability to grow independently of anchorage, can be assessed as a marker of the exposed cells tumor promotion capacity through secreted factors.

1.3.1.4. Anchorage-independent cell growth

Anchorage-independent growth is the ability of transformed cells to grow independently of a solid substrate. In normal tissues a correct adhesion to the extracellular matrix is essential for homeostasis and development; thus, cells are prevented from growing independently of anchorage through a particular type of apoptotic death (Taddei et al., 2012). During the transformation process cell-to-cell or cell-to-matrix contacts are altered and cells acquire the capacity of growing independently of anchorage, contributing to the cells' potential to disseminate. *In vitro*, anchorage-independent growth is evaluated via the soft-agar assay which is frequently used as a marker for an advanced transformed phenotype, given that only cells with transformed features are able to form colonies in the semi-solid matrix as seen in Figure 6. Interestingly it has been demonstrated that cells that grow independently of anchorage *in vitro* develop an expression signature also detected in metastatic human tumors (Mori et al., 2009).

1.3.1.5. Migration and invasion potential

The activation of invasion and metastasis is presumably the capacity of cancer cells that contributes the most to malignancy and an aggressive tumoral phenotype development. Cancer cells that undergo EMT activation, morphological changes, and loss of substrate attachment -mainly through E-cadherin suppression-, initiate the invasion-metastasis cascade. This involves a succession of events beginning with local invasion at the primary tumor site, followed by intravasation of cancer cells into the bloodstream and lymphatic vessels, circulation, extravasation into distant tissues and the eventual formation of metastatic lesions that can generate secondary tumors (Hanahan & Weinberg, 2011). *In vitro*, the cells' metastatic capacity can be evaluated through their migrating and invading potential. Migration assays assess the cells' capacity to disseminate in different surfaces such as transwells (Figure 6) and, thus, it is considered a marker of an advanced transformed phenotype. Regarding invasion assays, cells must not only exhibit a motile capacity but also are able to degrade layers that mimic extracellular matrix; therefore, invasion assays inform of the aggressiveness of the phenotype of *in vitro* transformed cells (Kramer et al., 2013) (Fiugre 6).

In the field of arsenic, it is well-established that long-term exposure induces the acquisition of an invasive phenotype in cell lines. As representative examples, the increase in the cells' invasion capacity has been reported in prostate epithelial RWPE-1 cells (Ngalame et al., 2014), in human lung peripheral epithelial HPL-1D cells (Person et al., 2015), and in mouse embryonic fibroblasts (Bach et al., 2016) after chronic arsenic exposure. This invasiveness of cells is closely linked to the cells' ability to form xenograft

tumors. In fact, a positive result when testing the cells' invasion ability is considered the step before xenograft studies (Tokar et al., 2010c). Thus, the invasion potential is proposed as a conclusive marker of advanced malignant transformation.

1.3.1.6. Cell stemness and tumorspheres formation

Accumulating evidence supports the idea that some cancer cells present or acquire stem cell-like properties, this subpopulation of cells are referred to as cancer stem cells (CSCs). CSCs self-renew and divide asymmetrically to give rise to the bulk of the tumor, formed by differentiated cancer cells (López de Andrés et al., 2020). Both non-tumoral cells and differentiated tumor cells interact with CSC in the tumor microenvironment, which contributes to modulate key oncogenic events. In fact, CSCs seem to be a normal constituent of many tumors, largely contributing to their heterogeneity, supporting tumor growth and metastatic potential, and being the cause of treatment resistance and recurrence (Tanabe & Sahara, 2020). Those cells that present stem-like properties are the ones able to form tumorspheres under specific *in vitro* culture conditions (Figure 6). Tumorspheres derived from cancer cells display characteristic CSCs features and present a highly invasive phenotype. Thus, the acquisition of this sphere-forming capability is considered a marker of aggressiveness and stemness in the cell population (Lee et al., 2016).

It has been suggested that exposure to heavy metals can lead to carcinogenesis either by promoting the selection of cell clones presenting survival and or proliferation advantages -clonal evolution model-, or by inducing dysregulation in cell processes, eventually providing cells with stem-like features and transforming them into CSCs which have the potential to initiate tumorigenesis -CSC model- (Wang & Yang, 2019). Although the role and characterization of CSC during arsenic-induced transformation has not been widely explored up to date, Dr. Michael P. Waalkes's group has carried out compelling studies showing that arsenic exposure increases the relative proportion of stem cells in culture. Thus, they found that long-term exposed RWPE-1 cells acquired features similar to those of RWPE-1-derived stem cells (WPE-stem) which contribute to the cells' adaptability to arsenic. Thissuggests that RWPE-1 transformation by arsenic involves an increase in CSC-like cells in the culture (Tokar et al., 2010c). These authors also described the transforming potential of arsenic in rat kidney stem cells that present aberrant regulation of differentiation pathways and aggressive features after the long-term exposure, showing that arsenic potentially targets stem cells and has the potential to transform them into CSC (Tokar et al., 2013).

1.4. POTENTIAL INTERACTIONS OF ARSENIC AND OTHER ENVIRONMENTAL POLLUTANTS

1.4.1. Co-exposures in the environment

The studies on arsenic impact on human populations, its biotransformation and mode of action are of utmost importance to mitigate and prevent the adverse effects derived from this exposure. However, arsenic is not an isolated contaminant in the environment, especially in water. It shares niche with many other major water pollutants from natural or anthropogenic sources such as fluoride, nitrates, metals, polycyclic hydrocarbons, pharmaceuticals (Fawell, 2012) or even nanoparticles (Malakar & Snow, 2020). Therefore, there is a need for a switch in the pollutants impact assessment model from the “one-exposure-for-one-health-effect” to a more comprehensive risk assessment that considers relevant co-exposures in a more real-life exposure scenario (Bjørklund et al., 2020).

Co-exposure assessment is complex to perform and interpret, given that the presence of an element may have synergistic or antagonistic effects on the impact induced by another. Thus, there is a lack of data on this regard. Some of the few studies available have reported that the co-exposure to metal mixtures -including lead, methylmercury, and arsenic-, increases neurodevelopmental toxicity compared to single metal exposure (Sanders et al., 2015). Indeed, arsenic and mercury (Bjørklund et al., 2020), as well as arsenic and lead (Freire et al., 2018) co-exposures in prenatal stages are associated to neurodevelopmental impairment. Further, epidemiological studies have found that the combined exposure to arsenic, chromium, lead, manganese, molybdenum, and zinc combined exposure is associated to increased genotoxicity levels (Annangi et al., 2016)

Although limited, this kind of approaches are critical to better understand the pleiotropic effects of environmental pollutants and, thus, more studies focusing on co-exposures are required for an adequate risk assessment.

1.4.2. Arsenic interaction with emergent pollutants

As previously described, arsenic is a classical pollutant inherent to life on Earth. In addition to other typical contaminants, arsenic also coexists with emerging pollutants, which are defined as synthetic or naturally occurring contaminants not commonly monitored and for which the fate, behavior, ecotoxicological effects, and health impact are still poorly understood. In our rapidly evolving world, anthropological sources increasingly contribute to the accumulation of emergent pollutants in the environment,

the most prominent being pharmaceuticals, pesticides, disinfection-by-products, industrial chemicals, and of course, plastics (Geissen et al., 2015).

Considering that the information on arsenic co-exposures with other classical contaminants is scarce, its interaction with emerging pollutants is no more characterized. Therefore, in the context of this Thesis, we aimed to contribute to fill this knowledge gap evaluating the potential interactions between arsenic and micro- and nano-plastics (MNPLs). This approach is not only relevant from the perspective of arsenic impact on health, but it is set in a new framework of study for risk assessment in a field with increasing interest as is the MNPLs exposure.

1.4.2.1. Arsenic and micro- and nano-plastic interaction

Plastics are widely used in uncountable applications due to their physicochemical properties, low cost, and high adaptability. This comes together with an exponential increase in plastic waste that is rapidly becoming a pressing environmental issue. In the environment, different physicochemical conditions favor plastic fragmentation and degradation into smaller particles called MNPLs, ranging the micro or nano scale (Bouwmeester et al., 2015).

While MNPLs are ubiquitously distributed throughout the environment, they are currently considered major water pollutants. In fact, it is estimated that up to 8.3 million MNPLs particles contaminate each m^3 of ocean water (Brandon et al., 2020). Thus, plastic pollution is becoming a serious issue in water ecosystems -rivers, lakes, open sea, and coasts-, where it co-exists with plenty of other pollutants, including arsenic.

As in the case of arsenic, there is accumulating evidence of the MNPLs uptake in humans through inhalation, ingestion and, in a lesser proportion, dermal contact. Furthermore, MNPLs' small size allows for adsorption and biodistribution, as it has been described that MNPLs translocate through physiological barriers and internalize intestinal cells (Domenech et al., 2020). Therefore, potential MNPLs adverse effects may arise in target organs, mainly the respiratory (RT) and gastrointestinal tract (GIT) (Campanale et al., 2020). The impact of MNPLs exposure has not been widely described yet and, while some studies have reported a lack of adverse effects, other have shown impact at different levels: cytotoxicity, ROS generation, DNA damage, and secretome and pro-inflammatory response alterations (Yong et al., 2020). However, the underlying mechanisms inducing these effects and the impact of long-term exposures remain unexplored.

Another compelling aspect of MNPLs pollution is their potential interaction with other pollutants and their possible role in the adsorption, aggregation, ingestion, retention, and release of chemicals in aquatic ecosystems. This interaction capacity can be influenced by factors such as salinity, temperature, pH, the particles' degree of aging, and distinct properties of specific MNPLs. Nonetheless it is largely recognized that the MNPLs' large surface-area-to-volume ratio and hydrophobicity make them potential carriers for other pollutants from the surrounding environment (Yu et al., 2019). Indeed, traces of cadmium, titanium, lead, and other metals have been detected on MNPLs samples collected at coasts and open sea (Massos & Turner, 2017; Prunier et al., 2019). Moreover, studies with fish models have associated MNPLs in the aquatic environment to increased uptake efficiency and bioaccumulation of contaminants such as bisphenol A (BPA) (Chen et al., 2017), polychlorinated biphenyls (PCB), or polycyclic aromatic hydrocarbons (PAH) (Rochman et al., 2013).

As previously introduced, the interaction between pollutants can determine their outcome and health impact. The joint toxicity of MNPLs and inorganic or organic pollutants remains widely unexplored but is now facing increasing interest and becoming a hot topic related to MNPLs risk. In this framework, we have broadened our scope and shift our focus from studies on the evaluation of arsenic effects as a single exposure, to the impact of arsenic and MNPLs co-exposure.

It is straightforward that arsenic and MNPLs coexist in the same environment, mainly in the water of highly contaminated areas. Indeed, arsenic adsorption onto MNPLs such as micro polystyrene (Dong et al., 2020a) and micro polytetrafluoroethylene (Dong et al., 2019) surface has already been described. As represented in Figure 7, arsenic and MNPLs also share exposure routes -predominantly ingestion and, to a lesser extent, via inhalation-, initial target organs -GIT and RT-, and certain exposure-related outcomes such as increased ROS levels and eventual genotoxicity.

Taken together, there is plenty of information that hints to potential joint effects of an arsenic and MNPLs co-exposure and, thus, these are explored in this Thesis dissertation, aiming to understand the probable health risk posed by the pollutant's interaction under long-term exposure conditions.

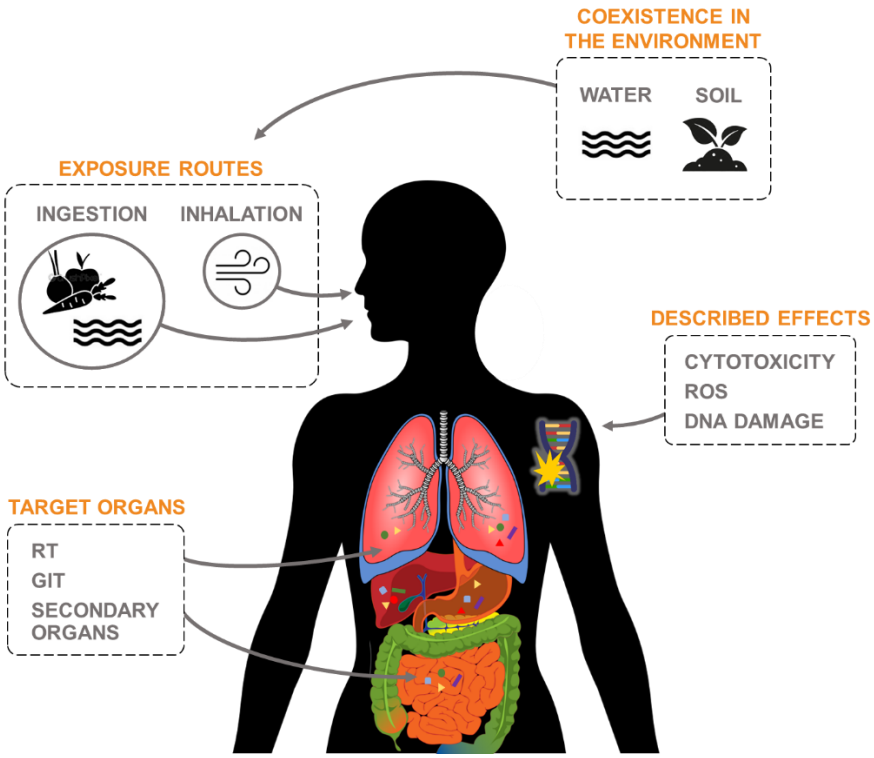

Figure 7. Arsenic and MNPLs share environmental compartment, exposure routes, and potential primary target organs and adverse effects.

2. OBJECTIVES

2. OBJECTIVES

As described in the Introduction, arsenic is a widespread environmental pollutant with a well-known carcinogenic potential. However, the mechanistic bases of arsenic carcinogenesis are not completely understood. Thus, the general objective of this Thesis is to expand the existing knowledge related to the molecular and functional effects induced by arsenic in an *in vitro* model of chronic (co)exposure. This will identify novel mechanisms of arsenic carcinogenesis operating under environmentally relevant exposure conditions.

To achieve this goal, we have set out the following three specific objectives:

1. To assess the levels of genotoxic and oxidative DNA damage during the cell transformation process induced by chronic arsenic exposure and to determine the potential involvement of AS3MT and MTH1. This objective is developed in *Chapter 1.*

2. To determine the role played by the transcription factor FRA1 in the arsenic-induced cell transformation process and to identify the influence of upstream and downstream components of FRA1 signaling axis. This objective is developed in *Chapter 2.*

3. To further advance in our model of study by evaluating the long-term (co)genotoxic and (co)carcinogenic impact of environmentally relevant mixtures of contaminants i.e. arsenic and nanoplastics. This objective is developed in *Chapter 3.*

3. RESULTS

3. RESULTS

The results of this Thesis have been divided in three different studies and classified by chapters. The first and second chapters comprise two studies published in peer-review journals, while the third study is currently submitted for evaluation.

Thus, the three articles/manuscripts arranged accordingly to the objectives of this Thesis are as follows:

3.1. Chapter 1 (Study 1): Role of *As3mt* and *Mth1* in the genotoxic and carcinogenic effects induced by long-term exposures to arsenic in MEF cells.

3.2. Chapter 2 (Study 2): FRA1 is essential for the maintenance of the oncogenic phenotype induced by *in vitro* long-term arsenic exposure.

3.3. Chapter 3 (Study 3): Oncogenic effects caused by *in vitro* long-term co-exposure to polystyrene nanoparticles and arsenic.

3.1. Chapter 1 (Study 1)

Role of *As3mt* and *Mth1* in the genotoxic and carcinogenic effects induced by long-term exposures to arsenic in MEF cells

Toxicology and Applied Pharmacology, 409: 115303.

Doi: 10.1016/j.taap.2020.115303

This chapter is a verbatim reproduction from the following published paper:

Barguilla, I., Peremartí, J., Bach, J., Marcos, R., Hernández, A. (2020) Role of *As3mt* and *Mth1* in the genotoxic and carcinogenic effects induced by long-term exposures to arsenic in MEF cells. *Toxicology and Applied Pharmacology*, 409: 115303.

Role of *As3mt* and *Mth1* in the genotoxic and carcinogenic effects induced by long-term exposures to arsenic in MEF cells

Irene Barguilla[1,*], Jana Peremartí[1,*], Jordi Bach[1], Ricard Marcos[1,2,§], Alba Hernández[1,2,§]

[*]Both authors contributed equally to this work.

[1]*Grup de Mutagènesi, Departament de Genètica i de Microbiologia, Facultat de Biociències, Universitat Autònoma de Barcelona, Bellaterra, Spain;* [2]*Consortium for Biomedical Research in Epidemiology and Public Health (CIBERESP), Carlos III Institute of Health, Madrid, Spain.*

[§]Corresponding authors at: Grup de Mutagènesi, Departament de Genètica i de Microbiologia, Universitat Autònoma de Barcelona, Edifici Cn, Campus de Bellaterra, 08193 Cerdanyola del Vallès (Barcelona), Spain.

E-mail: alba.hernandez@uab.cat (A. Hernández)

ricard.marcos@uab.es (R. Marcos)

Running title: *Mth1* and *As3mt* in arsenic-transformed cells.

ABSTRACT

DNA damage plays a crucial role in the transforming potential of the human carcinogen arsenic. The arsenic biotransformation enzyme AS3MT is known to participate in the generation of ROS after arsenic exposure, whereas MTH1 sanitizes oxidized dNTP pools to prevent the incorporation of damaged bases into DNA. In this work, we sought to assess the role of these two enzymes in the genotoxic and carcinogenic effects of arsenic exposure. Thus, mouse embryonic fibroblasts (MEF), transformed by chronic arsenite exposure, were monitored for DNA damage by the comet and the micronucleus assays at different time-of-exposure intervals lasting for 50 weeks. Results indicate that the oxidative and DNA damage of chronically exposed MEF cells increased time-dependently up to the point of transformation. *As3mt* expression followed a pattern like that of DNA damage, and its forced inhibition by shRNA technology before transformation resulted in a DNA damage decrease. On the other hand, *Mth1* mRNA levels increased after the transformation point, and its forced knock-down increased significantly the levels of DNA damage and decreased the aggressiveness of the oncogenic phenotype. Thus, *As3mt* and *Mth1* have important differential roles in the accumulation of DNA damage linked to the transformation process: while *As3mt* contributes to the genotoxic effects before the transformation, *Mth1* prevents the DNA damage fixation after the acquisition of the oncogenic phenotype. This study demonstrates the influence of *As3mt* and *Mth1* in arsenic DNA damage induction and it is the first to present *Mth1* as a candidate modulator biomarker of the tumoral phenotype.

Keywords: MEF, fibroblasts, arsenic *in vitro* long-term exposure, cell transformation, *Mth1*, *As3mt*, ODD, genotoxic DNA damage, oncogenic phenotype, carcinogenesis.

3.1.1. INTRODUCTION

Arsenic is a widespread and well-known human carcinogen. Chronic arsenic exposure is associated with skin, lung, bladder, liver, kidney, and prostate cancers (IARC, 2012). Even though chronic exposure to arsenic is known to be involved in carcinogenesis, the mechanism explaining its relationship with tumor development is unclear. The oxidative DNA damage (ODD) induced by the reactive oxygen species that are generated as by-products of inorganic arsenic biotransformation has traditionally been considered a plausible mechanism of arsenic carcinogenesis (Kojima et al., 2009; Flora, 2011) since ODD lesions such as 7,8-dihydro-2'-deoxyguanosine (8-OH-dG) are strongly linked to the potentially carcinogenic genotoxic DNA damage found in arsenic-exposed populations (Liu et al., 2001a; Hei and Filipic, 2004). In this sense, we have recently shown clear pieces of evidence of the involvement of ODD in arsenic-related oncogenic transformation (Bach et al., 2016). Noteworthy, arsenic induces cytogenetic damage as measured by the levels of chromosomal aberrations (CA), sister chromatid exchanges (SCE), and micronuclei (MN) formation in humans, as recently reviewed (Roy et al., 2018). Thus, humans exposed to inorganic arsenic via drinking water have high levels of DNA damage and increased frequencies of SCE, MN, CA, or 8-OH-dG lesions (Matsui et al., 1999; Yamauchi et al., 2004; Basu et al., 2005; Sampayo-Reyes et al., 2010). As for *in vitro* studies, compiling evidence also shows that arsenic increases the frequency of MN, CA, SCE, and oxidative effects (Hei and Filipic, 2004; Bustaffa et al., 2014).

In humans and most mammals, inorganic arsenic biotransformation involves alternating reduction and oxidation steps coupled to methylation events. The key enzyme for these multistep conversions is arsenic (+3 oxidation state) methyltransferase (AS3MT), which generates the methylated arsenic metabolites MMA^{V}, MMA^{III}, DMA^{V}, and DMA^{III} using S-adenosylmethionine (SAM) as the methyl donor (Waters et al., 2004; Thomas et al., 2007). Accumulating evidence indicates that the methylation of arsenic is not a detoxifying event; trivalent methylated arsenic metabolites -specially MMA^{III}- are more genotoxic and appear to stimulate the production of reactive oxygen species (ROS) more efficiently than inorganic arsenic compounds (Styblo et al., 2000; Mass et al., 2001; Tokar et al., 2014).

The ROS produced because of arsenic exposure can not only damage DNA directly but also oxidize free bases in the nucleotide pool that can be misincorporated into DNA. Thus, 7,8-dihydro-2′-deoxyguanosine (8-OH-dG), a major oxidized base lesion formed by ROS that causes G to T transversion mutations can originate as 8-OH-dGTP, formed in the nucleotide pool, or by direct oxidation of the DNA guanine base (Kasai and

Nishimura 1984). The MutT homolog 1 (MTH1), the major mammalian 8-oxoGTPase, is an 18kDa nudix pyrophosphorylase that effectively degrades oxidized nucleotides to avoid its incorporation into newly synthesized DNA, which otherwise can result in mispairing, mutations, and cell death (Nakabeppu, 2014). Thus, MTH1 sanitizes 8-oxodGTP from the nucleotide pool preventing its genomic incorporation by DNA polymerases. MTH1 protein is required for the efficient survival of cancer cells where it is commonly overexpressed, whereas it is non-essential in normal cells (Gad et al., 2014).

Due to the attributed role of DNA damage in arsenic-related carcinogenesis, this work aims to monitor ODD and DNA damage before, during, and after the acquisition of the transformed phenotype *in vitro*, using MEF cells previously transformed by around 30 weeks of chronic arsenic exposure (Bach et al., 2016). In such a study, MEF cells were exposed to 2 µM arsenite for 50 weeks. During this exposure-period, MEF cells acquired features of a transformed oncogenic phenotype around week 30. Indicators of such changes were their anchorage-independent cell growth capacity and invasive potential, the acquired spindle-like morphology, a de-regulated differentiation program -*C-myc, Oct3/4, Notch2, Sox2, Nanog* and *Klf4*-, and an oncogenic secretome with increased activity of matrix metalloproteinases MMP2+9, and with a capacity of functionally influence tumor growth and invasiveness (Bach et al., 2016).

Although most arsenic-induced tumors are originated from epithelial cells, there is evidence showing that stromal cells can also be affected (Shearer et al., 2015), supporting the use of this fibroblast-based model. The roles of *As3mt* and *Mth1* as the cause of the observed DNA damage and its correlation with the progressive development of a transformed phenotype are also evaluated here, applying the shRNA-based approach for gene expression inhibition. Interestingly, our findings set an association between *As3mt* and *Mth1* expression shifts and the acquisition of an aggressive tumor phenotype, introducing them as useful biomarkers of arsenic carcinogenesis.

3.1.2. MATERIALS AND METHODS

3.1.2.1. Culture conditions and *in vitro* arsenic exposure

Mouse embryonic fibroblasts (MEF) phenotypically sensitive to ODD were previously transformed by 20 - 30 weeks of arsenic exposure in the form of sodium arsenite -2 µM- (Bach et al., 2016). In the present work, MEFs were cultured after 0, 10, 20, 30, 40, and

50 weeks of exposure to analyze different end-points during the transformation process. MEF exposed cells and passaged-matched controls were grown in DMEM:F12 medium (Life Technologies, NY, USA) supplemented with 10% fetal bovine serum (FBS; PAA®, Pasching, Austria) and 2.5 µg/mL Plasmocin (InvivoGen, CA, USA) in a humidified atmosphere of 5% CO_2 and 95% air at 37 ºC.

3.1.2.2. Total RNA extraction and real-time RT-PCR

Total RNA from MEF cells at weeks 0, 10, 20, 30, 40, and 50 of exposure was extracted using TRIzol® Reagent (Invitrogen, CA, USA) following the manufacturer's instructions. RNase-free DNase I (DNAfreeTM kit; Ambion, UK) was used to remove DNA contamination. The first-strand cDNA synthesis was performed using 1 µg of total RNA and the transcriptor first-strand cDNA synthesis kit (Roche, Basel, Switzerland). The resulting cDNAs were subjected to real-time PCR analysis on a LightCycler 480 to evaluate the relative expression of the arsenite methylating enzyme As3mt and the mutT homolog Mth1. The expression of Actb was used as the housekeeping control. Each 20 µL of reaction volume contained 5 µL of cDNA, 10 µL of 2× LightCycler 480 SYBR Green I Master (Roche, Manheim, Germany), 3 µL of H_2O, and 1 µL of each primer pairs at a final concentration of 500 nM. The cycling parameters began with 95 °C for 5 min, then 45 cycles of 95 °C for 10 s, 61 °C for 15 s and 72 °C for 25 s. The primers used were: *As3mt* F (5'-GCATCGAGAAGTTGGCAGAG-3'), *As3mt* R (5'-ATCCTTCCAGTACAGAGCGC-3'), *Mth1* F (5'- GCAGGAAGGAGAGACCATTG-3'), *Mth1* R (5'-AACCAGTAGCTGTCATCCGG-3'), *Actb* F (5'-GGAGAAGATCTGGCACCACA-3'), and *Actb* R (5'-GCTCGGTCAGGATCTTCATG-3'). Cycle time (Ct) values were calculated with the LightCycler software package and then normalized with *Actb* data. The same protocol was followed for the enzymes' expression analysis in empty vectors or shRNA carrying cells to check the inhibition levels.

3.1.2.3. The micronucleus assay

The micronucleus assay (MN) was performed as a measure of chromosomal damage in MEF cells chronically exposed to arsenic, and passage-matched controls, throughout the exposure (weeks 0, 10, 20, 30, 40, and 50). Cells were seeded at a $1x10^6$ density in 60.8 cm^2 culture dishes, allowed to sit overnight, and placed in fresh medium containing 4 µg/mL of cytochalasin B (Cyt-B, Sigma, St Louis, MO, USA) to arrest cytokinesis. After 24 h, cells were harvested by trypsinization, washed, and subjected to hypotonic conditions with 0.075 M KCl. Finally, cells were centrifuged and fixed three times in a methanol/acetic acid (3:1 v/v) solution. Two or more slides were dropped, coded, and

stained with 10% of Giemsa (Merck, Darmstadt, Germany) in phosphate buffer (pH 6.8) for 5 min. Coded slides were manually scored blindly by an expert scorer under an Olympus BX50 microscope to determine the frequency of binucleated cells carrying MN (BNMN) in a total of 1000 binucleated cells with well- preserved cytoplasm (500 per replicate).

3.1.2.4. The comet assay

The ODD for MEF cells at weeks 0, 10, 20, 30, 40, and 50 of exposure and empty vector or shRNA carrying cells was evaluated by the alkaline comet assay with the use of formamidopyrimidine DNA glycosylase (FPG) as previously described by us (Bach et al., 2014). Sheet films of the type Gelbond® (GF) (McNamee et al., 2000) were used. Briefly, cells were collected by trypsinization, centrifuged, and resuspended in cold PBS at 17,500 cells/25 µL. Then cells were mixed with 0.75% LMP agarose at 37 ºC (1:10) and 7 µL of the mixture was dropped onto the GF. Two identical films with the same type of samples were processed simultaneously in each experiment. Then, GF were lysed overnight by immersion in ice-cold lysis buffer at 4 ºC (2.5 M NaCl, 0.1 M Na_2EDTA, 0.1 M Tris Base, 1% Triton X-100, 1% lauroyl sarcosinate, 10% DMSO), at pH 10. The GF replicates were gently washed twice (1x 5 min, 1x 50 min) in enzyme buffer at pH 8 (10 mM HEPES, 0.1 M KCl, 0.5 mM EDTA, 0.2 mg/mL BSA) at 4 ºC and then incubated for 30 min at 37 ºC in enzyme buffer (negative control) or FPG-containing enzyme buffer. The GF were then washed with electrophoresis buffer and placed into a horizontal gel electrophoresis tank where DNA was allowed to unwind for 23 min in 0.3 M NaOH and 1 mM Na_2EDTA pH 13.2 before the electrophoresis, which was carried out for 20 min at 0.8 V/cm and 300 mA at 4 ºC. After the electrophoresis, the GF were rinsed with cold PBS for 15 min and fixed in absolute ethanol for 2 h before air-drying overnight at room temperature. GF were stained for 20 min with SYBR Gold 1/10.000 in TE buffer (10 mM Tris, 1 mM EDTA pH 7.5). Finally, gels were mounted, visualized for comets using an epifluorescent microscope at 20X magnification, and analyzed with the Komet 5.5 Image analysis system (Kinetic Imaging Ltd, Liverpool, UK). Cells were analyzed according to their percentage of DNA in the tail, as an adequate measure of DNA damage. One hundred randomly selected comet images were analyzed per sample.

3.1.2.5. Short hairpin RNA (shRNA) and lentiviral particle production

MISSION® constructs carrying shRNA sequences targeting mouse genes *As3mt* and *Mth1*, and the control empty plasmid (pLKO.1) were purchased from Sigma-Aldrich (St Louis, MO, USA). The selected shRNA sequences were: *As3mt*

(CCGGCGAAGACGTTAGTTCGAGGTACTCGAGTACCTCGAACTAACGTCTTCGTTTTTG), *Mth1* (CCGGGAAGAAGTTCTGTGGGCACTTCTCGAGAAGTGCCCACAGAACTTCTTCTTTTTG). A maxiprep (Macherey-Nagel, Düren, Germany) was carried out following the manufacturer's protocol to obtain the plasmids at the desired concentration. Lentiviral transduction particles were produced transfecting HEK293 cells either with *As3mt* or *Mth1* shRNA vectors together with envelop (ENV) and packaging (PAX) plasmids, kindly provided by Dr. M. Bogliolo (Grup de Inestabilitat Genòmica, Universitat Autònoma de Barcelona). Briefly, the cells were seeded at 80% confluency and the next day they were transfected with the plasmids: shRNA carrying plasmid (10 µg), PAX (6.5 µg), and ENV (3.5 µg). After one day, the medium was aspirated and fresh medium was added. In the next two days, the medium was collected and centrifuged in Amicon Ultra-15 centrifugal filter units (Merck, Darmstadt, Germany) for 1 h at 3000 rpm. The concentrated medium containing the lentiviral particles was collected and stored at -80 ºC.

3.1.2.6. Cell transduction

For MEF cell transduction, 2 µM arsenic-exposed cells at weeks 20 and 40 (before and after transformation) were seeded at 25% confluency and transduced with lentiviral particles carrying *As3mt* shRNA and *Mth1* shRNA, respectively. After two days, the medium was changed and a fresh medium with puromycin was added for vector-expressing cells selection. To test the effect of *As3mt* and *Mth1* shRNA on the enzymes' expression, the cells were subjected to RNA extraction and real-time PCR analysis as previously described.

3.1.2.7. The cytotoxicity assay

To evaluate the effect of *As3mt* and *Mth1* inhibition on cell survival, cell viability was determined by the Beckman counter method with a ZTM Series Coulter-Counter (Beckman Coulter Inc., CA). 80,000 cells were seeded on 12-well plates. The next day, the cells were treated for 24 h with increasing doses of arsenic ranging from 10 to 40 µM. The cells were counted, the survival curves were obtained and the IC_{50}, defined as the As^{III} concentration that reduces viability by 50%, was calculated.

3.1.2.8. The soft-agar assay

Colony formation in soft-agar was performed in MEF cells at weeks 0, 10, 20, 30, 40, and 50 of 2 µM As^{III} exposure, as well as in the selected cells from the 40^{th} week either expressing the control empty vector or the Mth1 shRNA to assess the cells' anchorage-

independent growth potential. MEF cells were collected and filtered through a 40-µm mesh to obtain single-cell suspensions. Subsequently, a suspension of 65,000 cells in 1.75 mL of DMEM containing 10% of FBS and 2.5 µg/mL Plasmocin was prepared and mixed in a 1:1:1 ratio with 2X DMEM containing 20% of FBS, 2% NEEA, 2% L-Glu 200 mM and 2% penicillin-streptomycin, and with 1.2% of bacto-agar (DIFCO, MD, USA). This mixture was enough to prepare triplicates of 20,000 cells each by dispensing 1.5 mL over a 0.6% base agar (supplemented with 2X DMEM) in each well of a 6-well plate. The plates sat for 45 min and then kept in the incubator for 21 d. The cells able to form colonies were stained by a 24-h incubation with 1 mg/mL of (2-p-iodophenyl)-3-3(p-nitrophenyl)-5-phenyl tetrazolium chloride (INT; Sigma, MO, USA). Then, the plates were scanned, and the colonies were counted using the colony cell counter enumerator software OpenCFU (3.9.0).

A modified version of the protocol was also performed using 72 h conditioned media (CM) from long-term exposed MEF cells carrying the empty control vector or Mth1 targeted shRNA. The CM represents the cells' secretome, which varies in composition during the oncogenic transformation. Metalloproteinases 2 and 9 (MMP2+9) are oncogenic secretome-related proteins typically measured to support in vitro transformation from the secretome perspective, as they can influence cancer features such as migration and invasion in an autocrine and paracrine manner. Beyond identifying this or other particular changes in the secretome composition, the modified version of the soft-agar assay that we are conducting here evaluates changes in the functionality of the whole set of secreted factors, as it determines changes in the anchorage-independent cell growth capacity of cells that come in contact with the CM. To conduct the assay, HeLa cells (as a cancer cell model) were collected and passed through a 40-µm mesh to obtain single-cell suspensions. 35,000 cells were suspended in 1.75 mL of MEF cells' CM and mixed in a 1:1:1 ratio with 2X DMEM and 1.2% bacto-agar. This mixture was enough to prepare triplicates of 10,000 cells each. The remaining steps were performed as indicated above. Significant changes in the number or the size of the HeLa colonies present in the soft-agar plates are interpreted as having been exposed to an arsenic-induced oncogenic secretome.

3.1.2.9. The cell migration and invasion assays

To assess the effect of the 50-week chronic arsenic exposure and that of Mth1 expression inhibition on the invasive potential of transformed MEF cells, direct migration and invasion assays were performed. To carry out the invasion assay, empty control vector or Mth1 shRNA-carrying MEF cells at 80% confluency were deprived of FBS for

24 h before the assay. On the day of the assay, a 180 µL 1:2 dilution of Matrigel® (Costar-Corning, NY, USA) in FBS free DMEM:F12 with 0.1% BSA was used to coat each 8-µm pore size polycarbonate membrane 24 mm transwell insert (Costar-Corning, NY, USA). The Matrigel® mixture was left to sit and dry for 1 h in the cell incubator at 37 ºC. The bottom chamber of the transwell inserts was filled with 2.5 mL DMEM:F12 complemented with 15% FBS as the chemoattractant medium. A single-cell suspension containing 600,000 FBS-deprived MEF cells in 1.5 mL of FBS free DMEM:F12 with 0.1% BSA was added on top of the transwell Matrigel®-coated membrane. Cells were then allowed to invade for 48 h at 37 °C. Invading cells in the bottom chamber were photographed before being collected by trypsinization and counted using a Beckman Coulter® cell counter. A modified version of the assay was performed to evaluate cell migration. The main steps were followed as described above, however, the cells were seeded on the top of the transwell without the Matrigel® coating.

3.1.2.10. Statistics

Unpaired Student's *t*-test or analysis of variance followed by Dunnett's multiple comparison test was performed, as appropriate, to compare arsenic-treated cells with untreated time-matched controls at respective time points. In all cases, a two-sided $P < 0.05$ was considered statistically significant.

3.1.3. RESULTS

3.1.3.1. Chronic arsenic exposure leads to MEF cells transformation

In our previous work, MEF cells phenotypically sensitive to ODD were chronically exposed to 2 µM arsenite. This relevant subtoxic concentration induced the oncogenic transformation of the cells between the week 20 and 30 of exposure, as defined by the acquisition of a transformed phenotype *in vitro*, characterized by morphological changes, increased proliferation, deregulation of differentiation status, and a secretome with increased levels of MMPs able to enhance tumor effects of epithelial cells such as growth and invasiveness, all at levels known to induce malignant xenograft tumors in mice (Bach et al., 2016).

We confirmed the development of a transformed phenotype in this model by selecting MEFs at different time-points of the continuous 2 µM arsenic exposure -weeks 10, 20, 30, 40, and 50-. The anchorage-independent growth ability (Figure 1A), as well as the invasion potential of the cells (Figure 1B), show a progressive increase over weeks which

is significant when compared to the non-exposed time-matched controls from the week 20 onwards. Thus, corroborating the transforming effects induced by chronic arsenic exposure.

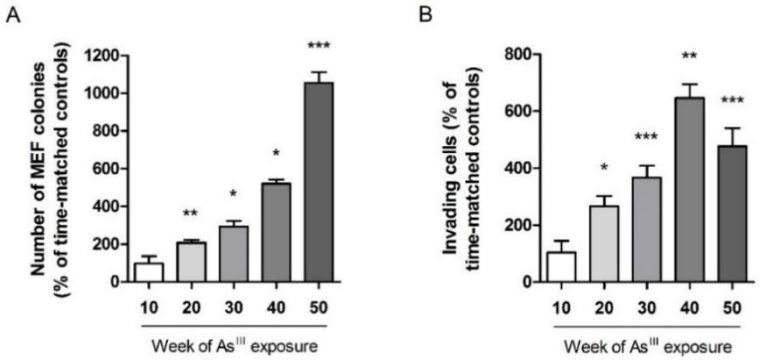

Figure 1. The progressive development of the *in vitro* transformed phenotype during chronic arsenic exposure. The ability of the MEF cells chronically exposed to 2 μM As^{III} to grow independently of anchorage in the soft-agar assay **(a)** and their invading potential **(b)** progressively increase throughout the weeks, starting to show significant variations with the non-exposed time-matched controls around week 20. The MEFs transformation point is reached between weeks 20 and 30. Data are presented as mean values with time-matched controls set to 100% (n=3); error bars represent standard error of the mean; $^{*}P < 0.05$, $^{**}P<0.01$, $^{***}P<0.001$ compared with time-matched controls.

3.1.3.2. Arsenic-induced oxidative and chromosomal damage peak at the time of transformation

Levels of ODD were measured in MEFs by the comet assay at exposure-time intervals covering the whole transformation process –before, during, and after transformation- (Figure 2A). Data revealed that 2 μM arsenic exposure induced a progressive increase in ODD in a time-dependent manner up to the point of transformation. Thus, the increase in % of tail DNA of exposed cells at week 10, when compared to passage-matched controls, was 2.77-fold, and at week 30, the increase on the % of tail DNA was 8.20-fold ($P<0.05$). Interestingly, the ODD dropped rapidly after the acquisition of the transformed phenotype. At week 40, the % DNA in tail decreased to 1.89-fold and those close-to-basal ODD levels were maintained at week 50, none of them being statistically different from their respective passage-matched controls. A similar pattern of damage was found when the level of MN was analyzed through the exposure, as a measure of chromosomal damage (Figure 2B). As shown, MN increased in a time-dependent manner up to the approximate point of transformation -peaking at 1.80-fold at week 20-, and then MN frequency in binucleated cells (BNMN) precipitously declined under baseline levels.

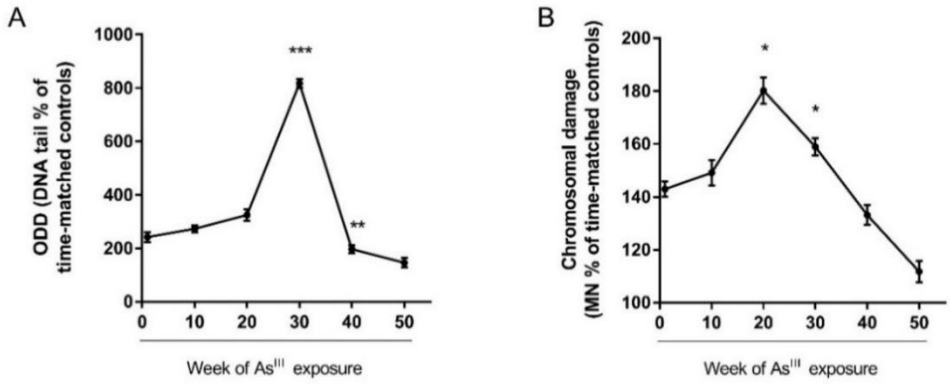

Figure 2. Oxidative and DNA damage in MEFs cells over the transformation process. **(a)** ODD levels measured by the comet assay show an increase up to week 30, the approximate point of transformation, and then drop close to basal levels. **(b)** Chromosomal damage measured as the frequency of MN in binucleated cells shows a similar tendency over the transformation process. Data are presented as mean values with time-matched controls set to 100% (n=3); error bars represent standard error of the mean; **P* < 0.05, ***P*<0.01, ****P*<0.001 compared with time-matched controls.

A global analysis of both ODD and chromosomal damage during the transformation process indicates that cells chronically exposed to subtoxic doses of arsenic gradually accumulate DNA damage up to the approximate point of transformation. From there on, the exposed cells acquire a resistant phenotype evidenced by a rapid decrease in DNA damage until it reaches control levels.

3.1.3.3. Arsenic-3-methyltransferase is involved in the increase of arsenic-induced DNA damage during the transformation process

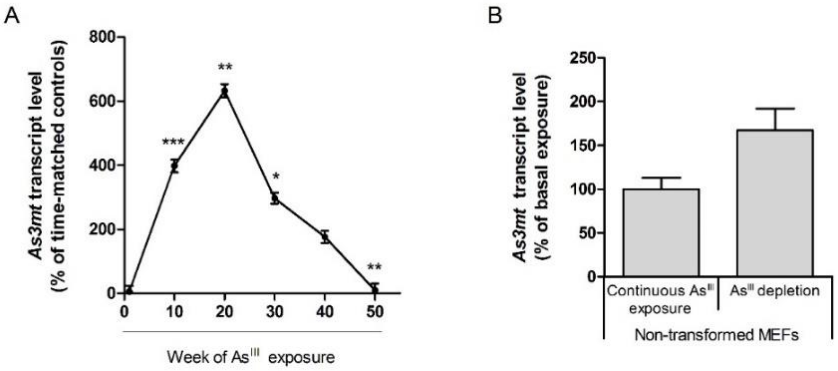

Figure 3. Expression changes of the *As3mt* gene in MEF cells under different conditions of arsenite exposure. **(a)** Throughout the chronic exposure, *As3mt* expression is upregulated up to the peak of transformation and follows a pattern similar to that of the DNA damage showing a drop to basal levels after the transformation point. **(b)** The *As3mt* expression levels did not diminish after a 2-week arsenic deprivation in cells before the transformation point. Data are presented as mean values with time-matched controls or with non-deprived cells set to 100% (n=3); error bars represent standard error of the mean; **P* < 0.05, ***P* < 0.01, ****P* < 0.001 compared with time-matched controls.

Under a chronic scenario of exposure, MEF cells increase *As3mt* expression time-dependently up to the point of transformation (Figure 3A), in parallel to what occurs with DNA damage. Thus, MEF cells at the time of transformation reached 6.5-fold expression when compared to controls. After, similarly to what happened with DNA damage, *As3mt* expression dropped and reached levels close to those of the first weeks of exposure. The differential expression of *As3mt* over time suggests its involvement in the DNA damage induction during the process of arsenic detoxification, supported by the fact that AS3MT is known to generate ODD during the biotransformation process -hence cells not expressing AS3MT do not generate detectable levels of ODD-. Moreover, when cells overexpressing *As3mt* (before transformation) are depleted from arsenic during 2 weeks, the levels of *As3mt* do not diminish (Figure 3B), supporting the view that the reduced expression found in the later weeks of chronic arsenic exposure is not a consequence of the reduction of DNA damage. On the contrary, when chronically exposed cells whose *As3mt* expression was 70% inhibited (Figure 4A) are exposed to arsenic for 2 more weeks, the levels of DNA damage and ODD are significantly reduced when compared to its non-inhibited counterparts (Figure 4B, C), showing that the increase in DNA damage before the transformation point can be explained by the AS3MT overexpression in our system.

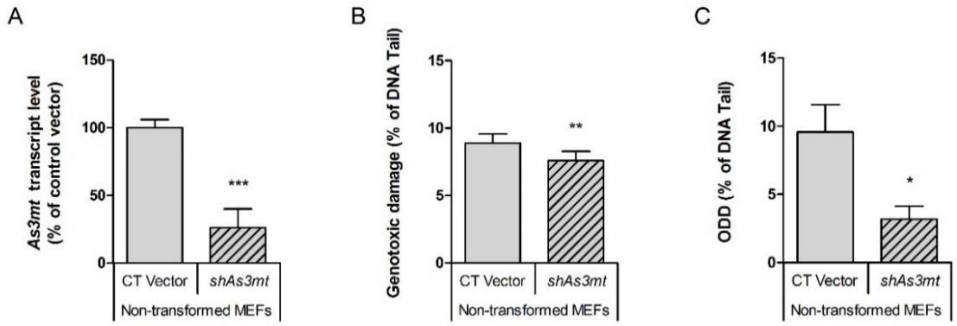

Figure 4. Oxidative and DNA damage in MEF cells transduced with *As3mt*-targeted shRNA before the transformation. **(a)** *As3mt* knock-down by shRNA efficiently reduced its expression by 70% before the transformation point. **(b,c)** *As3mt* shRNA-carrying MEFs show a higher resistance to the oxidative and DNA damage induced by a 2-week prolonged exposure to 2 μM AsIII after the inhibition. Data are represented as mean values (n=3); error bars represent standard error of the mean; **P* < 0.05, ***P* < 0.01, ****P* < 0.001 compared with *As3mt*-expressing cells.

3.1.3.4. Arsenic-transformed cells up-regulate Mth1 to avoid DNA damage and cell death

The involvement of the mutT homolog *Mth1* in the decline of ODD and DNA damage after transformation was studied by analyzing its expression through the transformation process.

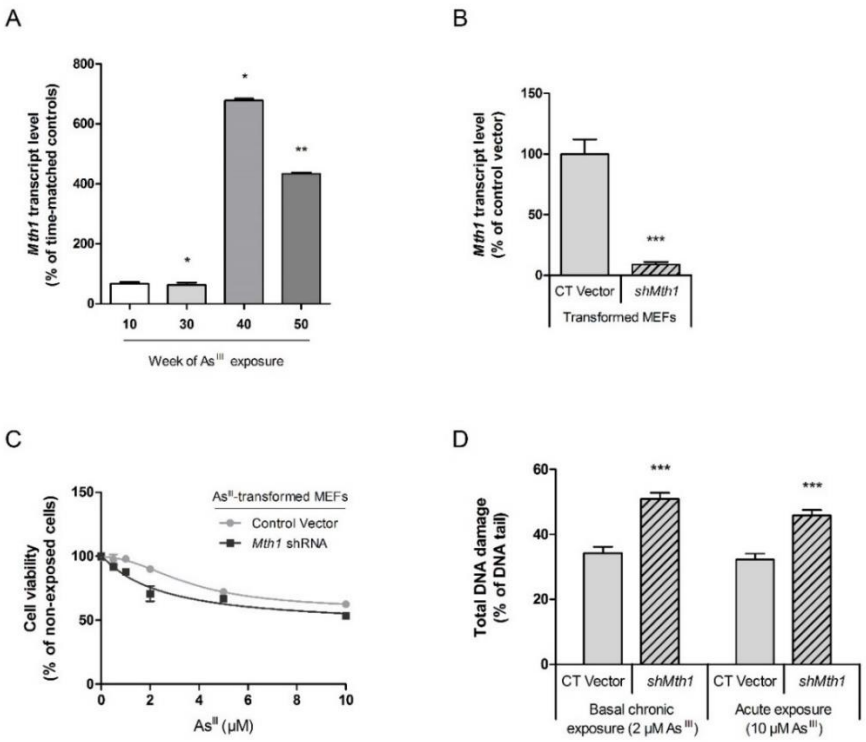

Figure 5. *Mth1* inhibition increases MEF cells' sensitivity to arsenic-related detrimental effects. **(a)** *Mth1* expression increases significantly after 40 and 50 weeks of continuous 2 μM arsenic exposure. **(b)** *Mth1* knock-down by shRNA efficiently reduced its expression by 90% after the transformation point. **(c)** Cell viability of *Mth1* knock-down MEFs is reduced when compared to control vector-carrying cells after acute exposure to low doses of arsenic for 24 h. **(d)** The DNA damage measured by the comet assay was increased in *Mth1* shRNA-carrying cells, both at the basal chronic exposure situation and after acute exposure to 10 μM As^{III} for 24 h, when compared to *Mth1*-expressing cells. Data are presented as mean values with time-matched controls (a) or control-vector carrying cells (b) set to 100% (n=3) when appropriate; error bars represent standard error of the mean; $^{*}P < 0.05$, $^{**}P < 0.01$, $^{***}P < 0.001$ compared with *Mth1*-expressing cells.

As MTH1 is non-essential in normal cells, but cancer cells require MTH1 activity to avoid incorporation of oxidized dNTPs resulting in DNA damage and cell death, a clear induction of gene expression was expected at those time-points where DNA damage relapsed. This occurs at weeks 40 and 50, after the acquisition of the *in vitro* transformed phenotype. *Mth1* transcript levels were found to be maintained close to control levels – or below- before transformation and at the point of transformation (weeks 10 and 30, Figure 5A). Notably, the upregulation of transcription was found after transformation. Hence, *Mth1* mRNA levels were 6.78-fold of control at week 40 of exposure ($P<0.05$), and similar levels were maintained at week 50 (Figure 5A). When the induction of expression was analyzed, comparing the point of maximal DNA damage -week 30- with that of DNA damage decline -week 40-, a clear and important induction of 21.7-fold was observed ($P<0.05$).

Mth1 expression knock-down with a 90% efficiency (Figure 5B) in transformed MEF cells -week 40 of chronic 2 µM As^{III} exposure- has shown its importance in these cells' survival and resistance to arsenic-induced DNA damage. When exposed to increasing doses of arsenic for 24 h, shRNA carrying cells' survival decreases from an IC_{50} = 15.01 ± 1.43 µM to IC_{50} = 9.208 ± 1.04 µM (Figure 5C). Accordingly, a significant increase in the DNA damage of the *Mth1* knock-down cells was observed at basal levels and after an acute arsenic exposure (Figure 5D), indicating that MTH1 activity is required for these cells to prevent the toxic and genotoxic effects of arsenic exposure and that *Mth1* overexpression found after arsenic-induced oncogenic transformation is responsible for the diminished levels of damage observed at this time.

3.1.3.5. MTH1 up-regulation is necessary for the development of an aggressive tumor phenotype

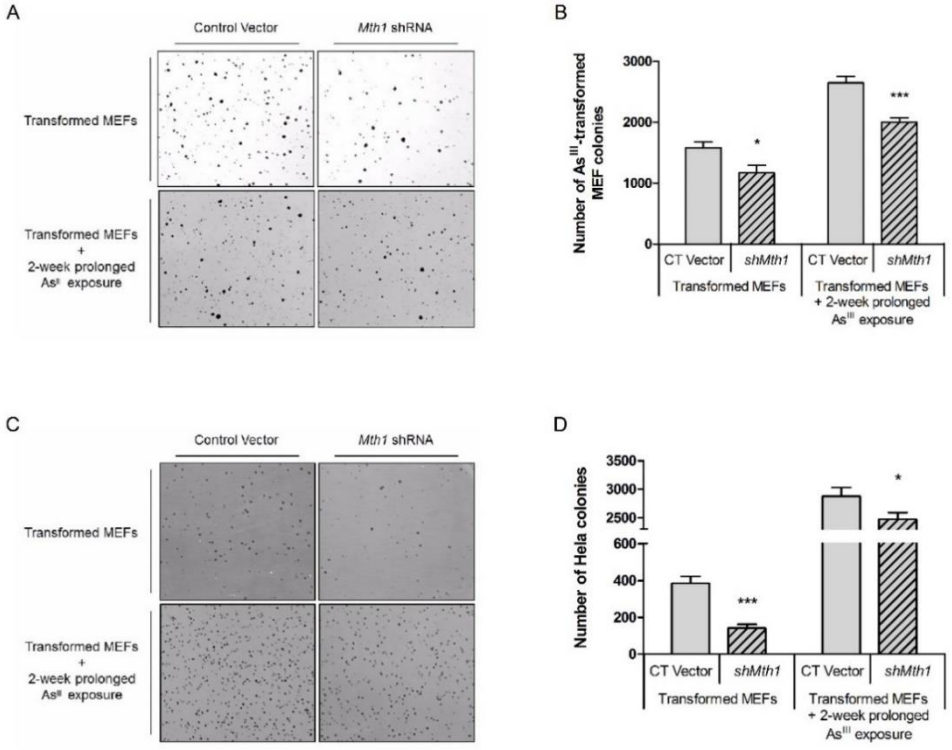

Figure 6. *Mth1* knock-down reduces the colony-forming ability of the cells transformed by chronic arsenic exposure. **(a, b)** The number of colonies able to grow independently of anchorage analyzed by the direct soft agar assay is reduced when comparing the *Mth1* shRNA-carrying cells with *Mth1*-expressing ones both immediately after the inhibition and after a 2-week prolonged exposure to 2 µM AsIII. **(c, d)** MEF cells' ability to promote the colony formation of HeLa cells was also diminished in *Mth1* knock-down conditioned media (CM) of cells before and after 2-week prolonged arsenic exposure. Data are presented as mean values (n=3); error bars represent standard error of the mean; **P* < 0.05, ***P* < 0.01, ****P* < 0.001 compared with *Mth1*-expressing cells.

Given the importance of MTH1 in cells' survival and genotoxicity after the transformation point, we analyzed the effect of its inhibition on several *in vitro* oncogenic phenotypic hallmarks. When studying the anchorage-independent cell growth capacity of arsenic-transformed MEF cells by the soft-agar assay, a decreased ability to form colonies was observed in those cells with inhibited *Mth1* expression both at the moment of inhibition and after two weeks of prolonged arsenic exposure (Figure 6A, B). As previously indicated, the CM represents the cells' secretome, which varies its composition during the oncogenic transformation. Our results indicate that the CM from the inhibited cells is less able to promote colony growth of known tumor HeLa cells than non-inhibited *Mth1* cells (Figures 6C, D). Accordingly, the migration and the invasion assay using transwells show that *Mth1* knock-down cells had a reduced migration (Figure 7A, B) and invasion (Figure 7 C, D) ability when compared with the *Mth1*-expressing cells.

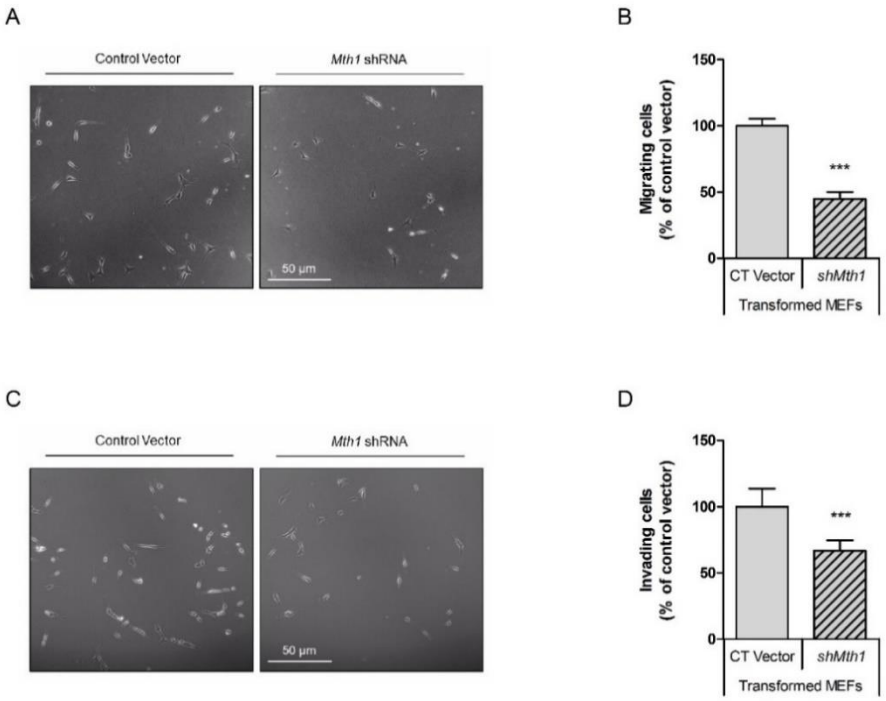

Figure 7. *Mth1* inhibition reduces the migration and invasion potential of arsenic-transformed cells. The number of cells able to migrate **(a, b)** and to invade **(c, d)** is significantly reduced in *Mth1* knock-down cells. Data are presented as mean values (n=3); error bars represent standard error of the mean; **P* < 0.05, ***P* < 0.01, ****P* < 0.001 compared with *Mth1*-expressing cells.

3.1.4. DISCUSSION

Understanding the mechanism(s) of arsenic carcinogenesis is of great relevance to protect human exposed populations. In this sense, arsenic-induced DNA damage -understood as the addition of genotoxic and oxidative DNA damage- has been proposed as a major player in the carcinogenicity of arsenic compounds, as it is considered to be essential for the initiation of malignancies (Rossman, 2003; Kitchin and Conolly, 2010).

Chronic exposure to arsenic has been involved with the *in vitro* oncogenic or malignant transformation of human bronchial epithelial cells (Xu et al., 2013), human HaCaT keratinocytes (Pi et al., 2008; Li et al., 2010), human lung epithelial BEAS-2B cells (Stueckle et al., 2012), human small airway epithelial cells (Wen et al., 2008), rat liver epithelial TRL1215 cells (Liu et al., 2006), human prostate epithelial RWPE-1 cells (Treas et al., 2013), breast epithelia (Xu et al., 2014) and mouse embryonic fibroblasts (Bach et al., 2016). Most of these cellular models are indeed epithelial since arsenic-induced tumors arise from epithelial cells, but emerging evidence shows that arsenic can affect stromal cells such as fibroblasts (Shearer et al., 2015), supporting the use of MEF cells in this type of experimental approaches. Under specific stimuli, including ROS generation, normal fibroblasts are known to acquire an activated state and give origin to the cancer-associated fibroblasts (CAFs) commonly found in the tumor microenvironment (Cirri and Chiarugi, 2012). Activated fibroblasts in a “CAF state” show a phenotype distinct from normal fibroblasts, characterized by enhanced secretion of factors and other ECM modulators that could help promote tumor growth and progression, facilitating the transformation process (Koontongkaew, 2013). Thus, the associated implications of fibroblasts being an arsenic target are certainly of interest, as not only can arsenic induce cell transformation directly, but it may also influence the organ or tumor stroma, thereby potentiating the carcinogenic effects of arsenic and/or other toxicants.

A broad number of molecular mechanisms of carcinogenesis including the newly described transcriptomic (Merrick et al., 2019) and epigenetic alterations (Chen et al., 2020) have been explored using the above-mentioned epithelial and stromal models of malignant transformation. Nonetheless, the behavior of DNA damage through the exposure/acquisition of the cancer phenotype has been poorly explored so far.

The present work monitored ODD and DNA damage in MEF cells during 50 weeks of exposure to 2 µM arsenite. During this exposure-period, MEF cells acquired features of a transformed oncogenic phenotype around week 30, as indicated by their anchorage-independent cell growth capacity and invasive potential (see Figure 1), together with an

acquired spindle-like morphology, a de-regulated differentiation program -*C-myc, Oct3/4, Notch2, Sox2, Nanog* and *Klf4*-, and an oncogenic secretome with increased activity of matrix metalloproteinases MMP2+9 and with the capacity of functionally influence tumor growth and invasiveness (Bach et al., 2016). Our results showed that DNA damage increased time-dependently up to the point of transformation and dropped radically ready after (see Figure 2).

The work of Kojima et al. (2009) explored the accumulation of ODD in chronically exposed rat liver TRL1215 cells and found concordant results, but no mechanistic explanation was proposed for the obtained observations (Kojima et al., 2009). We observed that *Mth1* was involved in the DNA damage resistant phenotype found after transformation since its expression was triggered by 21-fold at this time-point (see Figure 5A). MTH1 is required for cancer cells to sanitize oxidized dNTP pools and hence prevent the incorporation of oxidized bases into DNA (Gad et al., 2014). Then, arsenic-transformed cells appear to require Mth1 to avoid DNA damage and cell death (see Figure 5C and D). On one hand, this mechanism could explain the remarkable generalized apoptotic-resistant phenotype found by some authors in arsenic long-exposed cells (Qu et al., 2002, Pi et al., 2005), and could also contribute to the phenomenon of self-tolerance found to occur during chronic exposure in vitro (Romach et al., 2000; Liu et al., 2001b; Brambila et al., 2002). Interestingly, our findings set *Mth1* as a potential biomarker of arsenic carcinogenesis as arsenic-exposed cells are expected to increase its expression once malignant transformation has occurred. Remarkable is also the fact that *Mth1* is elicited here as having a role in the aggressiveness of the oncogenic phenotype, as *Mth1* inhibition led to a phenotype with diminished ability to grow independently of anchorage, reduced migration and invasion potential, and a secretome less capable of promoting tumor growth (see Figures 6 and 7). So far, the only role attributed to MTH1 in cancer cells is related to its function in DNA damage prevention, but this finding opens the door to a new role of this enzyme in the carcinogenesis process as inductor of a more aggressive phenotype.

In humans, ingested inorganic arsenic is biotransformed via multiple consecutive methylation steps into the methylated metabolites monomethyl-arsenic (MMAs) and dimethyl-arsenic (DMAs), which can be found in trivalent (MMAIII) and pentavalent (MMAV) oxidation states (Vahter, 2002). Originally thought to serve as a detoxifying mechanism, arsenic biotransformation is now considered a critical influencer of the adverse effects associated with arsenic exposure as trivalent intermediate metabolites are more genotoxic than pentavalent species (Styblo et al., 2000). As for its carcinogenic potential, MMAIII was able to induce a transformed phenotype in chronically exposed

TRL1215 and prostate RWPE cells more rapidly than its inorganic parental counterpart AsIII, by a mechanism involving genotoxicity, specifically the generation of ODD (Tokar et al., 2014). Notably, arsenic biotransformation appears mandatory for the generation of ODD by inorganic arsenic, but not for trivalent monomethyl-arsenic (Kojima et al., 2009; Tokar et al., 2014). Precisely due to the outstanding role of arsenic biotransformation in arsenic toxic, genotoxic, and carcinogenic potential consequences, the ability of our MEF cells to biotransform inorganic arsenic was previously analyzed by us by HPLC-ICP-MS, revealing that our MEF cells were able to biotransform arsenic, as indicated by the presence of all organic species resulting from inorganic arsenic metabolism in the cell lysates and the medium after exposure to AsIII and MMAIII for 24 and 48 h (Bach et al., 2014). It can be assumable that changes in the metabolic capacity of cells would strongly influence the outcome of a given exposure. Human liver HepG2 cells silenced for *AS3MT* gene and *As3mt* knockout mice drastically decreased arsenic methylation capacity (Drobna et al., 2006, 2009), and *As3mt* expression changes or polymorphisms found in chronic arsenic-exposed individuals are associated with individual arsenic metabolic patterns (Hernández et al., 2008a; Hernández et al., 2008b; Engström et al., 2011). In the present work, an interesting pattern of *As3mt* expression has been observed during arsenic-associated oncogenic transformation. Up to the point of transformation, *As3mt* increased time-dependently as occurred with ODD and chromosomal DNA damage (see Figures 2 and 3A). Presumably, the chronic stress and DNA damage accumulation induced the overexpression of *As3mt* as an attempt to enhance arsenic biotransformation and avoid cellular toxicity, which in turn aggravated the genotoxic accumulative effects by increasing ROS production and the highly-reactive intermediate metabolites. At the same time, the down-regulation of *As3mt* expression after transformation –by unknown reasons not explored here- contributes to the reduction of DNA damage found in transformed cells, as *As3mt* forced knock-down significantly diminish DNA damage (see Figure 4B and C). Therefore, our findings point out a link between AS3MT high activity and increase levels of DNA damage. It should be pointed out, however, that the biological significance of AS3MT-related DNA damage in vitro, in terms of toxicity, may differ from those taking place in vivo, where As3MT activity is necessary for a faster excretion of arsenic in many systems, including humans (Watanabe and Hirano, 2013). Thus, arsenic clearance and DNA damage induction are the two faces of the AS3MT-dependent biotransformation process

3.1.5. CONCLUSIONS

The present work demonstrates a time-dependent accumulation of ODD and chromosomal DNA damage during the acquisition of the arsenic-associated transformed phenotype, a carcinogenic mechanism where *As3mt* and *Mth1* are involved. Our results also demonstrate DNA damage resistant and tumor aggressive phenotype of arsenic-transformed cells, through *Mth1* induction. The evaluation of *Mth1* after a given exposure would help to define the associated risk, and we recommend its expression analysis in cells transformed by chronic arsenic exposure, in animal models of arsenic carcinogenesis, in environmentally exposed individuals and arsenic-induced skin lesions.

Acknowledgments

We wish to thank Mr. C. Valiente for his technical assistance. This work was supported by the *Universitat Autònoma de Barcelona* [PIF-UAB to I.B., J.P. and J.B.] and the Spanish Ministry of Education and Science [BFU2016-76831-R].

Competing financial interests

The authors declare they have no actual or potential competing financial interests.

3.1.6. REFERENCES

Bach, J., Marcos, R., Hernández, A. (2014). Ogg1 genetic background determines the genotoxic potential of environmentally relevant arsenic exposure. *Arch. Toxicol. 88*, 585-596.

Bach, J., Peremartí, J., Annangi, B., Marcos, R., Hernández, A. (2016). Oxidative DNA damage enhances the carcinogenic potential of in vitro chronic arsenic exposures. *Arch. Toxicol. 90*, 1893-1905.

Basu, A., Som, A., Ghoshal, S., Mondal, L., Chaubey, R.C., Bhilwade, H.N., Rahman, M.M., Giri, A.K. (2005). Assessment of DNA damage in peripheral blood lymphocytes of individuals susceptible to arsenic induced toxicity in West Bengal, India. *Toxicol. Lett. 159*, 100-112.

Brambila, E.M., Achanzar, W.E., Qu, W., Webber, M.M., Waalkes, M.P. (2002). Chronic arsenic-exposed human prostate epithelial cells exhibit stable arsenic tolerance: mechanistic implications of altered cellular glutathione and glutathione S-transferase. *Toxicol. Appl. Pharmacol. 183*, 99-107.

Chen, D., Chen, Q.Y., Wang, Z., Zhu, Y., Kluz, T., Tan, W., Li, J., Wu, F., Fang, L., Zhang, X., He, R., Shen, S., Sun, H., Zang, C., Jin, C., Costa, M. (2020). Polyadenylation of histone H3.1 mRNA promotes cell transformation by displacing H3.3 from gene regulatory elements. *iScience. 23*, 101518.

Cirri, P., Chiarugi, P. (2012). Cancer-associated-fibroblasts and tumour cells: a diabolic liaison driving cancer progression. *Cancer Metastasis Rev. 31*, 195-208.

Drobna, Z., Xing, W., Thomas, D.J., Stýblo, M. (2006). shRNA silencing of AS3MT expression minimizes arsenic methylation capacity of HepG2 cells. *Chem. Res. Toxicol. 19*, 894-898.

Drobna, Z., Naranmandura, H., Kubachka, K.M., Edwards, B.C., Herbin-Davis, K., Styblo, M., Le, X.C., Creed, J.T., Maeda, N., Hughes, M.F., Thomas, D.J. (2009). Disruption of the arsenic (+3 oxidation state) methyltransferase gene in the mouse alters the phenotype for methylation of arsenic and affects distribution and retention of orally administered arsenate. *Chem. Res. Toxicol. 22*, 1713-1720.

Engström, K., Vahter, M., Mlakar, S.J., Concha, G., Nermell, B., Raqib, R., Cardozo, A., Broberg, K. (2011). Polymorphisms in arsenic(+III oxidation state) methyltransferase (AS3MT) predict gene expression of AS3MT as well as arsenic metabolism. *Environ. Health Perspect. 119*, 182-188.

Flora, S.J.S. (2011). Arsenic-induced oxidative stress and its reversibility. *Free Radic. Biol. Med. 51*, 257-281.

Gad, H., Koolmeister, T., Jemth, A.S., Eshtad, S., Jacques, S.A., Ström, C.E., et al. (2014). MTH1 inhibition eradicates cancer by preventing sanitation of the dNTP pool. *Nature. 508*, 215-221.

Hei, T.K., Filipic, M. (2004). Role of oxidative damage in the genotoxicity of arsenic. *Free Radic. Biol. Med. 37*, 574-581.

Hernández, A., Xamena, N., Sekaran, C., Tokunaga, H., Sampayo-Reyes, A., Quinteros, D., Creus, A., Marcos, R. (2008a). High arsenic metabolic efficiency in AS3MT287Thr allele carriers. Pharmacogenet. *Genomics. 18*, 349-355.

Hernández, A., Xamena, N., Surrallés, J., Sekaran, C., Tokunaga, H., Quinteros, D., Creus, A., Marcos, R. (2008b). Role of the Met(287)Thr polymorphism in the AS3MT gene on the metabolic arsenic profile. *Mutat. Res. 637*, 80-92.

International Agency for Research on Cancer (IARC). (2012). Arsenic, metals, fibres and dusts. IARC Monographs on the evaluation of carcinogenic risk to humans, 100C. International Agency for reseach on Cancer, Lyon, France.

Kasai, H., Nishimura, S. (1984). Hydroxylation of deoxyguanosine at the C-8 position by ascorbic acid and other reducing agents. *Nucleic Acids Res. 12*, 2137-2145.

Kitchin, K.T., Conolly, R. (2010). Arsenic-induced carcinogenesis--oxidative stress as a possible mode of action and future research needs for more biologically based risk assessment. *Chem. Res. Toxicol. 23*, 327-335.

Kojima, C., Ramirez, D.C., Tokar, E.J., Himeno, S., Drobná, Z., Stýblo, M., Mason, R.P., Waalkest, M.P. (2009). Requirement of arsenic biomethylation for oxidative DNA damage. *J. Natl. Cancer Inst. 101*, 1670-1681.

Koontongkaew, S. (2013). The tumor microenvironment contribution to development, growth, invasion and metastasis of head and neck squamous cell carcinomas. *J. Cancer. 4*, 66-83.

Li, Y., Ling, M., Xu, Y., Wang, S., Li, Z., Zhou, J., Wang, X., Liu, Q. (2010). The repressive effect of NF-kappaB on p53 by mot-2 is involved in human keratinocyte transformation induced by low levels of arsenite. *Toxicol. Sci. 116*, 174-182.

Liu, S.X., Athar, M., Lippai, I., Waldren, C., Hei, T.K. (2001a). Induction of oxyradicals by arsenic: implication for mechanism of genotoxicity. *Proc. Natl. Acad. Sci. U.S.A. 98*, 1643-1648.

Liu, J., Chen, H., Miller, D.S., Saavedra, J.E., Keefer, L.K., Johnson, D.R., Klaassen, C.D., Waalkes, M.P. (2001b). Overexpression of glutathione S-transferase II and multidrug resistance transport proteins is associated with acquired tolerance to inorganic arsenic. *Mol. Pharmacol. 60*, 302-309.

Liu, J., Benbrahim-Tallaa, L., Qian, X., Yu, L., Xie, Y., Boos, J., Qu, W., Waalkes, M.P. (2006). Further studies on aberrant gene expression associated with arsenic-induced malignant transformation in rat liver TRL1215 cells. *Toxicol. Appl. Pharmacol. 216*, 407-415.

Mass, M.J., Tennant, A., Roop, B.C., Cullen, W.R., Styblo, M., Thomas, D.J., Kligerman, A.D. (2001). Methylated trivalent arsenic species are genotoxic. *Chem. Res. Toxicol. 14*, 355-361.

Matsui, M., Nishigori, C., Toyokuni, S., Takada, J., Akaboshi, M., Ishikawa, M., Imamura, S., Miyachi, Y. (1999). The role of oxidative DNA damage in human arsenic carcinogenesis: detection of 8-hydroxy-2'-deoxyguanosine in arsenic-related Bowen's disease. *J. Invest. Dermatol. 113*, 26-31.

McNamee, J.P., McLean, J.R., Ferrarotto, C.L., Bellier, P.V. (2000). Comet assay: rapid processing of multiple samples. *Mutat. Res. 466*, 63-69.

Merrick, B.A., Phadke, D.P., Bostrom, M.A., Shah, R.R., Wright, G.M., Wang, X., Gordon, O., Pelch, K.E., Auerbach, S.S., Paules, R.S., DeVito, M.J., Waalkes, M.P., Tokar, E.J. (2019). Arsenite malignantly transforms human prostate epithelial cells in vitro by gene amplification of mutated KRAS. *PLoS One, 14*, e0215504.

Nakabeppu, Y. (2014). Cellular levels of 8-Oxoguanine in either DNA or the nucleotide pool play pivotal roles in carcinogenesis and survival of cancer cells. *Int. J. Mol. Sci. 15*, 12543-12557.

Pi, J., He, Y., Bortner, C., Huang, J., Liu, J., Zhou, T., Qu, W., North, S.L., Kasprzak, K.S., Diwan, B.A., Chignell, C.F., Waalkes, M.P. (2005). Low level, long-term inorganic arsenite exposure causes generalized resistance to apoptosis in cultured human keratinocytes: potential role in skin co-carcinogenesis. *Int. J. Cancer. 116*, 20-26.

Pi, J., Diwan, B.A., Sun, Y., Liu, J., Qu, W., He, Y., Styblo, M., Waalkes, M.P. (2008). Arsenic-induced malignant transformation of human keratinocytes: involvement of Nrf2. *Free Radic. Biol. Med. 45*, 651-658.

Qu, W., Bortner, C.D., Sakurai, T., Hobson, M.J., Waalkes, M.P. (2002). Acquisition of apoptotic resistance in arsenic-induced malignant transformation: role of the JNK signal transduction pathway. *Carcinogenesis. 23*, 151-159.

Romach, E.H., Zhao, C.Q., Del Razo, L.M., Cebrián, M.E., Waalkes, M.P. (2000). Studies on the mechanisms of arsenic-induced self tolerance developed in liver epithelial cells through continuous low-level arsenite exposure. *Toxicol. Sci. 54*, 500-508.

Rossman, T.G. (2003). Mechanism of arsenic carcinogenesis: an integrated approach. *Mutat. Res. 533*, 37-65.

Roy, J.S., Chatterjee, D., Das ,N., Giri, A.K. (2018). Substantial evidences indicate that inorganic arsenic is a genotoxic carcinogen: a review. *Toxicol. Res. 34*, 311-324.

Sampayo-Reyes, A., Hernández, A., El-Yamani, N., López-Campos, C., Mayet-Machado, E., Rincón-Castañeda, C.B., et al. (2010). Arsenic induces DNA damage in environmentally exposed Mexican children and adults. Influence of GSTO1 and AS3MT polymorphisms. *Toxicol. Sci. 117*, 63-71.

Shearer, J.J., Wold, E.A., Umbaugh, C.S., Lichti, C.F., Nilsson, C.L., Figueiredo, M.L. (2016). Inorganic arsenic related changes in the stromal tumor microenvironment in a prostate cancer cell-conditioned media model. *Environ. Health Perspect. 124*, 1009-1015.

Stueckle, T.A., Lu, Y., Davis, M.E., Wang, L., Jiang, B.-H., Holaskova, I, Schafer, R., Barnett, J.B., Rojanasakul, Y. (2012). Chronic occupational exposure to arsenic induces carcinogenic gene signaling networks and neoplastic transformation in human lung epithelial cells. *Toxicol. Appl. Pharmacol. 261*, 204-216.

Styblo, M., Del Razo, L.M., Vega, L., Germolec, D.R., LeCluyse, E.L., Hamilton, G.A., Reed, W., Wang, C., Cullen, W.R., Thomas, D.J. (2000). Comparative toxicity of trivalent and pentavalent inorganic and methylated arsenicals in rat and human cells*. Arch. Toxicol. 74*, 289-299.

Thomas, D.J., Li, J., Waters, S.B., Xing, W., Adair, B.M., Drobna, Z., Devesa, V., Styblo, M. (2007). Arsenic (+3 oxidation state) methyltransferase and the methylation of arsenicals. *Exp. Biol. Med. (Maywood). 232*, 3-13.

Tokar, E.J., Kojima, C., Waalkes, M.P. (2014). Methylarsonous acid causes oxidative DNA damage in cells independent of the ability to biomethylate inorganic arsenic. *Arch. Toxicol. 88*, 249-261.

Treas, J., Tyagi, T., Singh, K.P. (2013). Chronic exposure to arsenic, estrogen, and their combination causes increased growth and transformation in human prostate epithelial cells potentially by hypermethylation-mediated silencing of MLH1. *Prostate. 73*, 1660-1672.

Vahter, M. (2002). Mechanisms of arsenic biotransformation. *Toxicology 181-182*, 211-217.

Watanabe, T., Hirano, S. (2013). Metabolism of arsenic and its toxicological relevance. *Arch. Toxicol. 87*, 969-979.

Waters, S.B., Devesa, V., Del Razo, L.M., Styblo, M., Thomas, D.J. (2004). Endogenous reductants support the catalytic function of recombinant rat cyt19, an arsenic methyltransferase. *Chem. Res. Toxicol. 17*, 404-409.

Wen, G., Calaf, G.M., Partridge, M.A., Echiburú-Chau, C., Zhao, Y., Huang, S., Chai, Y., Li, B., Hu, B., Hei, T.K. (2008). Neoplastic transformation of human small airway epithelial cells induced by arsenic. *Mol. Med. 14*, 2-10.

Xu, Y., Zhao, Y., Xu, W., Luo, F., Wang, B., Li, Y., Pang, Y., Liu, Q. (2013). Involvement of HIF-2α-mediated inflammation in arsenite-induced transformation of human bronchial epithelial cells. *Toxicol. Appl. Pharmacol. 272*, 542-550.

Xu, Y., Tokar, E.J., Waalkes, M.P. (2014). Arsenic-induced cancer cell phenotype in human breast epithelia is estrogen receptor-independent but involves aromatase activation. *Arch. Toxicol. 88*, 263-274.

Yamauchi, H., Aminaka, Y., Yoshida, K., Sun, G., Pi, J., Waalkes, M.P. (2004). Evaluation of DNA damage in patients with arsenic poisoning: urinary 8-hydroxydeoxyguanine. *Toxicol. Appl. Pharmacol. 198*, 291-296.

3.2. Chapter 2 (Study 2)

FRA1 is essential for the maintenance of the oncogenic phenotype induced by *in vitro* long-term arsenic exposure

Metallomics, Advanced article

Doi: 10.1039/d0mt00209g

This chapter is a verbatim reproduction from the following published paper:

Barguilla, I., Bach, J., Peremartí, J., Marcos, R., Hernández, A. (2020) FRA1 is essential for the maintenance of the oncogenic phenotype induced by *in vitro* long-term arsenic exposure. *Metallomics*, Advanced Article.

FRA1 is essential for the maintenance of the oncogenic phenotype induced by *in vitro* long-term arsenic exposure

Irene Barguilla[1], Jordi Bach[1], Jana Peremartí[1], Ricard Marcos[1,2,§], Alba Hernández[1,2,§]

[1]Group of Mutagenesis, Department of Genetics and Microbiology, Faculty of Biosciences, Universitat Autònoma de Barcelona, Cerdanyola del Vallès (Barcelona), Spain; [2]Consortium for Biomedical Research in Epidemiology and Public Health (CIBERESP), Carlos III Institute of Health, Madrid, Spain.

[§]Corresponding authors at: Group of Mutagenesis, Department of Genetics and Microbiology, Universitat Autònoma de Barcelona, Edifici Cn, Campus de Bellaterra, 08193 Cerdanyola del Vallès (Barcelona), Spain.

E-mail: alba.hernandez@uab.es (A. Hernández)

ricard.marcos@uab.es (R. Marcos)

Running title: *Role of FRA1* in arsenic carcinogenesis

ABSTRACT

Arsenic induces oncogenic effects activating stress-related signaling pathways. This can result in the over-activation of the AP-1 protein, specifically its FRA1 component. FRA1 is a transcription factor frequently overexpressed in epithelial tumors, where it can regulate the expression of different target genes. Accordingly, FRA1 could play an essential role in the *in vitro* cell transformation induced by arsenic. FRA1 levels were monitored in MEF cells throughout their transformation stages during 40-weeks long-term 2 μM arsenic exposure. Interestingly, results show a progressive FRA1 overexpression with time (60-fold and 11-fold for mRNA and pFRA/non-pFRA1, respectively, at week 40), which can be responsible for the observed altered expression in FRA1 downstream target genes *Pten*, *Pdcd4*, *Tpm1*, *Tgfb1*, *Tgfb2*, *Zeb1, Zeb2,* and *Twist*. The levels of MAPKs (ERK, p38, and JNK) and other known players upstream FRA1 were assessed at equivalent time-points, and ERK, p38 and RAS are pinpointed as potential candidates involved in arsenic-induced FRA1 activation. Further, FRA1 stable knockdown under chronic arsenic exposure settings elicits a remarkable impact on the features relative to cells' oncogenic phenotype. Notably, FRA1 knockdown cells present a 30% diminished proliferation rate, a 50% lowered migration and invasion potential, a 50% reduction in senescence, and a 30-60% reduced tumorsphere-forming ability. This work is the first to demonstrate the important role of FRA1 in the development and aggressiveness of the *in vitro* transformed phenotype induced by long-term arsenic exposure.

Keywords: Arsenic, AP1, FRA1 knockdown, long-term exposure, oncogenic transformation, tumorspheres

3.2.1. BRACKGROUND

Environmental and occupational exposures to arsenic are well known as hazardous for human health. In fact, this widely spread environmental contaminant has been classified by the IARC as a carcinogenic and genotoxic compound to humans (Group 1). Consequently, arsenic exposure is associated with a broad number of health effects, including an increased risk of skin, lung, bladder, liver, kidney, and prostate cancer development (Naujokas et al., 2013). Despite the evident threat that chronic arsenic exposure poses to human health, the underlying mechanisms of action of this compound have not been fully described (Tam et al., 2020; Zhu and Costa, 2020).

Arsenic is known to induce high levels of cellular stress through increased reactive oxygen species production, coupled with altered stress-response signaling pathways function (Qian et al., 2003; Flora, 2011). The activation of transcription factors such as NF-κβ or Nrf2 in cells exposed to sub-cytotoxic doses of arsenic is considered one of the mechanisms altering the expression of early stress-response genes (Druwe and Vaillantcourt, 2010). In this direction, the activator protein 1 (AP-1) is a transcription factor regulated by physical or chemical stressors, able to induce activation of mitogen-activated protein kinase (MAPK) cascades that, eventually, phosphorylate its different target substrates (Casalino et al., 2007; Dhillon and Tulchinsky, 2015). As a result, AP-1 can control the expression of different genes, including some involved in cell proliferation (TGFβ, Cyclin D1), differentiation (p38, Involucrin), invasion (MMP-1, MMP-9), and apoptosis (FasL, Bim, Bcl3) (Shaulian & Karin, 2002; Verde et al., 2007). Having such a broad range of regulatory functions and targets, alterations in AP-1 could lead to altered cellular processes related to tumor initiation or progression due to cell fate deregulation (Jiang et al., 2020). In fact, AP-1 has been classically linked to cancer and neoplastic transformation ever since the first representative members of the Jun and Fos gene family were shown to be cellular homologs of viral oncogenes (Curran and Franza, 1988).

AP-1 is formed by different dimeric pairs as a result of the combination of proteins from three subfamilies: including Jun (c-Jun, JunB, and Jun D), Fos (c-Fos, Fos B, FRA1, FRA2), and ATF (ATF-2, ATF-3, B-ATF) (Shaulian & Karin, 2002; Verde et al., 2007). The Fos-related antigen 1 (FRA1) subunit is frequently overexpressed in epithelial cancers. Its ability to cross-talk with TGFβ signaling (Diesch et al., 2014), to modulate the expression of epithelial-mesenchymal transition (EMT) transcription factors (Dhillon and Tulchinsky, 2015; Bakiri et al., 2015), and its involvement in tumor microenvironment development (Diesch et al., 2014; Luo et al., 2010), convert FRA1 in a central regulator

of many signaling and transcription networks that coordinate gene expression changes during tumor promotion. Until now, few studies have explored the possible relationship between arsenic exposure and AP-1/FRA1 activation. Only short and mid-term studies have shown a correlation between arsenic exposure and increased levels of active MAPKs that can eventually lead to AP-1 induction (Huang et al., 1999; Kim et al., 2016), while long-term studies have focused on MAPKs as the endpoint to explain arsenic-induced transformation (Person et al., 2015).

Our group has previously described that environmentally relevant chronic exposure to low non-cytotoxic doses of arsenic (0.5 to 2 μM) leads to carcinogenesis in cells with different genetic backgrounds. Thus, mouse embryonic fibroblasts (MEF) either sensitive or resistant to oxidative DNA damage showed features of oncogenic transformation after 20-30 weeks of chronic arsenic exposure, including morphological changes, increased proliferation, deregulation of differentiation status, and a secretome with increased levels of MMPs able to enhance tumor effects of epithelial cells such as growth and invasiveness, all at levels known to induce malignant xenograft tumors in mice (Bach et al., 2016). Thus, in the present study we have evaluated the importance of FRA1 in the above-mentioned arsenic-induced transformation context, this in MEF cells at different time-points during the transformation process. This is the first study describing a link between FRA1 overexpression and the development of cancer-like features in response to chronic arsenic exposure.

3.2.2. MATERIALS AND METHODS

3.2.2.1. Culture conditions and in vitro arsenic exposure

A bank of MEF cells phenotypically sensitive to oxidative damage and previously transformed by 20-30 weeks of continuous sodium arsenite (As^{III}; Sigma-Aldrich, MO, USA) exposure (0.5, 1, and 2 μM) (Bach et al., 2016) was used in this study. Representative time-points of the transformation process were considered, this are 0, 10, 20, 30, and 40 weeks of exposure. Cells were maintained in three separate T-75 flasks for each time-point. Cells were grown in Dulbecco's modified Eagle's medium (DMEM)/F12 medium (Life Technologies, NY, USA) supplemented with 10% foetal bovine serum (Biowest, France) and 2.5 μg/mL Plasmocin (InvivoGen, CA, USA) in a humidified atmosphere of 5% CO_2 and 95% air at 37 ºC. It should be pointed out that corresponding passage-matched controls were in all cases included for comparisons.

For the As^{III} treatments, a stock solution was prepared at a concentration of 10 mM in PBS (pH 7.4), then filtered, aliquoted and frozen until use.

3.2.2.2. Chemical inhibitors

PHA-665752 (ERK inhibitor) and SB203580 (p38 inhibitor) (Selleckchem, TX, USA) were dissolved in DMSO at the concentration of 10 mM.

3.2.2.3. Total RNA extraction and real-time RT-PCR

Total RNA from MEF, at different time points of the As^{III} chronic exposure, was extracted using TRI® Reagent (Sigma-Aldrich, MO, USA) following the manufacturer's instructions. The RNase-free DNase I (Turbo DNA-free Kit; Invitrogen, CA, USA) was used to remove DNA contamination. The reverse transcriptase step was performed using 1 µg of total RNA, and the high-capacity RNA-to-cDNA Kit (Applied Biosystems, CA, USA) based on the use of oligo d(T) primers. Real-time PCR analysis was performed on a LightCycler 480 to assess the relative expression of the target genes. *Actb* expression was used as a housekeeping control. Each 20 µL of reaction volume contained 5 µL of cDNA, 10 µL of 2X LightCycler 480 SYBR Green I Master (Roche, Manheim, Germany), 3 µL of H_2O, and 1 µL of each primer pairs at a final concentration of 500 nM. The target genes and the primer sequences are listed in Supplementary Table 1. The cycling parameters for the reaction were: 95 °C for 5 min, 45 cycles of 95 °C for 10 s, 61 °C for 15 s and 72 °C for 25 s. Cycle time (Ct) values were calculated with the LightCycler software package and then normalized with *Actb* data.

3.2.2.4. Total protein extraction and Western blot (WB)

MEFs from different exposure time-points were seeded, harvested, and homogenized in RIPA lysis buffer. The cell extracts were sonicated for 15 s at 10% amplitude on ice, and further incubated with 25 U of benzonase (EMD Chemicals Inc., CA). Total protein concentration was measured spectrophotometrically with the Bio-Rad Protein Assay (Bio-Rad, CA) following the manufacturer's instructions. 50 µg of total protein were separated on a 12% SDS/PAGE gel and blotted onto polyvinylidene difluoride (PVDF) membranes. After blocking the nonspecific binding sites for 1 h with 5% non-fat milk in Tris-buffered saline (TTBS), the membranes were incubated overnight at 4 ºC with the primary monoclonal antibodies of interest, listed in Supplementary Table 2. Then, the membranes were subjected to three 10-min washes with TTBS and incubated with the appropriate horseradish peroxidase (HRP)-conjugated secondary antibody at a 1:1000 dilution for 1 h at room temperature. The membranes were then washed three times with

TTBS and developed using an enhanced chemi-luminescence system (Millipore, MA). Before incubating the membrane with a different primary antibody, HRP was inactivated by adding 1% sodium azide in the 5% non-fat milk blocking solution, and following the subsequent steps as described above. Images of the membranes were captured with a GeneGnome imaging system (Syngene Cambridge, UK), and the relative quantification of protein expression was carried out using the analysis software Genome Tools (Syngene, Cambridge, UK).

3.2.2.5. Short hairpin RNA (shRNA) and lentiviral particle production

MISSION® constructs carrying shRNA sequences targeting mouse gene *Fra1*, and the control empty plasmid (pLKO.1) were purchased from Sigma-Aldrich (St Louis, MO, USA). The shRNA sequence for *Fra1* knock-down was: (CCGGCCAGTGCCTTGCATCTCCCTTCTCGAGAAGGGAGATGCAAGGCACTGGTTTTTG). A maxiprep (Macherey-Nagel, Düren, Germany) was carried out following the manufacturer's protocol, to obtain the plasmids at the desired concentration. Lentiviral transduction particles were produced by transfecting HEK293 cells either with the control empty plasmids or the *Fra1* shRNA-carrying one together with envelope (ENV) and packaging (PAX) plasmids They were kindly provided by Dr. M. Bogliolo (Group of Genomic Instability, UAB). Briefly, after 24 h of growth, cells at 80% confluency were transfected with the plasmids: shRNA-carrying or control plasmid (10 µg), PAX (6.5 µg), and ENV (3.5 µg). The next day, the medium was aspirated, and fresh medium was added. In the following two days, the medium was collected and centrifuged in Amicon Ultra-15 centrifugal filter units (Merck, Darmstadt, Germany) for 1 h at 3000 rpm and 4 ºC. The concentrated medium containing the lentiviral particles was collected and stored at -80 ºC.

3.2.2.6. Cell transduction

MEF cells showing different transformed features were selected from the As^{III}-chronic exposure. Cells from weeks 10, 30, and 40 of exposure (corresponding to non-transformed and transformed cells, and cells after the transformation point), were seeded at 25% confluence and transduced with lentiviral particles carrying either *Fra1* shRNA or the control empty vector. After two days, the medium was changed and a fresh medium with puromycin (10 µg/mL) was added for vector-expressing cells selection. To test the efficiency of *Fra1* knockdown, the cells were subjected to RNA extraction and real-time PCR analysis.

3.2.2.7. Cell population doubling time

Changes in the cell's proliferation rate due to the transformation process, or to *Fra1* inhibition, were evaluated tracking the time required for the cultured population to double in number. Non-transformed, transformed, and *Fra1* knockdown transformed cells, were seeded in 6-well plates. The total number of cells for each condition was evaluated with a ZTM Series coulter-counter (Beckman Coulter Inc., CA) for the following 72 h. The population doubling time was calculated as $PD = T*log(2)/log(fn) – log(in)$, where *in* is the initial number of cells and *fn* the final number of cells at each passage, and T is the time in hours.

3.2.2.8. Soft-agar assay

Colony formation in soft-agar was performed in As^{III}-transformed MEFs, expressing either the control empty vector or the *Fra1* shRNA, to assess the cells' anchorage-independent growth potential. MEF cells were collected and filtered through a 40-µm mesh, to obtain single-cell suspensions. Subsequently, a suspension of 65,000 cells in 1.75 mL of DMEM containing 10% of FBS and 2.5 µg/mL Plasmocin was prepared and mixed in a 1:1:1 ratio with 2x DMEM containing 20% of FBS, 2% NEEA, 2% L-Glu 200 mM and 2% penicillin-streptomycin and with 1.2% of bacto-agar (DIFCO, MD, USA). This mixture was enough to prepare triplicates of 20,000 cells each by dispensing 1.5 mL over a 0.6% base agar (supplemented with 2x DMEM) in each well of a 6-well plate. The plates were sitting for 45 min and then, kept in the incubator for 21 days. The cells able to form colonies were stained by a 24-h incubation with 1 mg/mL of (2-p-iodophenyl)-3-3(p-nitrophenyl)-5-phenyl tetrazolium chloride (INT; Sigma, MO, USA). Then, the plates were scanned with an HP Scanjet G4050, and the colonies were counted using the colony cell counter enumerator software OpenCFU (3.9.0).

3.2.2.9. Cell migration and invasion assays

The invasive potential, of both As^{III}-transformed control and *Fra1* knockdown MEFs, was evaluated performing direct migration and invasion assays. To carry out the invasion assay, cells at 80% confluence were deprived of FBS for 24 h. The day of the assay, a 180 µL 1:2 dilution of Matrigel® (Costar-Corning, NY, USA) in FBS free DMEM/F12 with 0.1% BSA was used to coat each 8-µm pore size polycarbonate membrane 24 mm transwell insert (Costar-Corning, NY, USA). The Matrigel® mixture was left to sit and dry for 1 h in the cell incubator at 37 ºC. The bottom chamber of the transwell inserts was filled with 2.5 mL DMEM/F12 complemented with 15% FBS as the chemoattractant medium. A single-cell suspension containing 600,000 FBS-deprived MEF cells in 1.5 mL

of FBS free DMEM/F12 with 0.1% BSA was added on top of the transwell Matrigel®-coated membrane. Cells were then allowed to invade for 48 h at 37 °C. Invading cells in the bottom chamber were photographed with a Zeiss Observer A1 microscope before being collected by trypsinization and counted using a Beckman Coulter cell counter. A modified version of the assay was performed to evaluate cell migration. The main steps were followed as described above; however, the cells were seeded on the top of the transwell without the Matrigel® coating.

3.2.2.10. Senescence detection

The number of senescent cells in the cell culture was assessed with the Senescence Detection Kit (ab65351, Abcam) following the manufacturer's instructions. Briefly, sub-confluent cells were fixed, and X-gal was added as a substrate. Thus, the SA-B-Gal activity, only present in senescent cells, can be observed after the addition of a staining solution for a qualitative analysis of senescence. Images of the senescent cells in the population were captured with a Zeiss Observer A1 microscope.

3.2.2.11. Tumorsphere formation assay

MEF cells were seeded at a density of 2,500 cells/mL in 96-well ultra-low-attachment plates (Corning, Costar-Corning, NY, USA) in serum-free DMEM/F12 supplemented with B27, 20 ng/mL basic fibroblast growth factor (bFGF) (both from Life Technologies, NY, USA), epithelial growth factor, and 4 µg/mL heparin (both from Sigma-Aldrich, Germany). After 6 days of incubation in a humidified atmosphere with 5% CO_2 and 95% air at 37 ºC, the tumorspheres were counted and photographed. Tumorspheres' size was assessed using ImageJ software.

3.2.2.12. Statistics

Unpaired Student's *t*-test, or analysis of variance followed by Dunn's multiple comparison test, as appropriate, were performed to compare As^{III}-treated cells with untreated time-matched controls at respective time points, transformed with non-transformed MEFs or *Fra1* knockdown cells with control vector-carrying ones. In all cases, a two-sided $P < 0.05$ was considered statistically significant.

3.2.3. RESULTS

3.2.3.1. FRA1 is overexpressed in arsenic-transformed cells

We observed a tendency towards a dose-dependent overexpression of *Fra1* in MEFs transformed cells exposed to environmentally relevant non-cytotoxic doses of As^{III} (0.5, 1, and 2 μM) for 40 weeks, being that of the 2 μM As^{III}-exposed cells 2.7-fold when compared to that of time-matched controls (Figure 1A). Moreover, when the effect of the highest selected dose (2 μM As^{III}) was analysed through the transformation process, we found a progressive increase in FRA1 levels throughout the weeks of exposure, both at RNA (Figure 1B) and protein levels (Figure 1C). Thus, the RNA levels of FRA1 transcript at the transformation point (20-30 weeks) is 3.7-fold when compared with time-matched controls (P<0.001), and the relevant ratio p-FRA versus non-p-FRA1 reach a >8-fold increase from the point of transformation.

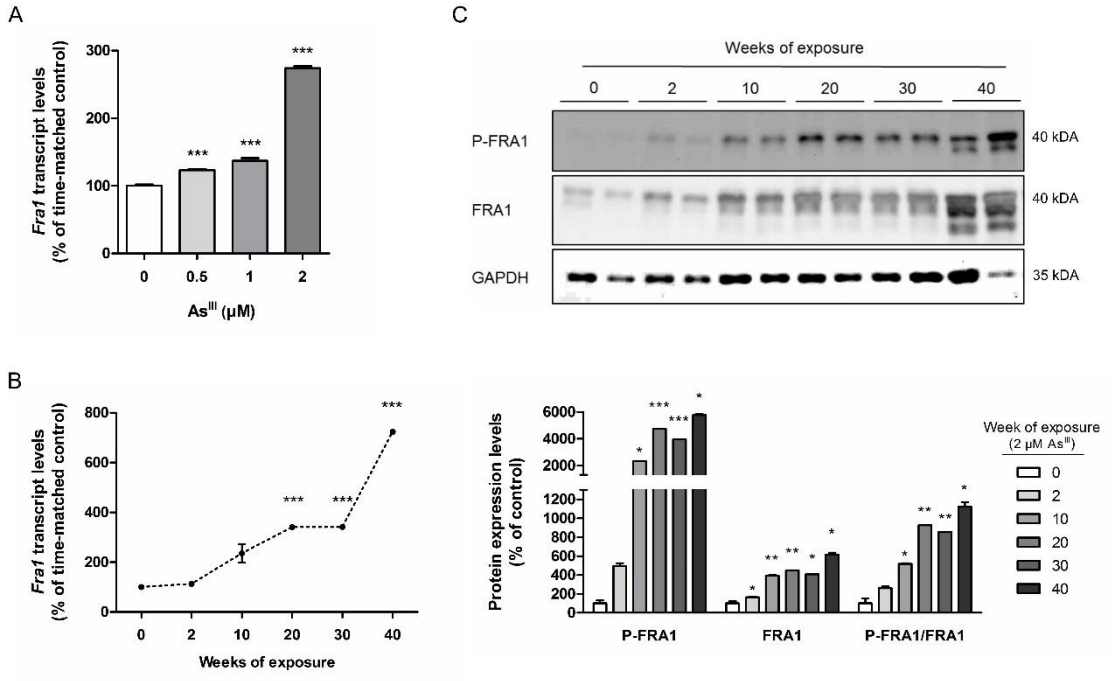

Figure 1: Variations in FRA1 levels during chronic arsenic exposure. Arsenic causes a dose **(A)** and time-dependent **(B)** increase of FRA1 mRNA expression, confirmed at a protein level by the representative western blot and quantification **(C)** of the phosphorylated and total forms of FRA1 along with the long-term AsIII exposure. Data are presented as mean values of independent experiments (n=3). Error bars represent the standard error of the mean. **P* < 0.05, ***P* < 0.01, ****P* < 0.001, compared to passage-matched controls or cells from the starting point of the chronic exposure (One-way ANOVA and Dunn's multiple comparisons test).

3.2.3.2. Arsenic-related FRA1 overexpression is MAPKs dependent

Given the known relevance of FRA1 activation and stabilization by MAPKs-induced phosphorylation (Xiang et al., 2020), we evaluated the levels of basal and active MAPKs during arsenic chronic exposure. A statistically significant increase in both phosphorylated and total levels of p38 (Figure 2B; 6 to 15-fold from the transformation point), and in P-ERK (Figure 2A; 5 to 6-fold from the transformation point), were observed, correlating with the FRA1 phosphorylation pattern. Conversely, JNK and PJNK levels remained unchanged or decreased (Figure 2C).

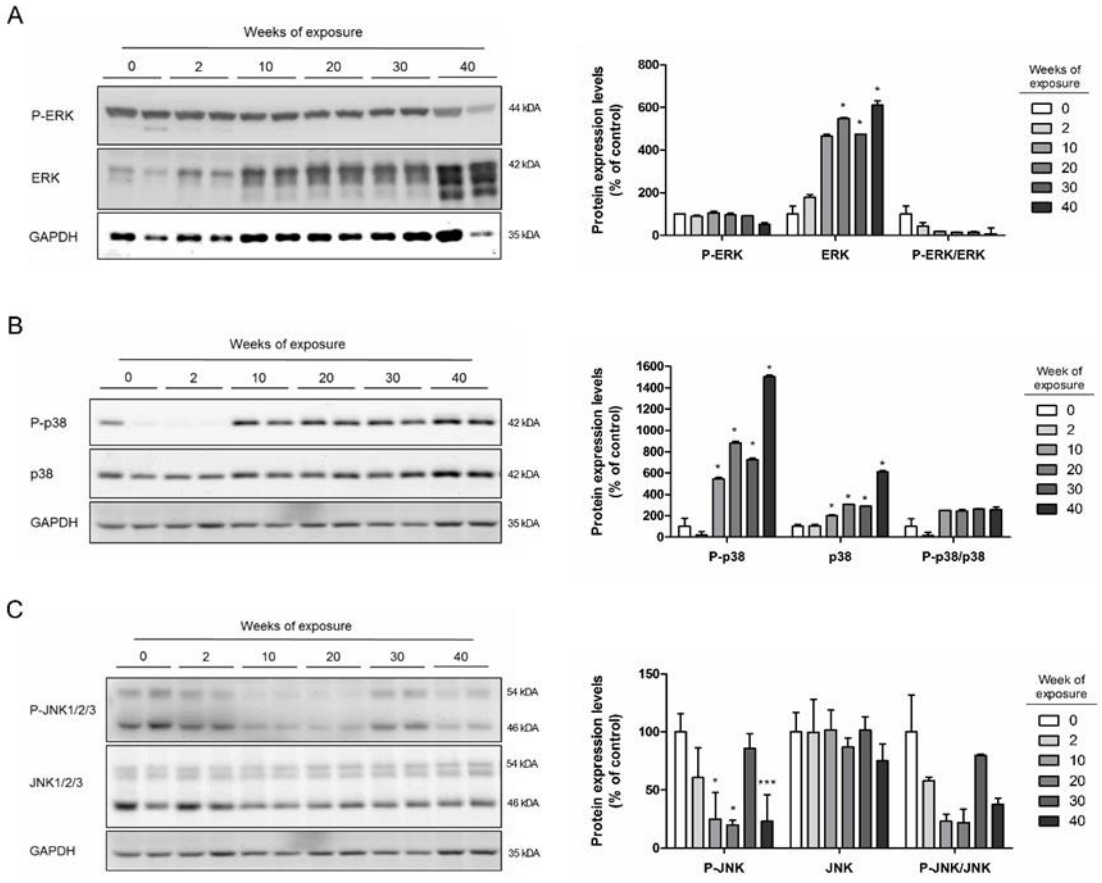

Figure 2: Evaluation of MAPKs levels at different time-points of arsenic chronic exposure. The western blot pictures and their quantification show the arsenic-induced variation in phosphorylated and total ERK **(A)**, p38 **(B),** and JNK **(C)** levels**.** Quantification was performed both normalizing against GAPDH and with the phosho/total ratio to evaluate the effects of As^{III} exposure in the protein expression and activation levels, respectively. Data shown are representative results from independent experiments (n=3). Error bars represent the standard error of the mean. **P* < 0.05, ****P* < 0.001 compared to the initial week of the long-term exposure set at 100% (One-way ANOVA test and Dunn's multiple comparisons test).

Thus, to confirm the involvement of p38 and ERK in the arsenic induced FRA1 activation, the effect of different MAPKs' chemical inhibitors over FRA1 protein levels were assessed at the point of maximum expression. PHA-665752, an ERK-related pathway

inhibitor, induced a close to 50% reduction in the P-ERK levels after 1 h of exposure, being able to significantly reduce P-FRA1 levels to 40% (Figure 3A). Similarly, SB203580 reduced both P-FRA1 and FRA1 by 40% in the cells after 1 h of exposure, via 60% p38 activity inhibition (Figure 3B). These results indicate a potential arsenic-related alteration of ERK and p38 signaling pathways, which could eventually lead to the changes in FRA1 activation observed during chronic As^{III} exposure.

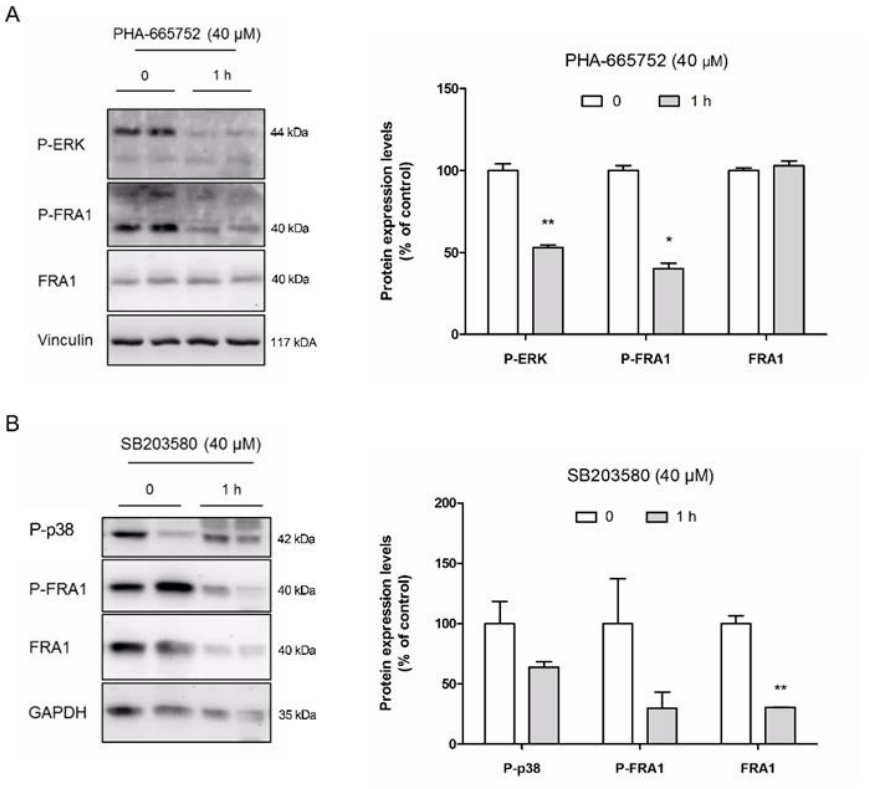

Figure 3: Effects in FRA1 expression after a transitory inhibition of MAPKs activity. Western blot quantification of the effects of a 1-hour-exposure to ERK inhibitor PHA-665752 show decreased levels of phosphorylated ERK and FRA1 active phosphorylated form when compared to those before the treatment **(A)**. The downregulation mediated by the short-term exposure to p38 inhibitor SB203580 leads to a marked reduction of phospho-p38, and both phospho- and total FRA1 levels compared to time 0 **(B)**. These assessments were performed in FRA1-overexpressing MEFs at the transformation point, reached after the continuous 30-week arsenic exposure. The data presented are a representative example of independent experiments (n=3). Error bars represent the standard error of the mean. **P* < 0.05, ***P* < 0.01 compared to the first measuring time-point set at 100% (Unpaired Student's t-test).

3.2.3.3. RAS involvement in the arsenic induced FRA1 activation pathway

The regulation of FRA1 expression has been linked to different MAPKs-activating pathways, such as cMET, RAS, and EGFR-related signaling, among others (Li et al., 2018). Therefore, we have explored the alterations in RAS and cMET expressions in arsenic chronically exposed cells before the transformation point, at the transformation

point, and after the transformation point. A progressive upregulation of RAS over the transformation process was observed (Figure 4A; 2-fold increase in transformed cells and 4.5-fold increase in post-transformed cells, when compared to that of non-transformed cells) while cMET levels decreased (Figure 4B), indicating the rather relevant role of RAS in arsenic-related carcinogenesis.

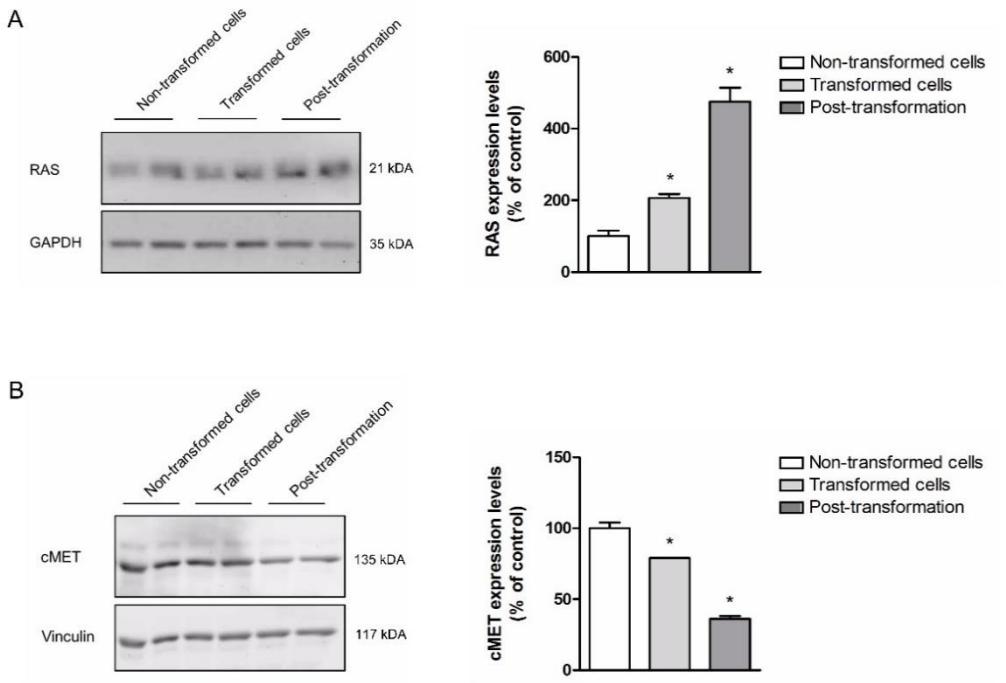

Figure 4: RAS and cMET levels at different points during the arsenic-induced transformation process. The WB analysis and quantification of RAS shows its overexpression along the process of the acquisition of the tumoral phenotype **(A)** while cMET protein levels follow the opposite trend **(B)**. Data are presented as mean values of independent experiments (n=3). Error bars represent the standard error of the mean. *$P < 0.05$, compared to non-transformed cells set at 100% (One-way ANOVA and Dunn's multiple comparisons test).

3.2.3.4. FRA1 target genes are altered during the arsenic chronic exposure

It has been described how increased FRA1 activity can regulate the expression of many different target genes, including those related to the development of a transformed cellular phenotype and further aggressive features.

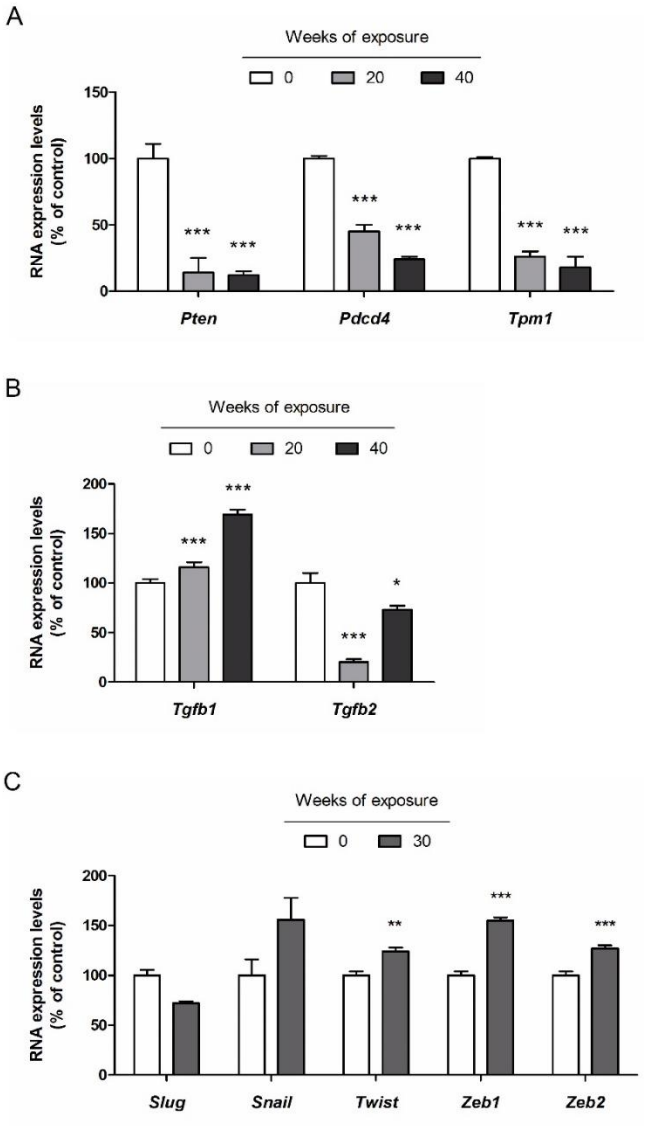

Figure 5: Arsenic-induced alteration of FRA1 target genes relevant for carcinogenesis. Tumor suppressor genes **(A)**, TGFβ components **(B),** and EMT-TFs **(C)** coding genes mRNA levels shift significantly at different time-points during the chronic As^{III} exposure. Displayed data show the mean values of independent experiments (n=3). Error bars represent the standard error of the mean. *P < 0.05, **P < 0.01, ***P < 0.001, compared to cells from the starting point of the chronic exposure set at 100% (One-way ANOVA and Dunn's multiple comparisons test (A, B); Unpaired Student's t-test (C))

Thus, FRA1 activity leads to the reduction of various tumor suppressor genes such as *Pten*, *Pdcd4,* and *Tpm1*. When the expression of these genes was evaluated, a significant decrease over the weeks of chronic arsenic exposure was observed (Figure 5A; less than 20%, 40% and 25% expression for *Pten*, *Pdcd4,* and *Tpm1,* respectively, when compared to controls). *Tgfb1* and *Tgfb2* genes, known for their tumor-promoting and suppressing dual function, are also FRA1 targets. The significant 120 to 170% increase in the expression of *Tgfb1* and the significant 20 to 70% downregulation of *Tgfb2* levels (Figure 5B), together with the above-mentioned reduction of the tumor suppressors expression during the long-term arsenic exposure suggest that, at least partially, the mechanisms for arsenic to induce cell transformation depend on the As^{III}-induced FRA1 overexpression. Moreover, we analyzed the variations in EMT-related genes, also known to be regulated by the FRA1 transcription factor. While *Slug*

expression did not vary significantly after a 30-week-exposure, increased levels of *Snail*, *Twist*, *Zeb1,* and *Zeb2* at the transformation point were observed (120%, 150%, and 130%, respectively), when compared to those at the beginning of the exposure (Figure 5C). These results show that FRA1 upregulation in response to chronic arsenic exposure contributes to the deregulation of some of the many different AP-1 target genes that can promote the acquisition of tumoral phenotypical features.

3.2.3.5. Involvement of FRA1 in the progression of an aggressive transformed phenotype

At a functional level, the observed arsenic induced FRA1 upregulation could play an important role in the progression of an aggressive transformed phenotype. To evaluate this endpoint, we performed a stable *Fra1* knockdown by shRNA in MEF cells after 10, 30, and 40 weeks of continuous arsenic exposure with a 57%, 43%, and 51% of inhibition rate, respectively ($P \leq 0.05$ in all cases). After confirming that the growth rate of the knockdown cells was not affected, a battery of different oncogenic features were analyzed in order to define variations in the transformation status of the 30-week-exposed *Fra1*-expressing MEFs in comparison with that of *Fra1*-deficient cells. Interestingly, we observed that the >2-fold increase in the population proliferation at 72 h, found in transformed cells, was restored in knockdown MEFs and became equivalent to that of the non-transformed (Figure 6A). Thus, while non-transformed and knockdown cells presented a doubling time of 15.31 and 13.97 h, respectively, the transformed cells were able to double their population in 10.56 h. Moreover, transformed *Fra1* shRNA-carrying cells exhibited a 20% reduced ability to form colonies in the soft-agar assay (Figures 6B and C), and their migrating (Figure 6D), and invading potential (Figure 6E) was reduced by 50%, when compared with their control vector-expressing counterparts. Regarding the senescence evaluation in the cultured cells, we observed a 50% lower number of senescent cells in the knockdown population than in the *Fra1*-expressing MEFs (Figure 6F). This suggests that FRA1 overexpression contributes to the escape from senescence, as found in tumoral cells.

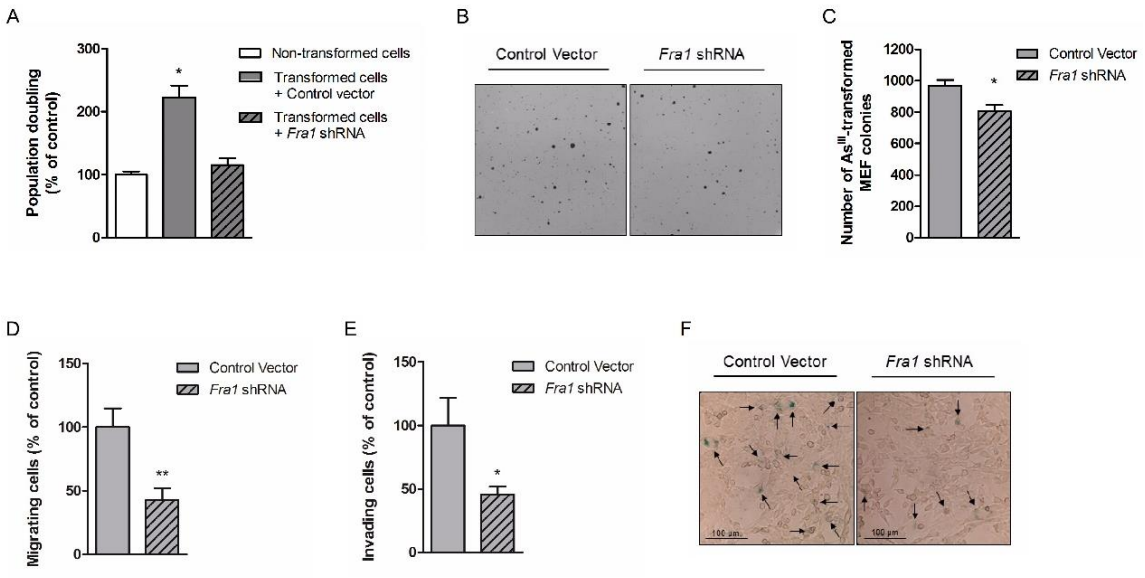

Figure 6: Importance of FRA1 overexpression in the development of an aggressive tumoral phenotype. Proliferation rate **(A)**, the anchorage independent cell growth capacity **(B, C),** and the assessment of the migrating **(D)** and invading potential **(E)** of cells show a reduction of the aggressive features of arsenic-transformed FRA1 knock-down cells compared with the control vector carrying counterparts. **(F)** The representative picture of senescent cells shows a reduction in the number of senescent cells in the knockdown cells population. Quantified data are presented as representative results of independent experiments (n=3). Error bars represent the standard error of the mean. **P* < 0.05, ***P* < 0.01, compared to non-transformed cells set at 100% (A) or control vector-carrying cells (C, D, E) (Unpaired Student's t-test (A, C, D, E)).

The ability of cells to grow as tumorspheres was tested in both control and *Fra1* knockdown cells from the selected time-points during the arsenic chronic exposure: 10, 30, and 40 weeks of exposure. We observed a drastic change in the tumorspheres' size from non-transformed cells at the early stages of the exposure, compared with the close to 3- or 4-fold bigger spheres observed from MEFs at later stages of the transformation process (Figure 7A and B). It is also very relevant the comparison between the *Fra1* knockdown cells and the control vector-expressing ones, as *Fra1* inhibition leads to a significant decrease in the tumorspheres' size at all time-points studied, specially from the transformation point (Figure 7A and B; reduction in the tumorspheres diameter of 240 µm and 120 µm at the point of transformation and after the transformation point, respectively). Moreover, tumorspheres from cells past the transformation point were harvested, lysed, and protein extracts were obtained to perform a WB analysis on the FRA1 levels. We found that FRA1 is 5-fold overexpressed in tumorsphere-forming cells, compared with its presence in adherent cells from the same time of exposure (Figure 7C and D). Therefore, FRA1 enrichment in tumoral cells may be a sign not only of the development of a more aggressive phenotype but also of the acquisition of stem cell-like features in response to long-term arsenic exposure.

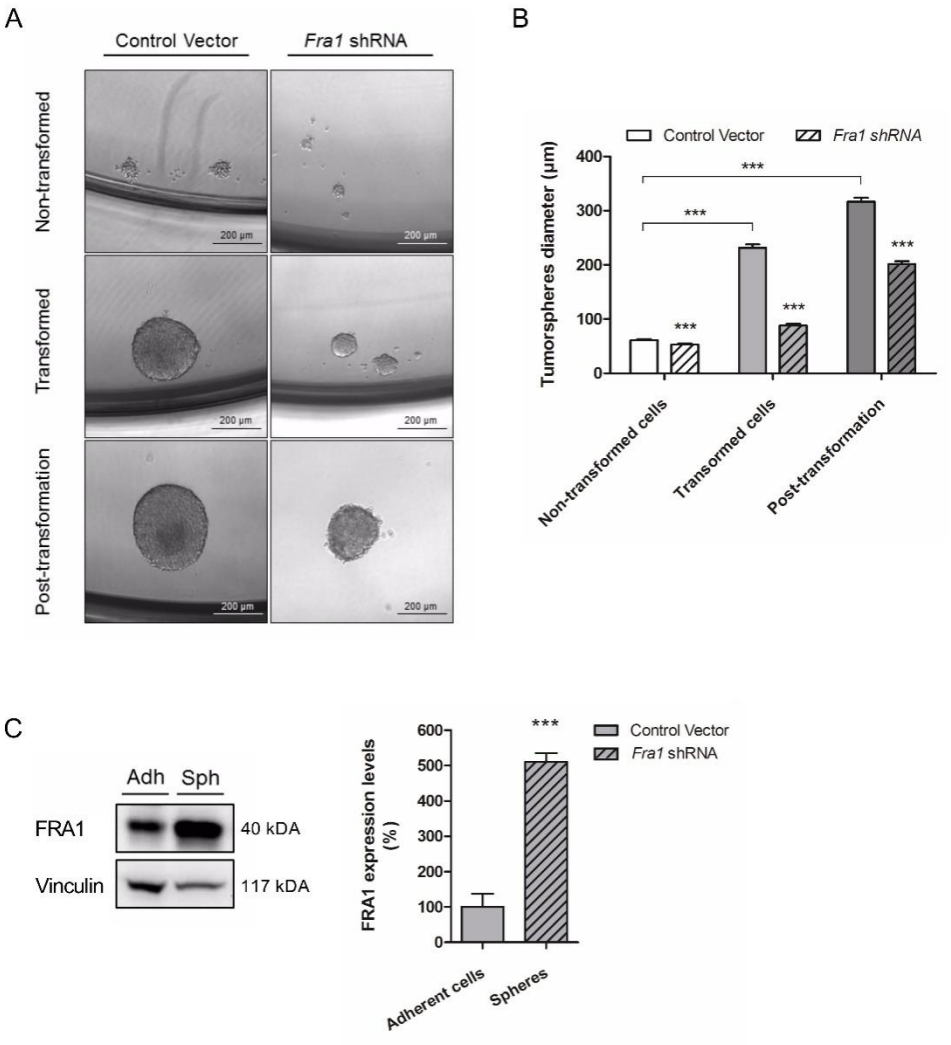

Figure 7: Involvement of FRA1 in stem-cell-like features development. The tumorspheres formed by the arsenic-exposed cells are significantly bigger as the cells acquire a more transformed state. This increase drops in FRA1 shRNA-carrying cells **(A, B).** The analysis of FRA1 levels by western blot shows its significant upregulation in tumorspheres, compared to the adherent culture **(C)**. Quantified data show representative results of independent experiments (n=3). Error bars represent the standard error of the mean. **P* < 0.05, ****P* < 0.001 compared to non-transformed cells or the control vector carrying cells as appropriate (One-way ANOVA and Dunn's multiple comparisons test (B); Unpaired Student's t-test (C)).

3.2.4. DISCUSSION

Arsenic is a naturally occurring metalloid widely distributed throughout the Earth's crust. Human exposure to arsenic occurs primarily from the consumption of potable water containing high amounts of inorganic arsenic, as well as from the consumption of crops cultivated in arsenic-contaminated agricultural fields or irrigated with arsenic-containing water (Arslan et al., 2017). Therefore, human exposure to arsenic mainly occurs on a chronic basis, leading to a variety of adverse health effects (Naujokas et al., 2013; Khan et al., 2020), such as dermatological, developmental, neurological, respiratory (Siddique et al.; 2020), cardiovascular, immunological (Jamal et al., 2020; Zhao et al., 2020), endocrine effects and early-life effects (Song et al., 2020). Most remarkably, arsenic is a known carcinogen associated with skin, lung, bladder, kidney, and liver cancer (Palma et al., 2020), and new evidence links arsenic exposure with prostate, pancreatic (Wei et al., 2020) and breast (Marciniak, et al., 2020) cancers as well. Published research has demonstrated that several important molecular mechanisms are involved in arsenic-induced carcinogenesis (Tchounwou et al., 2019). However, despite the evidence, the mechanisms of arsenic-related hazardous effects remain only partially understood.

3.2.4.1. FRA1 overexpression during arsenic-induced transformation

Oxidative stress induction is one of the most explored mechanisms-of-action of this compound (Druwe and Vaillancourt, 2010). Previous studies with the MEF cells used in the present study have shown their sensitivity to arsenic-induced oxidative stress (Bach et al., 2014) which eventually leads to the genotoxic damage and chromosomal instability also observed by other authors (Bach et al., 2014; Paul et al., 2014). Cells under these stress conditions present altered signaling pathways, leading to changes in some of the major transcription factors' role in stress-related responses. Nrf2 is activated by short-term arsenic exposures showing a protective effect, although under long-term exposure conditions its induction can produce the over-activation of the genes downstream in its signaling pathway, leading to the onset of tumorigenesis (Hubaux et al., 2013; Schmidlin et al., 2020; Wang et al., 2018). In the same direction, increased expression of NF-kb in the presence of low doses of arsenic induce detrimental effects on the inflammatory response (Druwe and Vaillancourt, 2010). AP-1 is classified within the same category of stress-response proteins, as the previous examples, since it is involved in a wide variety of processes including the regulation of cell differentiation, survival, proliferation, migration, and transformation (Vesely et al., 2009). Few studies have analyzed AP-1 in the context of arsenic-related transformation. Among the most relevant, it has been reported that acute arsenite exposure leads to an increase in AP-1 transcriptional

activity, which protects bronchial epithelial cells from apoptosis (Aodengqimuge et al., 2014). Therefore, the sensitivity of AP-1 to arsenic exposure, and its relevant role in cell fate-regulating processes, makes this transcription factor an attractive target for more studies.

Linked to the above-mentioned oxidative stress and AP-1 signaling pathway activation, FRA1 is an interesting component in the context of cancer research. It is often overexpressed in different tumors such as squamous cell skin carcinoma (Zhang et al., 2016), glioma (Zhang et al., 2017), or breast cancer (Sundqvist et al., 2013; Gu et al., 2016), where it is mainly involved in the development of aggressive tumoral features by increasing the invasiveness potential of cells. Concordantly, we have observed that FRA1 can respond to increasing levels of As^{III} exposure, and that this activation escalates over time.

3.2.4.2. Involvement of FRA1 upstream activators during arsenic-induced transformation

We have explored the activation state of the FRA1 upstream MAPKs during 40 weeks of arsenic exposure, observing a correlating increase of ERK and p38 phosphorylation in a similar pattern to that of FRA1. Moreover, after a transient inhibition of these MAPKs' activity, FRA1 phosphorylation decreases accordingly. The observed involvement of ERK and p38 in FRA1 activation is reinforced by the fact that other authors have previously observed the ability of arsenic exposure of deregulating ERK (Person et al., 2015), p38 (Kim et al., 2016), and JNK activity (Dong, 2002). Continuing with the potential activators upstream FRA1, we then evaluated the levels of RAS and c-MET. RAS, because it is a well-described arsenic molecular target involved in the onset and maintenance of the tumoral phenotype in exposed cells (Ngalame et al., 2014; Zhou et al., 2018; Soza-Ried et al., 2019). c-MET, since it is a transformation driver found overexpressed after chronic arsenic trioxide exposure (Kryeziu et al., 2016), and able to stimulate FRA1 expression in the tumor microenvironment (Lau et al., 2016). While our observations indicate that the c-MET expression changes did not correlate with those of FRA1 and its upstream MAPKs in response to the exposure, RAS was found to be significantly overexpressed during and after the acquisition of a transformed phenotype, suggesting that arsenic interaction with RAS can eventually result in FRA1 induction.

3.2.4.3. Downstream FRA1 gene dysregulation during arsenic-induced transformation

Because of FRA1 stimulation, the regulation of many relevant genes for the development and progression of a transformed phenotype is altered. Tumor suppressor genes, usually highly expressed in non-transformed cells, are inhibited by the FRA1-induced miR-21 overexpression (Talotta et al., 2009). Therefore, the observed downregulation of *Pten*, *Pdcd4,* and *Tpm1* levels in our chronic arsenic-exposure model hints to the involvement of FRA1 in the transformation onset. All this supports the role of FRA1 as an oncogenic driver. Different studies have described the crosstalk between FRA1 transcription factor and the TGFβ signaling pathways, reporting that FRA1 can modulate TGFβ1 and TGFβ2 expression by directly binding to their promoters' regulatory regions (Diesch et al., 2014; Bakiri et al., 2015). TGFβ1 pathway is related to tumor suppression in the initial stages of carcinogenesis; however, once the tumor has developed, its function switches and becomes a tumor promoter, while TGFβ2 remains as a tumor suppressor (Levy and Hill 2006). Then, the progressive upregulation and the downregulation of *Tgfβ1* and *Tgfβ2*, respectively, during the chronic As^{III} exposure observed by us can be a consequence of the FRA1/TGFβ crosstalk, and lead to the further development of the transformed phenotype. Nonetheless, FRA1 is known in oncogenesis because of its tumor-promoting function through the regulation of epithelial-to-mesenchymal transition transcription factors (EMT-TFs) (Dhillon and Tulchinsky, 2015). The correlation of FRA1 overexpression with the altered levels of *Snail, Twist*, *Zeb1,* and *Zeb2* at the transformation point of the As^{III}-exposed cells supports the role of FRA1 in the acquisition of the arsenic-induced aggressive phenotype.

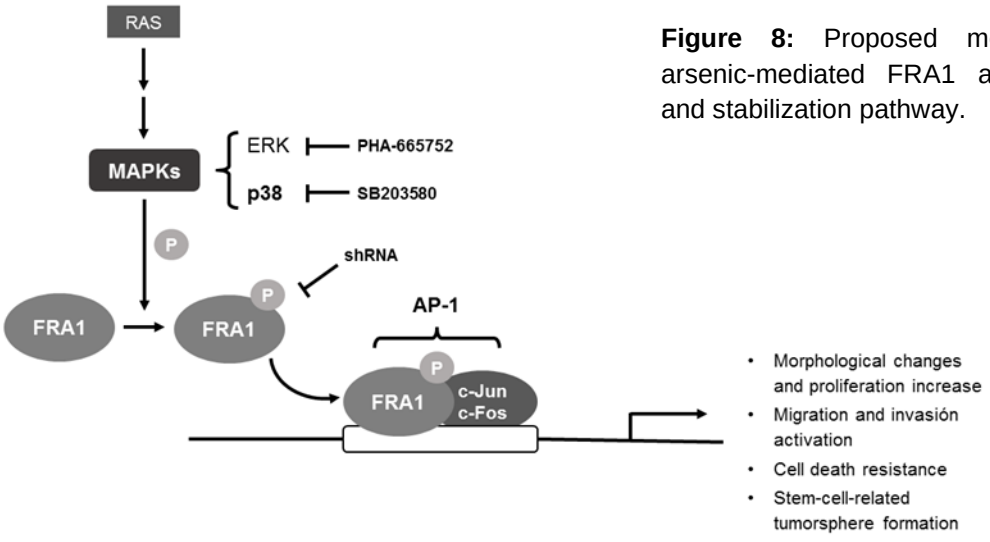

Figure 8: Proposed model of arsenic-mediated FRA1 activation and stabilization pathway.

3.2.4.4. Stable FRA1 knockdown impacts the arsenic-induced oncogenic phenotype

Remarkably, experiments on the stable inhibition of FRA1 show a significant decrease in the aggressiveness of the oncogenic phenotype induced by arsenic long-term exposure. Specifically, a marked reduction on the proliferation rate, anchorage-independent cell growth, migrating and invading potential has been observed, all accompanied by a reduced senescent status of the arsenic-exposed cells. Regarding this last point, the impact of arsenic in senescence has been recently pointed out by other authors under similar chronic exposure conditions (Chung et al., 2020). To further examine potential mechanisms of oncogenic transformation- we have evaluated the tumorsphere-forming ability of our transformed cells. The progressively bigger tumorspheres formed by MEFs cells in more advanced weeks of arsenic exposure, compared to those from the non-transformed cells, indicate an increase in the proportion of cells exhibiting stem-like features, namely cancer stem cells. Concordantly, the arsenic impact on stem cell populations have been previously described by other authors (Ngalame et al., 2018; Wang et al., 2020; Xiao et al., 2020). Upon FRA1 knockdown, a significant reduction of the tumorspheres' size was observed in all cases. Moreover, we have found a significant enrichment of FRA1 in the tumorspheres population in comparison with that in the adherent culture. Given that among FRA1 target genes we can find *Nanog* and *Sox2* (Wang and Yang, 2019), often considered as direct stemness markers, and miR-21 (Sekar et al., 2016), related to cancer progression through cancer stem cells promotion, these findings bring the opportunity to re-evaluate the essential role of FRA1 transcription factor as a driver in the oncogenesis mediated by arsenic, and a necessary component for the emergence of cancer stem cells during the process.

3.2.5. CONCLUSIONS

The present work demonstrates for the first time that FRA1 is progressively overexpressed during the acquisition of an in vitro oncogenic phenotype induced by chronic arsenic exposure (long-term, non-cytotoxic doses). Rather than being related to tumor initiation, our results point out a role of FRA1 in the progression of the oncogenic phenotype, potentially mediated by the dysregulation of downstream relevant target genes such as tumor suppressors or EMT-TFs. The FRA1 increase during the transformation process leads to an accelerated proliferation, an increased anchorage-independent growth, and an increase in the migrating and invading potential, which are significantly reduced after FRA1 stable knock-down. Moreover, we are the first to

describe a link between FRA1 and the development of stem-cell-like features, which evidences the importance of this transcription factor in arsenic-associated carcinogenesis. This finding may not be restricted to the arsenic field only but could also be translated to other types of carcinogenesis processes where FRA1 is known to be involved.

Declaration of interests

The authors declare they have no actual or potential competing interests.

Author contribution statement:

RM and AH planned the experiments. IB, JB, and JP carried out the experimental part, analyzed the data, carried out the statistical analysis, and prepared the figures. IB, RM, and AH wrote the final manuscript.

3.2.6. REFERENCES

Aodengqimuge, Liu, S., Mai, S., Li, X., Li, Y., Hu, M., Yuan, S., Song, L. (2014). AP-1 activation attenuates the arsenite-induced apoptotic response in human bronchial epithelial cells by up-regulating HO-1 expression. *Biotech. Lett. 36,* 1927-193628.

Arslan, B., Djamgoz, M.B.A., Akün, E. (2017). Arsenic: A review on exposure pathways, accumulation, mobility and transmission into the human food chain. *Rev. Environ. Contam. Toxicol. 243*, 27-51.

Bach, J., Sampayo-Reyes, A., Marcos, R., Hernández, A. (2014). Ogg1 genetic background determines the genotoxic potential of environmentally relevant arsenic exposures. *Arch. Toxicol. 88*, 585-596.

Bach, J., Peremartí, J., Annangi, B., Marcos, R., Hernández, A. (2016). Oxidative DNA damage enhances the carcinogenic potential of in vitro chronic arsenic exposures. *Arch. Toxicol*. *90*, 1893-1905.

Bakiri, L., Macho-Maschler, S., Custic, I., Niemiec, J., Guió-Carrión, A., Hasenfuss, S.C., Eger, A., Müller, M., Beug, H., Wagner, E.F. (2015). Fra-1/AP-1 induces EMT in mammary epithelial cells by modulating Zeb1/2 and TGFβ expression. *Cell Death Differ. 22*, 336-350.

Casalino, L., Bakiri, L., Talotta, F., Weitzman, J. B., Fusco, A., Yaniv, M., Verde, P. (2007). Fra-1 promotes growth and survival in RAS-transformed thyroid cells by controlling cyclin A transcription. *EMBO J. 26*, 1878-1890.

Chung, Y. P., Chen, Y. W., Weng, T. I., Yang, R. Sen, Liu, S. H. (2020). Arsenic induces human chondrocyte senescence and accelerates rat articular cartilage aging. *Arch. Toxicol*. *94,* 89-101.

Curran, T., Franza, B. R. (1988). Fos and jun: The AP-1 connection. *Cell*. *55*, 395-397.

Dhillon, A.S., Tulchinsky, E. (2015). FRA-1 as a driver of tumor heterogeneity: A nexus between oncogenes and embryonic signalling pathways in cancer. *Oncogene*. *34*, 4421-4428.

Diesch, J., Sanij, E., Gilan, O., Love, C., Tran, H., Fleming, N.I., Ellul, J., Amalia, M., Haviv, I., Pearson, R.B., Tulchinsky, E., Mariadason, J.M., Sieber, O.M., Hannan, R.D., Dhillon, A.S. (2014) Widespread FRA1-dependent control of mesenchymal transdifferentiation programs in colorectal cancer cells. *PLoS One*. *9*, 1-11.

Dong, Z. (2002). The molecular mechanisms of arsenic-induced cell transformation and apoptosis. *Environ. Health Perspect. 110*, 757-759.

Druwe, I. L., Vaillancourt, R.R. (2010). Influence of arsenate and arsenite on signal transduction pathways: an update. *Archiv. Toxicol*. *84*, 585-596.

Flora, S.J.S. (2011). Arsenic-induced oxidative stress and its reversibility. *Free Radic. Biol. Med*. *51*, 257-281.

Gu, X., Lu, C., He, D., Lu, Y., Jin, J., Liu, D., Ma, X. (2016). Notch3 negatively regulates chemoresistance in breast cancers. *Tumor Biol*. *37*, 15825-15833.

Huang, C., Ma, W.Y., Li, J., Goranson, A., Dong, Z. (1999). Requirement of Erk, but not JNK, for arsenite-induced cell transformation. *J. Biol. Chem. 274*, 14595-14601.

Hubaux, R., Becker-Santos, D.D., Enfield, K.S.S., Rowbotham, D., Lam, S., Lam, W.L., Martinez, V.D. (2013). Molecular features in arsenic-induced lung tumors. *Mol. Cancer. 12*, 1-11.

Jamal, Z., Das, J., Ghosh, S., Gupta, A., Chattopadhyay, S., Chatterji, U. (2020). Arsenic-induced immunomodulatory effects disorient the survival-death interface by stabilizing the Hsp90/Beclin1 interaction. *Chemosphere*. *238*, 124647.

Jiang, X., Xie, H., Dou, Y., Yuan, J., Zeng, D., Xiao, S. (2020). Expression and function of FRA1 protein in tumors. *Mol. Biol. Rep. 47,* 737-752.

Khan, K. M., Chakraborty, R., Bundschuh, J., Bhattacharya, P., Parvez, F. (2020). Health effects of arsenic exposure in Latin America: An overview of the past eight years of research. *Sci. Total Environ. 710*, 136071.

Kim, H.G., Shi, C., Bode, A.M., Dong, Z. (2016). p38α MAPK is required for arsenic-induced cell transformation. *Mol. Carcinog*. *55*, 910-917.

Kryeziu, K., Pirker, C., Englinger, B., van Schoonhoven, S., Spitzwieser, M., Mohr, T., Körner, W., Weinmüllner, R., Tav, K., Grillari, J., Cichna-Markl, M., Berger, W., Heffeter, P.(2016). Chronic arsenic trioxide exposure leads to enhanced aggressiveness via Met oncogene addiction in cancer cells. *Oncotarget*. *7*, 27379-27393.

Lau, E.Y.T., Lo, J., Cheng, B.Y.L., Ma, M.K.F., Lee, J.M.F., Ng, J.K.Y., Chai, S., Lin, C.H., Tsang, S.Y., Ma, S., Ng, I.O., Lee, T.K.W. (2016). Cancer-associated fibroblasts regulate tumor-initiating cell plasticity in hepatocellular carcinoma through c-Met/FRA1/HEY1 signaling. *Cell Rep. 15*, 1175-1189.

Levy, L., Hill, C.S. (2006). Alterations in components of the TGF-β superfamily signaling pathways in human cancer. *Cytokine Growth Factor Rev*. *17*, 41-58.

Li, Q. R., Ni, W. P., Lei, N. J., Yang, J. Y., Xuan, X. Y., Liu, P. P., Gong, G. M., Yan, F., Feng, Y. S., Zhao, R., Du, Y. (2018). The overexpression of Fra1 disorders the inflammatory cytokine secretion by mTEC of myasthenia gravis thymus. *Scand. J. Immunol*. *88*, 1-10.

Luo, Y.P., Zhou, H., Krueger, J., Kaplan, C., Liao, D., Markowitz, D., Liu, C., Chen, T., Chuang, T.H., Xiang, R., Reisfeld, R.A. (2010). The role of proto-oncogene Fra-1 in remodeling the tumor microenvironment in support of breast tumor cell invasion and progression. *Oncogene. 29*, 662-673.

Marciniak, W., Derkacz, R., Muszyńska, M., Baszuk, P., Gronwald, J., Huzarski, T., Cybulski, C., Jakubowska, A., Falco, M., Dębniak, T., Lener, M., Oszurek, O., Pullella, K., Kotsopoulos, J., Sun, P., Narod, S. A., Lubiński, J. (2020). Blood arsenic levels and the risk of familial breast cancer in Poland. *Int. J. Cancer*. *146*, 2721-2727.

Naujokas, M. F., Anderson, B., Ahsan, H., Vasken Aposhian, H., Graziano, J. H., Thompson, C., Suk, W. A. (2013). The broad scope of health effects from chronic arsenic exposure: Update on a worldwide public health problem. *Environ. Health Perspect. 121*, 295-302.

Ngalame, N.N.O., Tokar, E.J., Person, R.J., Waalkes, M.P. (2014). Silencing KRAS overexpression in arsenic-transformed prostate epithelial and stem cells partially mitigates malignant phenotype. *Toxicol. Sci. 142*, 489-496.

Ngalame, N. N. O., Luz, A. L., Makia, N., Tokar, E. J. (2018). Arsenic alters exosome quantity and cargo to mediate stem cell recruitment into a cancer stem cell-like phenotype. *Toxicol. Sci. 165*, 40-49.

Palma-Lara, I., Martínez-Castillo, M., Quintana-Pérez, J. C., Arellano-Mendoza, M. G., Tamay-Cach, F., Valenzuela-Limón, O. L., García-Montalvo, E. A., Hernández-Zavala, A. (2020). Arsenic exposure: A public health problem leading to several cancers. *Reg. Toxicol. Pharmacol*. *110*, 104539.

Paul, S., Banerjee, N., Chatterjee, A., Sau, T. J., Das, J. K., Mishra, P. K., Chakrabarti, P., Bandyopadhyay, A., Giri, A. K. (2014). Arsenic-induced promoter hypomethylation and over-expression of ERCC2 reduces DNA repair capacity in humans by non-disjunction of the ERCC2-Cdk7 complex. *Metallomics*. *6*, 864-873.

Person, R.J., Olive Ngalame, N.N., Makia, N.L., Bell, M.W., Waalkes, M.P., Tokar, E.J. (2015). Chronic inorganic arsenic exposure in vitro induces a cancer cell phenotype in human peripheral lung epithelial cells. *Toxicol. Appl. Pharmacol. 286*, 36-43.

Qian, Y., Castranova, V., Shi, X. (2003). New perspectives in arsenic-induced cell signal transduction. *J. Inorg. Biochem*. *96*, 271-278.

Schmidlin, C. J., Zeng, T., Liu, P., Wei, Y., Dodson, M., Chapman, E., Zhang, D. D. (2020). Chronic arsenic exposure enhances metastatic potential via NRF2-mediated upregulation of SOX9. *Toxicol. Appl. Pharmacol*. *402*, 115138.

Sekar, D., Krishnan, R., Panagal, M., Sivakumar, P., Gopinath, V., Basam, V. (2016). Deciphering the role of microRNA 21 in cancer stem cells (CSCs). *Genes Dis*. *3*, 277-281.

Shaulian, E., Karin. M. (2002). AP-1 as a regulator of cell life and death. *Nat. Cell Biol. 4*, E131-136.

Siddique, A. E., Rahman, M., Hossain, M. I., Karim, Y., Hasibuzzaman, M. M., Biswas, S., Islam, M. S., Rahman, A., Hossen, F., Mondal, V., Banna, H. U., Huda, N., Hossain, M., Sultana, P., Nikkon, F., Saud, Z. A., Haque, A., Nohara, K., Xin, L., Himeno, S., Hossain, K. (2020). Association between chronic arsenic exposure and the characteristic features of asthma. *Chemosphere*. *246*, 12579.

Song, L., Liu, B., Wang, L., Wu, M., Zhang, L., Liu, Y., Bi, J., Yang, S., Zhang, B., Xia, W., Xu, S., Chen, R., Cao, Z., Wang, Y. (2020). Exposure to arsenic during pregnancy and newborn mitochondrial DNA copy number: A birth cohort study in Wuhan, China. *Chemosphere*. *243*, 125335.

Soza-Ried, C., Bustamante, E., Caglevic, C., Rolfo, C., Sirera, R., Marsiglia, H. (2019). Oncogenic role of arsenic exposure in lung cancer: A forgotten risk factor. *Crit. Rev. Oncol./Hematol*. *139*, 128-133.

Sundqvist, A., Zieba, A., Vasilaki, E., Herrera Hidalgo, C., Söderberg, O., Koinuma, D., Miyazono K, Heldin, C.H., Landegren, U., Ten Dijke, P., Van Dam, H. (2013). Specific interactions between Smad proteins and AP-1 components determine TGFβ-induced breast cancer cell invasion. *Oncogene*. *32*, 3606-3615.

Talotta, F., Cimmino, A., Matarazzo, M.R., Casalino, L., De Vita, G., D'Esposito, M., Di Lauro, R., Verde, P. (2009). An autoregulatory loop mediated by miR-21 and PDCD4 controls the AP-1 activity in RAS transformation. *Oncogene*. *28*, 73-84.

Tam, L. M., Price, N. E., Wang, Y. (2020). Molecular mechanisms of arsenic-induced disruption of DNA repair. *Chem. Res. Toxicol*. *33*, 709-726.

Tchounwou, P.B., Yedjou, C.G., Udensi, U.K., Pacurari, M., Stevens, J.J., Patlolla, A.K., Noubissi, F., Kumar, S. (2019). State of the science review of the health effects of inorganic arsenic: Perspectives for future research. *Environ. Toxicol*. *34*, 188-202.

Verde, P., Casalino, L., Talotta, F., Yaniv, M., Weitzman, J.B. (2007). Deciphering AP-1 function in tumorigenesis: Fra-ternizing on target promoters. *Cell Cycle*. *6*, 2633-2639.

Vesely, P.W., Staber, P.B., Hoefler, G., Kenner, L. (2009). Translational regulation mechanisms of AP-1 proteins. *Mutat. Res. Rev. 682*, 7-12.

Wang, Y., Zhao, H., Guo, M., Shao, Y., Liu, J., Jiang, G., Xing, M. (2018). Arsenite renal apoptotic effects in chickens co-aggravated by oxidative stress and inflammatory response. *Metallomics*. *10,* 1805-1813.

Wang, Z., Yang, C. (2019). Metal carcinogen exposure induces cancer stem cell-like property through epigenetic reprograming: A novel mechanism of metal carcinogenesis. *Semin. Cancer Biol. 57*, 95-104.

Wang, Z., Yang, P., Xie, J., Lin, H. P., Kumagai, K., Harkema, J., Yang, C. (2020). Arsenic and benzo[a]pyrene co-exposure acts synergistically in inducing cancer stem cell-like property and tumorigenesis by epigenetically down-regulating SOCS3 expression. *Environ. Int*. *137*, 105560.

Wei, S., Qiu, T., Yao, X., Wang, N., Jiang, L., Jia, X., Tao, Y., Wang, Z., Pei, P., Zhang, J., Zhu, Y., Yang, G., Liu, X., Liu, S., Sun, X. (2020). Arsenic induces pancreatic dysfunction and ferroptosis via mitochondrial ROS-autophagy-lysosomal pathway. *J. Hazard. Mater*. *384*, 121390.

Xiao, T., Xue, J., Shi, M., Chen, C., Luo, F., Xu, H., Chen, X., Sun, B., Sun, Q., Yang, Q., Dai, X., Zhang, A., Tang, H., Liu, Q. (2018). Circ008913, via miR-889 regulation of DAB2IP/ZEB1, is involved in the arsenite-induced acquisition of CSC-like properties by human keratinocytes in carcinogenesis. *Metallomics*. *10*, 1328-1338.

Zhang, X., Wu, J., Luo, S., Lechler, T., Zhang, J.Y. (2016). FRA1 promotes squamous cell carcinoma growth and metastasis through distinct AKT and c-Jun dependent mechanisms. *Oncotarget*. *7*, 34371-34383.

Zhang, L., Liu, H., Mu, X., Cui, J., Peng, Z. (2017). Dysregulation of Fra1 expression by Wnt/β-catenin signaling promotes glioma aggressiveness through epithelial–mesenchymal transition. *Biosci. Rep. 37*, BSR20160643.

Zhao, L., Liu, X., Xu, G., Guo, Y., Sun, L., Zhang, C., Li, X., Li, B. (2020). Arsenic induces mTOR-dependent autophagy, whereas it impairs the autophagy-lysosome pathway and the potential role of TFEB in cultured dendritic cells. *Metallomics*. *12*, 1230-1245.

Zhou, Q., Jin, P., Liu, J., Wang, F., Xi, S. (2018). HER2 and Src co-regulate proliferation, migration and transformation by downstream signaling pathways in arsenite-treated human uroepithelial cells. *Metallomics. 10*, 1141-1159.

Zhu, Y., Costa, M. (2020). Metals and molecular carcinogenesis. *Carcinogenesis*. *41*, 1161-1172.

3.3. Chapter 3 (Study 3)

Oncogenic effects caused by *in vitro* long-term co-exposure to polystyrene nanoparticles and arsenic

Submitted paper

Oncogenic effects caused by *in vitro* long-term co-exposure to polystyrene nanoparticles and arsenic

Irene Barguilla[1], Josefa Domenech[1], Ricard Marcos[1,2,§], Alba Hernández[1,2,§]

[1]Group of Mutagenesis, Department of Genetics and Microbiology, Faculty of Biosciences, Universitat Autònoma de Barcelona, Cerdanyola del Vallès (Barcelona), Spain; [2]Consortium for Biomedical Research in Epidemiology and Public Health (CIBERESP), Carlos III Institute of Health, Madrid, Spain.

[§]Corresponding authors at: Group of Mutagenesis, Department of Genetics and Microbiology, Universitat Autònoma de Barcelona, Edifici Cn, Campus de Bellaterra, 08193 Cerdanyola del Vallès (Barcelona), Spain.

E-mail: alba.hernandez@uab.es (A. Hernández)

ricard.marcos@uab.es (R. Marcos)

Running title: Co-carcinogenenic potential of nanopolystyrene and arsenite

ABSTRACT

The increasingly widespread presence of micro- and nanoplastics (MNPLs) in the environment calls for urgent evaluation of their potential risks. These particles may enter the human body, and translocate through physiological barriers i.e. the gastrointestinal barrier, therefore an important aspect of their potential health impact is their role as carriers for other hazardous environmental contaminants (*Trojan horse* effect). In this sense, we have examined the interaction and joint effects of two relevant water contaminants: arsenic (As^{III}) and polystyrene nanoparticles (PSNPs). Thus, cells previously transformed by chronic arsenic exposure, were further exposed to PSNPs, As^{III} and the combination As^{III}/PSNPs for 12 weeks. Interestingly, a physical interaction between both pollutants is demonstrated. Results also indicate that the continuous co-exposure enhances the DNA damage and the aggressive features of the initial transformed phenotype. Remarkably, co-exposed cells present a higher proportion of spindle-like cells within the population, an increased capacity to grow independently of anchorage, as well as enhanced migrating and invading potentials, when compared to cells exposed to arsenic or PSNPs alone. Hence, this study highlights theneed to further explore the long-term effects of contaminants of emerging concern, such as MNPLs, and the importance of considering the behavior of mixtures as part of the hazard and human risk assessment approaches.

Graphical abstract:

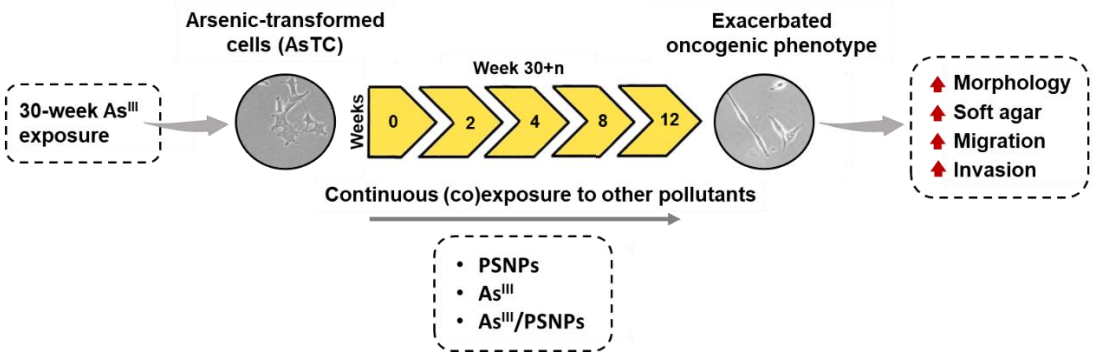

Keywords: polystyrene nanoparticles, arsenic, long-term co-exposure, cell transformation, genotoxic DNA damage, oncogenic phenotype, carcinogenesis.

3.3.1. INTRODUCTION

The generalized utilization of single-use plastic in uncountable applications comes together with an alarming rise in plastic waste, which is becoming a pressing environmental issue. Under environmental conditions, plastic litter is subjected to fragmentation and degradation into the so-called micro- and nanoplastics (MNPLs) (Bouwmeester et al., 2015; EFSA, 2016). While macroplastic pollution is the noticeable facet of this issue, the extensive presence of MNPLs in water, soil and air is equally worrisome, especially in aquatic ecosystems. Indeed, it has recently been estimated that 8.3 million MNPLs particles contaminate each cubic meter of ocean water (Brandon et al., 2020) and they are ubiquitously distributed on open sea and coasts (Li et al., 2016). Although there are still many questions to be answered on the potential hazard that MNPL pollution poses to human health, recent studies evidence the MNPLs' potential to translocate through physiological barriers and internalize cells (Hesler et al., 2019; Domenech et al., 2020), to produce cytotoxicity (Xu et al., 2019), to increase the levels of reactive oxygen species (ROS) (Liu et al., 2020), to induce DNA damage (Rubio et al., 2020), and to trigger the altered secretion of pro-inflammatory cytokines (Ballesteros et al., 2020). It is noteworthy the lack of exploration of MNPL exposure long-term effects, which would be more descriptive of a real environmental exposure scenario.

In an actual context of environmental pollution, diverse contaminants coexist in the same site and can interact with each other. Therefore, increasing interest is being directed towards the potential role of MNPLs as carriers for other contaminants. MNPLs' surface features give them the capacity to interact with and adsorb other compounds from heavy metals (Godoy et al., 2019), to organic pollutants (Hüffer and Hofmann, 2016; Lin et al., 2019). Interestingly, cadmium, titanium, and lead have already been detected in MNPL samples collected on marine ecosystems (Massos and Turner, 2017). Despite the potential risk derived from the role of MNPLs as carriers for other pollutants, the information on their combined effects is still very limited.

Arsenic is one of those metals potentially sharing environmental compartments with MNPLs. Inherently present in the Earth's crust, arsenic is part of geological formations widespread worldwide. The weathering of these rocks and minerals releases inorganic forms -arsenates (As^{V}) and arsenites (As^{III})- which enter the arsenic cycle as dust or dissolved in water, and are carried by rivers, rain and groundwater (Smedley and Kinniburgh, 2002; Ravenscroft et al., 2009). Hence, the intake of contaminated water or food is the main route of exposure to this classic genotoxic and carcinogen pollutant. Arsenic exposure affects large human populations which are at a higher risk to develop

cardiovascular abnormalities, neurological alterations, hepatotoxicity, and most importantly, cancer. Being a well-described carcinogen, the long-term exposure to arsenic has been associated with lung, bladder, liver, skin, prostate and kidney cancer (IARC, 2012). Multiple studies have addressed arsenic-induced carcinogenesis following diverse *in vitro*, *in vivo*, and epidemiological approaches. *In vitro*, 12-30 weeks of chronic arsenic exposure have been described to transform very different *in vitro* models, including lung epithelial cells (Stueckle et al., 2012), prostate epithelial cells (Treas et al., 2013), breast epithelial cells (Xu et al., 2014), keratinocytes (Pi et al., 2008; Li et al., 2010) and fibroblasts (Shearer et al., 2016).

To the hazard of classic contaminants, we now have to add the potential adverse effects of emergent pollutants. MNPLs are likely found together with arsenic in highly contaminated water and could act as arsenic carriers, altering its toxicity. Therefore, considering the existing evidence of arsenic adsorption onto MNPLs (Dong et al., 2019, Dong et al., 2020), it is very relevant to evaluate the probable health risk posed by this interaction, which remains widely unexplored up to date.

In this work, we have evaluated the arsenic interaction with polystyrene nanoparticles (PSNPs), being one of the most abundant MNPLs in the environment (Bouwmeester et al., 2015). Further, to assess the co-exposure impact on the long-term, we selected mouse embryonic fibroblasts previously transformed by 30 weeks of chronic exposure to sodium arsenite (As^{III}), hereafter referred to as arsenic-transformed cells (AsTC). The phenotypic and molecular changes that AsTC undergo during the chronic arsenic exposure were characterized by Bach et al. (2016). AsTC showed characteristic cancer-associated features such as morphological changes, differentiation status deregulation and invasiveness potential (Bach et al., 2016). Aiming to assess whether the chronic PSNPs exposure or the As^{III}/PSNPs co-exposure exacerbate the arsenic-induced transformed phenotype, AsTC were further exposed for 12 weeks to PSNPs, As^{III}, or the combination of both compounds and different hallmarks of carcinogenesis were evaluated.

3.3.2. MATERIALS AND METHODS

3.3.2.1. PSNPs and y-PSNPs characterization

Pristine PSNPs (PP-008-10) and yellow fluorophore-conjugated PSNPs (y-PSNPs) (FP-00552-2) were purchased from Spherotech (Chicago, USA). The pristine form of polystyrene (PS) particles was used for all the experiments carried out except for those in which the fluorescent marker was required, such as the visualization and the quantification of PS particles internalization by confocal microscopy and flow cytometry, respectively. PSNPs used for the assays were characterized by Z-sizer and transmission electron microscopy (TEM). To that purpose, the obtained dispersions were diluted to a final concentration of 100 µg/mL in distilled water. PSNPs and y-PSNPs dilutions were analyzed in a Malvern Zetasizer Nano ZS zen3600 device (Malvern, UK) to determine the hydrodynamic size and the Z-potential parameters using dynamic light scattering (DLS) and laser Doppler velocimetry (LDV) methodologies. All the parameters for each sample were measured in triplicates. On the other hand, carbon coated TEM grids were dipped into the PSNPs and y-PSNPs dilutions and samples were visualized on a JEOL JEM-1400 instrument (JEOL LTD, Tokyo, Japan). To determine the mean size, Image J software with the Fiji extension was used to measure 100 randomly selected PS nanoparticles.

3.3.2.2. Cell culture conditions

Mouse embryonic fibroblasts phenotypically sensitive to oxidative damage and previously transformed by 30 weeks of continuous sodium arsenite (As^{III}) exposure (2 µM) (Bach et al., 2016), were used in this study and will be henceforth referenced as arsenic-transformed cells (AsTC). AsTC were grown in Dulbecco's modified Eagle's medium (DMEM)/F12 medium (Life Technologies, NY, USA) supplemented with 10% fetal bovine serum (Biowest, France) and 2.5 µg/mL Plasmocin (InvivoGen, CA, USA) in a humidified atmosphere of 5% CO_2 and 95% air at 37 ºC.

3.3.2.3. PSNPs uptake by AsTC

The cellular localization of y-PSNPs was determined by confocal microscopy with the aim of assessing PSNPs internalization by AsTC. To this end, 80,000 AsTC were seeded in Glass Bottom Microwell dishes (MatTek, USA) and exposed to 25 and 100 µg/mL y-PSNPs for 24 h. Samples were then washed with PBS 1X and nuclei and cell membranes were stained with 1:500 Hoechst 33342 (ThermoFisher Scientific, USA) and 1:500 Cellmask™ Deep Red plasma (Life Technologies, USA), respectively, for 15 min at room

temperature. y-PSNP were detected thanks to the fluorophore to which they are conjugated. A Leica TCS SP5 confocal microscope was used to visualize two different randomly selected fields per sample and images were processed with the software Image J with the Fiji extension. In addition, a quantification of the y-PSNPs internalization was carried out by flow cytometry. Briefly, after the AsTC exposure to 25 and 100 µg/mL of y-PSNPs, cells were washed with PBS 1X, trypsinized, centrifuged and recovered in PBS 1X at a final concentration of 1 x 10^6 cells/mL in FACS tubes. To select alive cells from the total population of the samples, 1:1000 propidium iodide was added before the analysis with a BD FACSCanto Flow Cytometer (BD Bioscience, USA). 10,000 events from the living cells population per sample were analyzed and the y-PSNPs uptake was extrapolated from the mean fluorescence intensity of the living cells population. AsTC incubated with DMEM/F12 medium were used as control in both assays.

3.3.2.4. As^{III}/PSNPs interaction detection

The interaction between As^{III} and PSNPs was assessed by TEM. With this aim, the highest doses of both treatments were used. Concisely, a dilution in distilled water with a final concentration of 20 µM As^{III} and 100 µg/mL PSNPs was incubated for 3 h at room temperature. Carbon coated TEM grids were then dipped into the sample and analyzed by transmission electron microscopy coupled with energy-dispersive X-ray spectroscopy (TEM-EDX). A TEM JEOL-2011 (200kV) instrument (JEOL LTD, Tokyo, Japan) was used to visualize the sample and take images while the INCA detector (Oxford Instruments, United Kingdom) was used to determine the elementary composition of the sample with the aim of detecting arsenic on PSNPs surface.

3.3.2.5. As^{III} internalization by AsTC

To evaluate and quantify As^{III} uptake by AsTC, an analysis with inductively coupled plasma mass spectrometry (ICP-MS) was performed. AsTC were exposed to 20 µM As^{III} combined with 0, 25, and 100 µg/mL PSNPs for 24 h. AsTC non-exposed to As^{III}, but exposed to 0, 25, and 100 µg/mL PSNPs for 24 h were used as negative controls. After that, cells were washed with PBS 1X and trypsinized. Then, samples were centrifuged at 1,000 rpm for 8 min, supernatants were discarded, and pellets were frozen at -20 ºC until samples were digested on a heat block in concentrated HNO_3 (Merck, suprapure) at 105 ºC for 30 min. Finally, the amount of arsenic in each sample was determined using an ICP-MS 7500-ce device (Agilent Technologies).

3.3.2.6. *In vitro* chronic PSNP and arsenic (co)exposure

AsTC were (co)exposed for 12 weeks to 25 µg/mL PSNPs, 2 µM As^{III}, or the combination of both treatments: 2 µM As^{III}/ 25 µg/mL PSNPs. Replicates of exposed and passage-matched AsTC were maintained in two separate T-25 flasks and grown under the culture conditions previously described.

3.3.2.7. Comet assay

The total and oxidative DNA damage (ODD) for AsTC under the different exposure scenarios was evaluated by the alkaline comet assay with the use of formamidopyrimidine DNA glycosylase (FPG) as previously described by us (Bach et al., 2014). Sheet films of the type Gelbond® (GF) (McNamee et al., 2000) were used. Briefly, cells were collected by trypsinization, centrifuged, and resuspended in cold PBS at 17,500 cells/25 µL. Then cells were mixed with 0.75% LMP agarose at 37 ºC (1:10) and 7 µL of the mixture was dropped onto the GF. Two identical films with the same type of samples were processed simultaneously in each experiment. Then, GF were lysed overnight by immersion in ice-cold lysis buffer at 4 ºC (2.5 M NaCl, 0.1 M Na2EDTA, 0.1 M Tris Base, 1% Triton X-100, 1% lauroyl sarcosinate, 10% DMSO), at pH 10. The GF replicates were gently washed twice (1x 5 min, 1x 50 min) in enzyme buffer at pH 8 (10 mM HEPES, 0.1 M KCl, 0.5 mM EDTA, 0.2 mg/mL BSA) at 4 ºC and then incubated for 30 min at 37 ºC in enzyme buffer (negative control) or FPG-containing enzyme buffer. The GF were then washed with electrophoresis buffer and placed into a horizontal gel electrophoresis tank where DNA could unwind for 23 min in 0.3 M NaOH and 1 mM Na2EDTA pH 13.2 before the electrophoresis, which was carried out for 20 min at 0.8 V/cm and 300 mA at 4 ºC. After the electrophoresis, the GF were rinsed with cold PBS for 15 min and fixed in absolute ethanol for 2 h before air-drying overnight at room temperature. GF were stained for 20 min with SYBR Gold 1/10.000 in TE buffer (10 mM Tris, 1 mM EDTA pH 7.5). Finally, gels were mounted, visualized for comets using an epifluorescent microscope at 20X magnification and analyzed with the Komet 5.5 Image analysis system (Kinetic Imaging Ltd, Liverpool, UK). Cells were analyzed according to their percentage of DNA in the tail, as an adequate measure of DNA damage. One hundred randomly selected comet images were analyzed per sample.

3.3.2.8. Cell morphology

Cell morphology was qualitatively evaluated, and cells were photographed with a Zeiss Observer A1 microscope.

3.3.2.9. Soft-agar assay

Colony formation in soft-agar was performed for AsCT and the different exposure conditions to assess the cells' anchorage-independent growth potential. Cells were collected and filtered through a 40 µm mesh, to obtain single-cell suspensions. Subsequently, a suspension of 65,000 cells in 1.75 mL of DMEM containing 10% of FBS and 2.5 µg/mL Plasmocin was prepared and mixed in a 1:1:1 ratio with 2x DMEM containing 20% of FBS, 2% NEEA, 2% L-Glu 200 mM, and 2% penicillin-streptomycin and with 1.2% of bacto-agar (DIFCO, MD, USA). This mixture was enough to prepare triplicates of 20,000 cells each by dispensing 1.5 mL over a 0.6% base agar (supplemented with 2x DMEM) in each well of a 6-well plate. Plates were allowed to sit for 45 min and then, kept in the incubator for 21 days. The cells able to form colonies were stained by a 24 h incubation with 1 mg/mL of (2-p-iodophenyl)-3-3(p-nitrophenyl)-5-phenyl tetrazolium chloride (INT; Sigma, MO, USA). Then, the plates were scanned with a HP Scanjet G4050, and the colonies were counted using the colony cell counter enumerator software OpenCFU (3.9.0).

3.3.2.10. Invasion and migration assays

The invasive potential of AsTC and those subjected to further As^{III} and PSPNs exposures, was evaluated performing direct migration and invasion assays. To carry out the invasion assay, cells at 80% confluency were deprived of FBS for 24 h. The day of the assay, a 180 µL 1:2 dilution of Matrigel® (Costar-Corning, NY, USA) in FBS free DMEM/F12 with 0.1% BSA was used to coat each 8 µm pore size polycarbonate membrane 24 mm transwell insert (Costar-Corning, NY, USA). The Matrigel® mixture was left to sit and dry for 1 h in the cell incubator at 37 ºC. The bottom chamber of the transwell inserts was filled with 2.5 mL DMEM/F12 complemented with 15% FBS as the chemoattractant medium. A single-cell suspension containing 600,000 FBS-deprived MEF cells in 1.5 mL of FBS free DMEM/F12 with 0.1% BSA was added on top of the transwell Matrigel®-coated membrane. Cells were then allowed to invade for 48 h at 37 °C. Invading cells in the bottom chamber were collected by trypsinization and counted using a Beckman Coulter cell counter.

A modified version of the assay was performed to evaluate cell migration. The main steps were followed as described above; however, the cells were seeded on the top of the transwell without the Matrigel® coating.

3.3.2.11. Tumorsphere formation assay

AsTC and exposed cells were seeded at a density of 2,500 cells/mL on 96-well ultra-low-attachment plates (Corning, Costar-Corning, NY, USA) in serum-free DMEM/F12 supplemented with B27, 20 ng/mL basic fibroblast growth factor (bFGF) (both from Life Technologies, NY, USA), epithelial growth factor and 4 µg/mL heparin (both from Sigma-Aldrich, Germany). After 6 days of incubation in a humidified atmosphere of 5% CO_2 and 95% air at 37 ºC, the tumorspheres were counted and photographed. Tumorspheres' size was assessed using ImageJ software.

3.3.3. RESULTS

3.3.3.1. PS materials characterization

Both, PSNPs and y-PSNPs were visualized by TEM. As shown in Figure 1A, the commercial PSNPs and y-PSNPs dispersions consist of electrodense round shaped particles. The particles' size was measured from TEM images by Image J, obtaining a median size of 45.91 nm and 42.42 nm for PSNPs and y-PSNPs, respectively (Figure 1B). PS materials were further characterized by Z-sizer and data obtained is summarized in Figure 1B. PSNPs and y-PSNPs hydrodynamic radius measured by DLS were larger than those measured from TEM images. Besides, polydispersity index (PdI) values close to 0 indicates the samples are consistent monodispersions, and Z-potential measurements indicate a high stability of the dispersions.

A

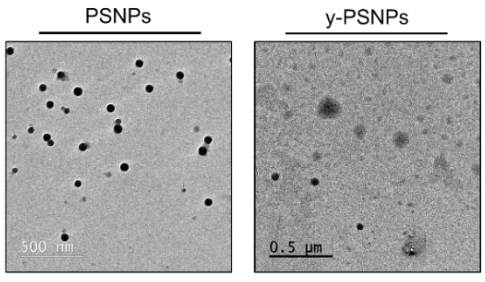

B

	PSNPs	y-PSNPs
Median size (nm) (TEM)	45.91	42.42
Size (nm) (DLS)	86.33 ± 10.20	112.87 ± 3.11
PdI (DLS)	0.10 ± 0.09	0.35 ± 0.02
Z-potential (mV) (LDV)	-36.00 ± 7.88	-45.97 ± 3.84
Mobility (µm cm/Vs) (LDV)	-2.29 ± 0.10	-3.76 ± 0.38

Figure 1: PS materials characterization. **(A)** Representative TEM images of PSNP and y-PSNP. **(B)** PSNPs and y-PSNPs characterization by TEM (median size) and Zetasizer Nano ZS (mean ± SD). 100 µg/mL dilutions in distilled water of each material were used for the visualization and characterization.

3.3.3.2. Determination and quantification of y-PSNPs uptake by AsTC

The cellular location of y-PSNPs after the internalization by AsTC was assessed by confocal microscopy. y-PSNPs were found inside the cell cytoplasm at all the conditions analyzed (Figure 2A). However, no difference in the plastic internalization pattern at the different concentrations of y-PSNPs analyzed could be deduced at first sight. To quantify y-PSNPs cellular uptake, the mean fluorescence intensity of the living AsTC exposed to 25 and 100 µg/mL y-PSNPs was determined by flow cytometry. As shown in Figure 2B, there is a dose-dependent significant increase of the fluorescence intensity that is translated in a greater internalization of y-PSNPs as the selected doses increase.

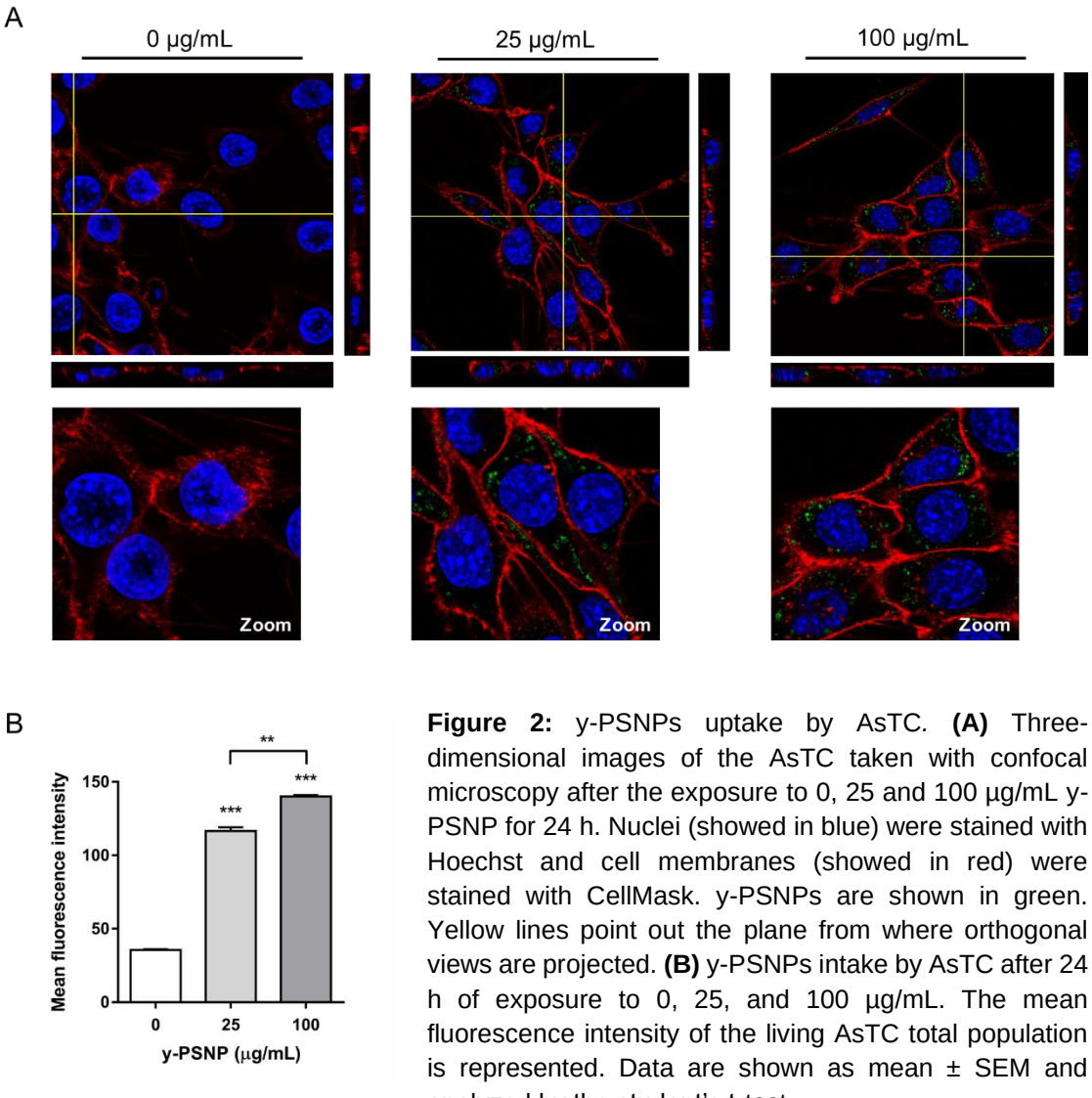

Figure 2: y-PSNPs uptake by AsTC. **(A)** Three-dimensional images of the AsTC taken with confocal microscopy after the exposure to 0, 25 and 100 µg/mL y-PSNP for 24 h. Nuclei (showed in blue) were stained with Hoechst and cell membranes (showed in red) were stained with CellMask. y-PSNPs are shown in green. Yellow lines point out the plane from where orthogonal views are projected. **(B)** y-PSNPs intake by AsTC after 24 h of exposure to 0, 25, and 100 µg/mL. The mean fluorescence intensity of the living AsTC total population is represented. Data are shown as mean ± SEM and analyzed by the student's t-test.

3.3.3.3 Visualization of the As^{III}/PSNPs interaction in dispersion and quantification of As^{III} uptake by AsTC

As^{III} and PSNPs interactions in dispersion were visualized by TEM and the presence of arsenic was confirmed with the EDX analysis. As shown in Figure 3A, different types of associations between As^{III} and polystyrene particles were observed. On the one hand, arsenic was found associated to single PSNPs. Differently, arsenic was also visualized forming aggregates that were, in turn, ringed by PSNPs. The plot of the arsenic electrons transition shown in the diagrams obtained with EDX, confirmed that the electrodense shadow detected with TEM consists of As^{III}. Once confirmed the interaction and the formation of As^{III}/PSNPs complexes, arsenic uptake by AsTC was determine by ICP-MS. The amount of arsenic detected inside the cells did not show a PSNPs dependency. As shown in Figure 3B, the amount of internalized arsenic was remained unchangeable at the different PSNPs concentrations assayed. The pg of arsenic measured were normalized to the number of cells in each sample. In the negative control samples, arsenic was under the limit of detection as expected. Since the ICP-MS device was unable to detect it, data are arbitrarily represented as 0.005 pg As^{III}/cell.

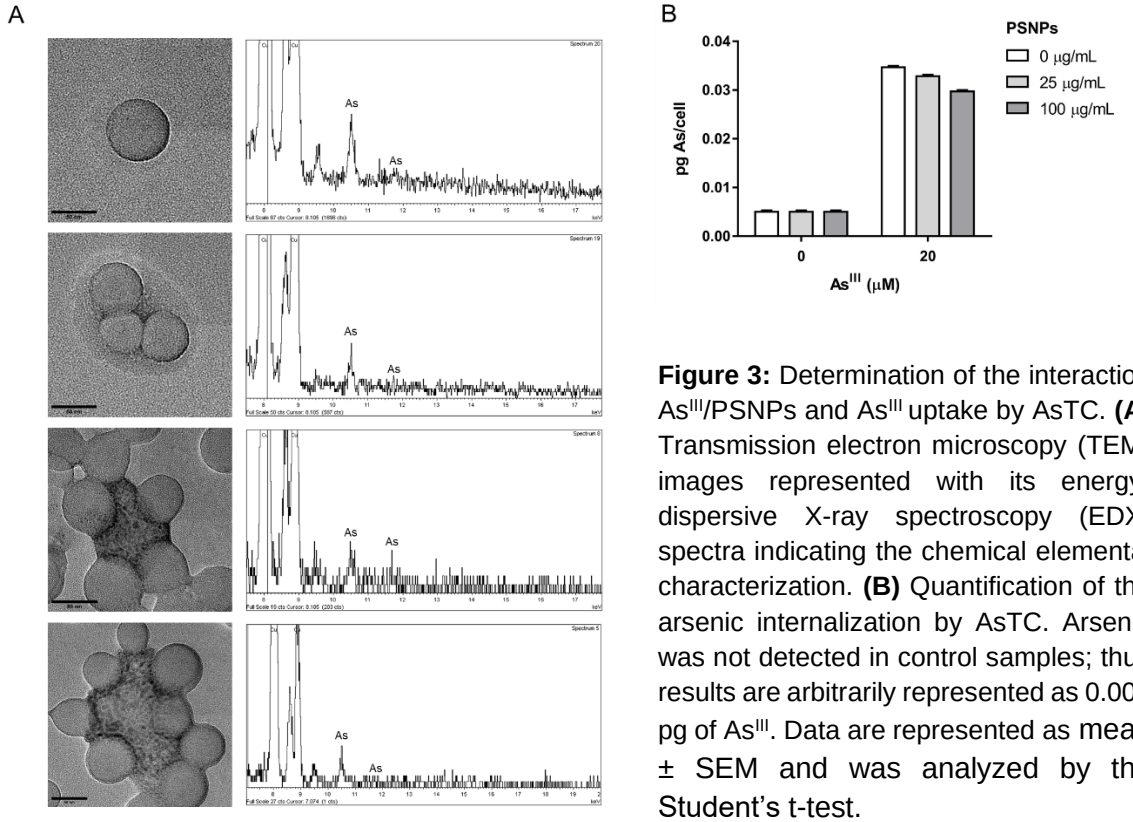

Figure 3: Determination of the interaction As^{III}/PSNPs and As^{III} uptake by AsTC. **(A)** Transmission electron microscopy (TEM) images represented with its energy-dispersive X-ray spectroscopy (EDX) spectra indicating the chemical elemental characterization. **(B)** Quantification of the arsenic internalization by AsTC. Arsenic was not detected in control samples; thus results are arbitrarily represented as 0.005 pg of As^{III}. Data are represented as mean ± SEM and was analyzed by the Student's t-test.

3.3.3.3. Both the co-exposure and the single pollutant exposure induce DNA damage

Given the obtained evidence supporting the pollutants interaction, we evaluated the genotoxic potential of the chronic (co)exposure to arsenic and the MNPLs. The levels of DNA damage and oxidative DNA damage (ODD) of AsTC were assessed after 12-weeks of prolonged PSNPs, As^{III}, and As^{III}/PSNPs exposure. As seen in Figure 4, all exposure scenarios tested led to an increase of total (Figure 4A) and oxidative (Figure 4B) DNA damage compared to the damage levels of AsTC. Interestingly, the levels of ODD were also significantly higher than those of PSNPs-exposed AsTC.

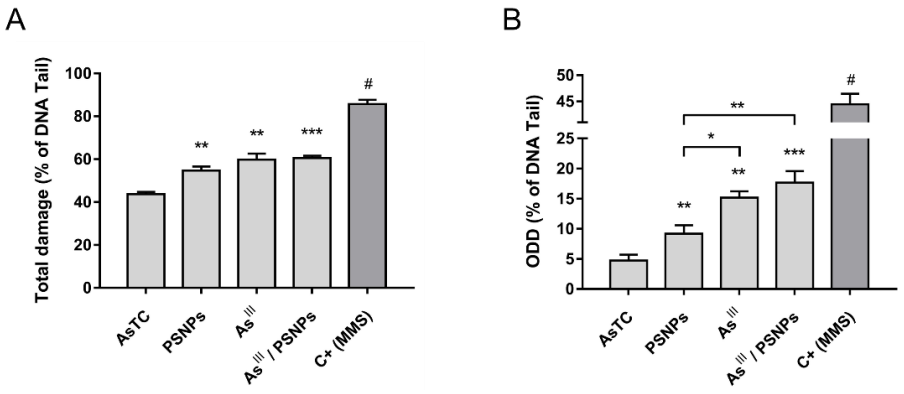

Figure 4: DNA damage induced by the long-term (co)exposure to As^{III} and PSNPs measured by the comet assay. **(A)** Total and **(B)** oxidative DNA damage levels after a 12-week exposure of AsTC to 25 µg/mL PSNPs, 2 µM As^{III} and the combination of both As^{III}/PSNPs treatments. MMS (200 µM) was used as a positive control. Data are presented as mean ± SEM analyzed by one-way ANOVA with Dunnett's post-test (***$P < 0.001$, **$P < 0.01$, *$P < 0.05$ compared to passage-matched AsTC or other conditions as indicated; $^{\#}P < 0.001$ when compared to all conditions tested).

3.3.3.4. AsCT oncogenic phenotype is exacerbated by the long-term co-exposure to As^{III} and PSNPs

To determine whether the aggressiveness of the oncogenic phenotype of AsTC is enhanced after the 12-week-extended exposure to As^{III}, PSNPs or the combination As^{III}/PSNPs, several carcinogenesis markers were evaluated. As shown in Figure 5, certain level of morphological changes are evidenced by the increase in the proportion of spindle-like cells in the culture of PSNPs- and As^{III}-exposed cells and in those subjected to the co-exposure in comparison to both non-exposed controls and AsTC.

At a functional level, the soft-agar assay showed a significant 6-fold increase in the number of colonies formed by AsTC under As^{III}/PSNPs exposure settings, when compared with passage-matched or single-exposed AsTC (Figure 6A).

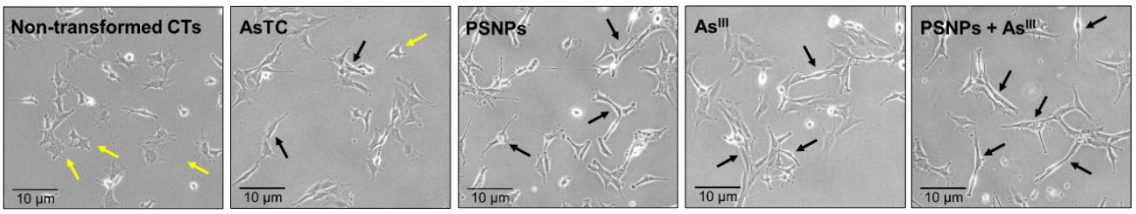

Figure 5: Chronically (co)exposed AsTC morphology evaluation. Representative images of non-transformed MEF cells, non-exposed AsTC, and AsTC after the chronic exposure to 25 µg/mL PSNPs, 2 µM As^{III} and the combination of both As^{III}/PSNPs. Arrows point to cells with evident flattened stellate shape (yellow) or to spindle-like cells (black).

Interestingly, no effects of the chronic PSNPs exposure were observed. Regarding the cells' migrating (Figure 6B) and invading (Figure 6C) potential, PSNP- and As^{III}-exposed cells showed a similar ability to cross the porous membrane and translocate to the basolateral part of the transwell as that of AsTC, while the number of As^{III}/PSNPs co-exposed cells able to migrate and invade, was 2-fold and 3-fold higher, respectively.

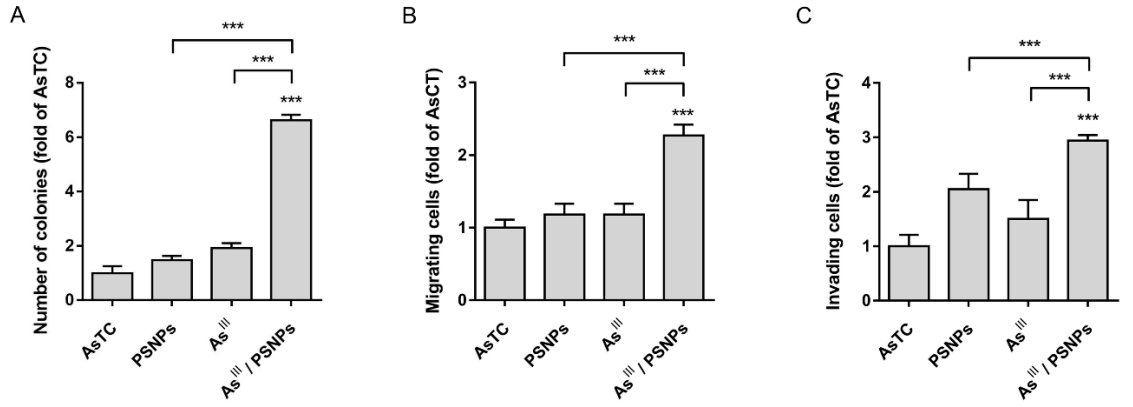

Figure 6: Determination of the *in vitro* transformed phenotype after the chronic (co)exposure. **(A)** Quantitative data derived from the number of colonies formed in the anchorage-independent growth assay. **(B)** Proportion of cells able to translocate to the basolateral side of the transwell in the migration, and **(C)** invasion assay. Data are represented as fold of the mean comparing exposed AsTC with the passage-matched AsTC. Error bars represent SEM. $^{\#}P < 0.001$ when compared to all conditions tested by one-way ANOVA with Dunnett's post-test.

3.3.3.5. The increased aggressiveness of AsTC's oncogenic phenotype is not related with an increasing stem-like cells' population

The cells' capacity to grow as tumorspheres is associated with the presence of stem or progenitor cells in tumor cell populations. When we evaluated if the potential of AsTC to form tumorspheres was exacerbated by the extended PSNPs, As^{III} and combined exposures, no differences were found (Figure 7).

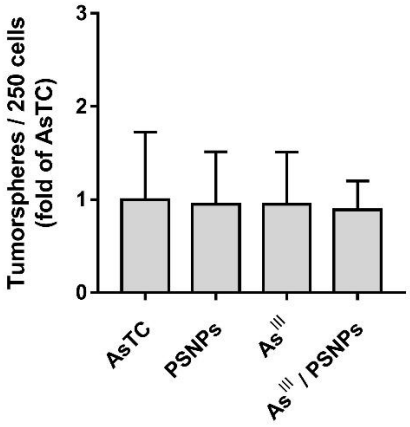

Figure 7: Evaluation of the proportion of stem-like cells in chronically (co)exposed cultures. Number of tumorspheres formed for every 250 AsTC seeded under tumorsphere-inducing conditions. Data are represented as fold of the mean comparing exposed AsTC with the passage-matched AsTC. Error bars represent SEM.

3.3.4. DISCUSSION

The widespread and ever-rising amount of plastic litter is closely linked to the increasing levels of MNPLs found in all environmental compartments. These tiny particles (< 5 mm) are ubiquitously distributed in soil, air, freshwater and marine ecosystems from where they easily enter the trophic chain (Correia-Prata et al., 2020). As a result, humans are believed to be mainly exposed to MNPLs via the ingestion of contaminated food or water, but also through other routes such as inhalation or dermal deposition (Lehner et al., 2019). Under this potential broad human exposure scenario, urgent hazard assessment is required.

Great efforts are being addressed to understanding the environmental and ecotoxicological effects of these emergent contaminants. However, studies based on mammal and human models focusing on the characterization of MNPLs' impact on human health, are still limited (Toussaint et al., 2019). Among those available in the literature, it has been fairly described that MNPLs significantly internalize cells and translocate through physiological barriers (Hesler et al., 2019; Domenech et al., 2020); however, whether this uptake results in a biological impact is not sufficiently clear. While some authors describe a lack of cytotoxic and cytostatic effects (Cortés et al., 2020; Stock et al., 2019), others have reported MNPL-induced ROS production and pro-inflammatory responses *in vitro*, as well as mild histological lesions and metabolic disorders in rodent systems (Yong et al., 2020). Regardless of these disparities, overall, MNPLs are considered to have low acute toxicity. Nonetheless, much remains to be unveiled in terms of MNPLs' long-term effects and their role as carriers of different

environmental pollutants, which is now attracting attention as a potential toxicological risk associated to MNPLs exposure.

In this context, our work contributes to the field in in two ways: (1) by the analysis of the impact of MNPLs and arsenic (co)exposures in the long-term, and (2) by the establishment of a model in which the already damaged genetic background of cells may render them more susceptible to the alterations induced by MNPLs, thus allowing for the detection of typically unnoticed mild effects.

Our selected co-contaminants of study are As^{III} and PSNPs, representative legacy and emergent contaminants, respectively. They share a ubiquitous environmental distribution although both have major implications in terms of human exposure via the intake of contaminated water and, at a lesser proportion, inhalation. As a result, primary target organs (gastrointestinal and respiratory tracts) are potentially affected by both contaminants (Palma-Lara et al., 2020; Stapleton, 2019). Thus, these coexisting contaminants potentially could have a joint impact on human health. Indeed, there is accumulating evidence hinting to arsenic/MNPLs interaction. Arsenic adsorption onto MNPLs has already been reported in debris samples collected from open sea (Prunier et al., 2019). Besides, laboratory studies have confirmed arsenic adsorption onto polystyrene microplastic particles (Dong et al., 2020) and other MNPLs such as polytetrafluoroethylene microparticles (Dong et al., 2019). Accordingly, our data demonstrates that arsenic adsorbs onto single PS particles and it can also form As^{III}/PSNPs aggregates (see Figure 3A). Although the proportion of interactions within our samples are not quantifiable with the use of TEM/EDX, the physical interaction is clear and, thus, the generation of a certain number As^{III}/PSNPs complexes could induce differential effects compared to those of the addition of the arsenic and MNPLs as independent compounds.

Aiming to test the long-term impact of the As^{III}/PSNPs interaction and whether the effects induced by arsenic exposure are exacerbated under a co-exposure scenario, we have evaluated endpoints regarding genotoxicity and carcinogenicity after the chronic (co)exposure of AsTC, our selected *in vitro* model. AsTC derive from MEF cells previously demonstrated to have sensitivity to oxidative stress which is closely linked with genotoxicity, genomic and chromosomal instability, and the eventual transformation driven by 30-weeks of chronic arsenic exposure (Bach et al., 2014, Bach et al., 2016). The compromised genetic background of these cells can be helpful to make more evident the biological impact of MNPLs and their co-exposures.

The high cellular uptake of PSNPs in our system (see Figures 2A and 2B), led us to consider whether the As^{III}/PSNPs interaction would translate into an increased arsenic bioavailability and a higher internalization rate. This phenomenon has already been described upon *in vitro* co-exposures to arsenic and nanoparticles (NPs) such as TiO_2 and SiO_2NPs (Wang et al., 2017; Ahamed et al., 2019). However, as shown in Figure 3B, the levels of arsenic internalized in AsTC remained stable with increasing doses of PSNPs. Therefore, the remarkable genotoxic/oncogenic effects we observed upon As^{III}/PSNPs co-exposure are not due to the PSNP-mediated facilitation of As^{III} uptake, but rather due to potential alterations of the As^{III}/PSNPs at the molecular level.

Among those notable effects of arsenic and MNPLs (co)exposure in our system, we have found a significative induction of both total and oxidative DNA damage. Arsenic is a well-known genotoxic compound and one of its most studied mechanisms-of-action is the induction of ROS and oxidative stress (Jomova et al., 2011). Also, plenty of those studies reporting adverse effects of MNPLs have detected increased ROS levels and DNA damage after short-term exposures (Schirinzi et al., 2017; Ballesteros et al., 2020; Liu et al., 2020; Rubio et al., 2020). Concordantly, in the analysis of the long-term effects of the (co)exposure to PSNPs, As^{III} and As^{III}/PSNPs we found a significant increase in the total and oxidative DNA damage when compared with passage matched AsTC (see Figure 4). Interestingly, the oxidative damage derived from the As^{III}/PSNPs co-exposure is significantly higher than that observed after single exposures (see Figure 4B). This effect of contaminant mixtures enhancing arsenic-induced oxidative stress and genotoxicity has also been recently reported at short-term when analyzing the impact of the coexposure to As^{III}/TiO_2 NPs (Wang et al., 2017), As^{III}/SiO_2 NPs (Ahamed et al., 2019), and the As^{III}/polystyrene microplastics (Wu et al., 2019). Therefore, our results and those from other groups contribute to support the existence of a positive interaction between contaminants.

Remarkably, the positive interaction between As^{III} and PSNPs also adds to the aggressiveness of the arsenic-induced oncogenic phenotype. Arsenic capacity to drive *in vitro* carcinogenicity is well-established (Zhou and Xi, 2018), while this potential aspect of MNPLs long-term impact has not been explored up to date. *In vitro*, a battery cancer hallmarks is evaluated to assess the transformed status of cells (Hanahan and Weinberg, 2011). These include morphological changes, accelerated proliferation, secretome alterations, metastatic potential and deregulation of the differentiation status. The measure of these features has been proven useful to assess arsenic-induced carcinogenesis before (Ganapathy et al., 2019; Person et al., 2015; Tokar et al., 2010). In the present study, all endpoints are met by passage matched AsTC which, as

previously mentioned, display an evident transformed phenotype (Bach et al., 2016). Interestingly, according to our data, these hallmarks remain unchanged for AsTC subjected to 12 weeks of PSNPs or As^{III} single exposure but are significantly enhanced under As^{III}/PSNPs co-exposure settings. The increment on the proportion of spindle-like cells within the population (see Figure 5), and specially the dramatic increased capacity of cells to grow independently of anchorage (see Figure 6A), migrate (see Figure 6B) and invade (see Figure 6C) confirm the co-exposure-mediated acquisition of a further aggressive transformed phenotype. To further characterize the oncogenic phenotype of the (co)exposed AsTC, we have evaluated their tumorsphere-forming ability as a marker of the stemness status in our cell population; given the existing evidence linking the conversion of non-stem cells to cancer stem cells with carcinogenesis (Afify and Seno, 2019) and, specifically, arsenic-induced carcinogenesis (Ngalame et al., 2018; Ooki et al., 2018; Z. Wang et al., 2020; Xiao et al., 2018). However, we did not find significative difference under the different exposure scenarios tested, thus stemness induction seems not to be the mechanism by which As^{III}/PSNPs promotes tumor aggressiveness. Taken together, these findings highlight the urgent need to explore MNPLs' long-term effects and their potential role as co-carcinogens.

3.3.5. CONLCUSIONS

As a summary, in the present work we have demonstrated that the long-term concurrent exposure to subtoxic doses of arsenic and PSNPs significantly enhances the arsenic-associated aggressive transformed phenotype and genotoxicity. Further, we have demonstrated that PSNPs and arsenic physically interact. However, this interaction is not associated to an increased arsenic bioavailability and, therefore, the mechanism by which PSNPs add to arsenic's impact requires further research. Importantly, while the evaluation of single exposure to MNPLs effects is still of great relevance, it is also necessary to ask whether together with other contaminants new differential effects arise. Indeed, our results support considering co-exposure scenarios as an essential part on emergent pollutants' hazard assessment.

Acknowledgments

We wish to thank Mr. C. Valiente for his technical assistance. This work was supported by the *Universitat Autònoma de Barcelona* [PIF-UAB to I.B. and J.D.] and the Spanish Ministry of Education and Science [BFU2016-76831-R].

Competing financial interests

The authors declare they have no actual or potential competing financial interests.

3.3.6. REFERENCES

Afify, S. M., & Seno, M. (2019). Conversion of stem cells to cancer stem cells: Undercurrent of cancer initiation. *Cancers, 11*(3), 1–19.

Ahamed, M., Akhtar, M. J., & Alhadlaq, H. A. (2019). Co-exposure to SiO2 nanoparticles and arsenic induced augmentation of oxidative stress and mitochondria-dependent apoptosis in human cells. *International Journal of Environmental Research and Public Health, 16*(17).

Bach, J., Sampayo-Reyes, A., Marcos, R., & Hernández, A. (2014). Ogg1 genetic background determines the genotoxic potential of environmentally relevant arsenic exposures. *Archives of Toxicology, 88*(3), 585–596.

Bach, J., Peremartí, J., Annangi, B., Marcos, R., & Hernández, A. (2016). Oxidative DNA damage enhances the carcinogenic potential of in vitro chronic arsenic exposures. *Archives of Toxicology, 90*(8), 1893–1905.

Ballesteros, S., Domenech, J., Barguilla, I., Cortés, C., Marcos, R., & Hernández, A. (2020). Genotoxic and immunomodulatory effects in human white blood cells after ex vivo exposure to polystyrene nanoplastics. *Environmental Science: Nano. 7*, 3431-3446.

Bouwmeester, H., Hollman, P. C. H., & Peters, R. J. B. (2015). Potential Health Impact of Environmentally Released Micro- and Nanoplastics in the Human Food Production Chain: Experiences from Nanotoxicology. *Environmental Science and Technology, 49*(15), 8932–8947.

Brandon, J. A., Freibott, A., & Sala, L. M. (2020). Patterns of suspended and salp-ingested microplastic debris in the North Pacific investigated with epifluorescence microscopy. *Limnology and Oceanography Letters, 5*(1), 46–53.

Correia-Prata, J., da Costa, J. P., Lopes, I., Duarte, A. C., & Rocha-Santos, T. (2020). Environmental exposure to microplastics: An overview on possible human health effects. *Science of the Total Environment, 702*, 134455.

Cortés, C., Domenech, J., Salazar, M., Pastor, S., Marcos, R., & Hernández, A. (2020). Nanoplastics as a potential environmental health factor: Effects of polystyrene nanoparticles on human intestinal epithelial Caco-2 cells. *Environmental Science: Nano, 7*(1), 272–285.

Domenech, J., Hernández, A., Rubio, L., Marcos, R., & Cortés, C. (2020). Interactions of polystyrene nanoplastics with in vitro models of the human intestinal barrier. *Archives of Toxicology, 94*(9), 2997–3012.

Dong, Y., Gao, M., Song, Z., & Qiu, W. (2019). Adsorption mechanism of As(III) on polytetrafluoroethylene particles of different size. *Environmental Pollution, 254*, 112950.

Dong, Y., Gao, M., Song, Z., & Qiu, W. (2020). As(III) adsorption onto different-sized polystyrene microplastic particles and its mechanism. *Chemosphere, 239*, 124792.

EFSA. (2016). Presence of microplastics and nanoplastics in food, with particular focus on seafood. *EFSA Journal, 14*(6), 1-30 .

Ganapathy, S., Liu, J., Xiong, R., Yu, T., Makriyannis, A., & Chen, C. (2019). Chronic low dose arsenic exposure preferentially perturbs mitotic phase of the cell cycle. *Genes and Cancer, 10*(1–2), 39–51.

Godoy, V., Blázquez, G., Calero, M., Quesada, L., & Martín-Lara, M. A. (2019). The potential of microplastics as carriers of metals. *Environmental Pollution, 255*(Pt 3):113363.

Hanahan, D., & Weinberg, R. A. (2011). Hallmarks of cancer: The next generation. *Cell, 144*(5), 646–674.

Hesler, M., Aengenheister, L., Ellinger, B., Drexel, R., Straskraba, S., Jost, C., Wagner, S., Meier, F., von Briesen, H., Büchel, C., Wick, P., Buerki-Thurnherr, T., & Kohl, Y. (2019). Multi-endpoint toxicological assessment of polystyrene nano- and microparticles in different biological models in vitro. *Toxicology in Vitro, 61*(May), 104610.

Hüffer, T., & Hofmann, T. (2016). Sorption of non-polar organic compounds by micro-sized plastic particles in aqueous solution. *Environmental Pollution, 214*, 194–201.

IARC (2012). Arsenic, metals fibres and dusts. Monographs on the evaluation of carcinogenic risk to humans. *Int. Agency. Res. Cancer, 100*, 407–443.

Jomova, K., Jenisova, Z., Feszterova, M., Baros, S., Liska, J., Hudecova, D., Rhodes, C. J., & Valko, M. (2011). Arsenic: Toxicity, oxidative stress and human disease. *Journal of Applied Toxicology, 31*(2), 95–107.

Lehner, R., Weder, C., Petri-Fink, A., & Rothen-Rutishauser, B. (2019). Emergence of Nanoplastic in the Environment and Possible Impact on Human Health. *Environmental Science and Technology, 53*(4):1748-1765.

Li, Y., Ling, M., Xu, Y., Wang, S., Li, Z., Zhou, J., Wang, X., & Liu, Q. (2010). The repressive effect of NF-κB on p53 by mot-2 is involved in human keratinocyte transformation induced by low levels of arsenite. *Toxicological Sciences, 116*(1), 174–182.

Li, W. C., Tse, H. F., & Fok, L. (2016). Plastic waste in the marine environment: A review of sources, occurrence and effects. *Science of the Total Environment, 566–567*, 333–349.

Lin, W., Jiang, R., Wu, J., Wei, S., Yin, L., Xiao, X., Hu, S., Shen, Y., & Ouyang, G. (2019). Sorption properties of hydrophobic organic chemicals to micro-sized polystyrene particles. *Science of the Total Environment, 690*, 565–572.

Liu, Z., Huang, Y., Jiao, Y., Chen, Q., Wu, D., Yu, P., Li, Y., Cai, M., & Zhao, Y. (2020). Polystyrene nanoplastic induces ROS production and affects the MAPK-HIF-1/NFkB-mediated antioxidant system in Daphnia pulex. *Aquatic Toxicology, 220*(November 2019), 105420.

Massos, A., & Turner, A. (2017). Cadmium, lead, and bromine in beached microplastics. *Environmental Pollution, 227*, 139–145.

Ngalame, N. N. O., Luz, A. L., Makia, N., & Tokar, E. J. (2018). Arsenic alters exosome quantity and cargo to mediate stem cell recruitment into a cancer stem cell-like phenotype. *Toxicological Sciences, 165*(1), 40–49.

Ooki, A., Begum, A., Marchionni, L., Vandenbussche, C. J., Mao, S., Kates, M., & Hoque, M. O. (2018). Arsenic Promotes the COX2/PGE2-SOX2 Axis to Increase the Malignant Stemness Properties of Urothelial Cells. *International Journal of Cancer, 143*(1), 113–126.

Palma-Lara, I., Martínez-Castillo, M., Quintana-Pérez, J. C., Arellano-Mendoza, M. G., Tamay-Cach, F., Valenzuela-Limón, O. L., García-Montalvo, E. A., & Hernández-Zavala, A. (2020). Arsenic exposure: A public health problem leading to several cancers. *Regulatory Toxicology and Pharmacology, 110*, 104539.

Person, R. J., Olive Ngalame, N. N., Makia, N. L., Bell, M. W., Waalkes, M. P., & Tokar, E. J. (2015). Chronic inorganic arsenic exposure in vitro induces a cancer cell phenotype in human peripheral lung epithelial cells. *Toxicology and Applied Pharmacology, 286*(1), 36–43.

Pi, J., Diwan, B. A., Sun, Y., Liu, J., Qu, W., He, Y., Styblo, M., & Waalkes, M. P. (2008). Arsenic-induced malignant transformation of human keratinocytes: Involvement of Nrf2. *Free Radic Biol Med, 45*(5), 651–658.

Prunier, J., Maurice, L., Perez, E., Gigault, J., Pierson Wickmann, A. C., Davranche, M., & Halle, A. ter. (2019). Trace metals in polyethylene debris from the North Atlantic subtropical gyre. *Environmental Pollution, 245*, 371–379.

Ravenscroft, P., Brammer, H., & Richards, K. (2009). Arsenic Pollution. In Arsenic Pollution: A Global Synthesis. Wiley-Blackwell. A John Wiley and Sons Ltd.

Rubio, L., Barguilla, I., Domenech, J., Marcos, R., & Hernández, A. (2020). Biological effects, including oxidative stress and genotoxic damage, of polystyrene nanoparticles in different human hematopoietic cell lines. *Journal of Hazardous Materials, 398*(April), 122900.

Schirinzi, G. F., Pérez-Pomeda, I., Sanchís, J., Rossini, C., Farré, M., & Barceló, D. (2017). Cytotoxic effects of commonly used nanomaterials and microplastics on cerebral and epithelial human cells. *Environmental Research, 159*(June), 579–587.

Shearer, M. J. J., Wold, E. A., Umbaugh, C. S., Lichti, C. F., Nilsson, C. L., & Figueiredo, M. L. (2016). Inorganic arsenic-related changes in the stromal tumor microenvironment in a prostate cancer cell-conditioned media. *Environmental Health Perspectives, 124*(7), 1009–1015.

Smedley, P. L., & Kinniburgh, D. G. (2002). A review of the source, behaviour and distribution of arsenic in natural waters. Applied Geochemistry, 17, 517–568.

Stapleton. (2019). Toxicological considerations of nano-sized plastics. AIMS *Environmental Science, 6*(5), 367–378.

Stock, V., Böhmert, L., Lisicki, E., Block, R., Cara-Carmona, J., Pack, L. K., Selb, R., Lichtenstein, D., Voss, L., Henderson, C. J., Zabinsky, E., Sieg, H., Braeuning, A., & Lampen, A. (2019). Uptake and effects of orally ingested polystyrene microplastic particles in vitro and in vivo. *Archives of Toxicology, 93*(7), 1817–1833.

Stueckle, T. A., Lu, Y., Davis, M. E., Wang, L., Jiang, B.-H., Holaskova, I., Schafer, R., Barnett, J. B., & Rojanasakul, Y. (2012). Chronic occupational exposure to arsenic induces carcinogenic gene signaling networks and neoplastic transformation in human lung epithelial cells. *Toxicology and Applied Pharmacology, 61*(2), 204–216.

Tokar, E. J., Diwan, B. A., & Waalkes, M. P. (2010). Arsenic exposure transforms human epithelial stem/progenitor cells into a cancer stem-like phenotype. Environmental Health Perspectives, 118(1), 108–115.

Toussaint, B., Raffael, B., Angers-Loustau, A., Gilliland, D., Kestens, V., Petrillo, M., Rio-Echevarria, I. M., & Van den Eede, G. (2019). Review of micro- and nanoplastic contamination in the food chain. Food Additives and Contaminants - Part A Chemistry, Analysis, Control, Exposure and Risk Assessment, 36(5), 639–673.

Treas, J., Tyagi, T., & Singh, K. P. (2013). Chronic exposure to arsenic, estrogen, and their combination causes increased growth and transformation in human prostate epithelial cells potentially by hypermethylation-mediated silencing of MLH1. *Prostate, 73*(15), 1660–1672.

Wang, X., Liu, Y., Wang, J., Nie, Y., Chen, S., Hei, T. K., Deng, Z., Wu, L., Zhao, G., & Xu, A. (2017). Amplification of arsenic genotoxicity by TiO2 nanoparticles in mammalian cells: new insights from physicochemical interactions and mitochondria. *Nanotoxicology, 11*(8), 978–995.

Wang, Z., Yang, P., Xie, J., Lin, H. P., Kumagai, K., Harkema, J., & Yang, C. (2020). Arsenic and benzo[a]pyrene co-exposure acts synergistically in inducing cancer stem cell-like property and tumorigenesis by epigenetically down-regulating SOCS3 expression. *Environment International, 137*(February), 105560.

Wu, B., Wu, X., Liu, S., Wang, Z., & Chen, L. (2019). Size-dependent effects of polystyrene microplastics on cytotoxicity and efflux pump inhibition in human Caco-2 cells. *Chemosphere, 221*, 333–341.

Xiao, T., Xue, J., Shi, M., Chen, C., Luo, F., Xu, H., Chen, X., Sun, B., Sun, Q., Yang, Q., Dai, X., Zhang, A., Tang, H., & Liu, Q. (2018). Circ008913, via miR-889 regulation of DAB2IP/ZEB1, is involved in the arsenite-induced acquisition of CSC-like properties by human keratinocytes in carcinogenesis. *Metallomics, 10*(9), 1328–1338.

Xu, Y., Tokar, E. J., & Waalkes, M. P. (2014). Arsenic-induced cancer cell phenotype in human breast epithelia is estrogen receptor-independent but involves aromatase activation. *Archives of Toxicology, 88*(2), 263–274.

Xu, M., Halimu, G., Zhang, Q., Song, Y., Fu, X., Li, Y., Li, Y., & Zhang, H. (2019). Internalization and toxicity: A preliminary study of effects of nanoplastic particles on human lung epithelial cell. *Science of the Total Environment, 694*, 133794.

Yong, C. Q. Y., Valiyaveetill, S., & Tang, B. L. (2020). Toxicity of microplastics and nanoplastics in Mammalian systems. *International Journal of Environmental Research and Public Health, 17*(5), 1509.

Zhou, Q., & Xi, S. (2018). A review on arsenic carcinogenesis: Epidemiology, metabolism, genotoxicity and epigenetic changes. *Regulatory Toxicology and Pharmacology, 99*(September), 78–88.

4. DISCUSSION

4. DISCUSSION

Arsenic is a naturally occurring pollutant ubiquitously distributed in all environmental compartments: soil, air, and mainly water. Worldwide, more than 200 million people (WHO, 2019) are subjected to arsenic exposure mainly via the consumption of arsenic-containing water as well as crops cultivated in arsenic-contaminated soil or irrigated with contaminated water (Arslan et al., 2017). The exposed populations are at a high risk of developing diverse pathologies and, most importantly, several types of cancer, including skin, lung, bladder, kidney, and liver cancers (IARC, 2012). Therefore, arsenic's unavoidable presence in nature, widespread exposure potential and severe adverse effects on human health calls for an in-depth risk assessment. To achieve this, it is essential to expand the existing knowledge of arsenic mechanisms-of-action as an environmental contaminant.

Over time, the experimental approaches for the evaluation of arsenic mechanisms-of-action and effects have adapted, aiming to emulate the actual environmental exposure conditions. Indeed, *in vitro* models have gradually become more sophisticated and new cell biology techniques have allowed a great contribution to the knowledge base regarding the carcinogenic potential of multiple compounds, including arsenic (Breheny et al., 2011). Around 20 years ago, pioneer studies in the arsenic field established a new experimental design based on the use of *in vitro* models subjected to the chronic exposure to subtoxic doses of arsenic (Zhao et al., 1997; Achanzar et al., 2002). Since then, our group and many others have followed this approach, centering the attention on the study of long-term arsenic-induced carcinogenesis. Indeed, the model developed in our group by Bach et al. (2016), based on MEF cells sensitive to oxidative stress, evidenced the relevant role of arsenic-induced oxidative damage in the genotoxicity and carcinogenicity derived from the chronic exposure to arsenic. In such model, cells were chronically exposed to 2 μM As^{III} for up to 50 weeks, reaching transformation after 20-30 weeks of exposure. At that time-point, cells developed the defining features of an *in vitro* oncogenic phenotype, showing an acquired spindle-like cell morphology, an enhanced anchorage-independent cell growth capacity and invasive potential, the de-regulation of the expression of central genes in the cell differentiation program -*c-myc*, *Oct3/4*, *Notch2*, *Sox2*, *Nanog,* and *Klf4*-, and an oncogenic secretome with increased activity of matrix metalloproteinases MMP2+9, which functionally influence tumor growth and invasiveness. This model was extended by our group to evaluate the effects of different nanomaterials (Rubio et al., 2018; Barguilla et al., 2020) and it has also been used in the

work presented in this Thesis, aiming to gain further insight in the role of central drivers involved in arsenic-induced genotoxicity and carcinogenesis.

Thus, in the field of arsenic carcinogenesis, the long-term experimental approach has been of great use for the identification of mechanisms-of-action, key elements and alterations distinctive of the oncogenic process derived from this environmental exposure.

The most classically explored mechanism is arsenic-induced oxidative stress and genotoxicity (Flora, 2011). Kojima and colleagues were the first to describe an association between the oxidative damage generated during the arsenic biotransformation process and the oncogenic transformation of cell lines chronically exposed to low As^{III} doses. Interestingly, they described a progressive increase of ODD in the chronically exposed cells, associated with an acceleration in the development of the oncogenic phenotype. In their work, once the rat liver TRL1215 cells reached a transformed status at week 18 of 1 µM As^{III} exposure, the ODD was significantly reduced reaching basal levels (Kojima et al., 2009). Later, Tokar et al. (2014) found similar variations of the ODD levels as the human prostate epithelial RWPE-1 cells acquired a transformed phenotype during 20 weeks of chronic exposure to subtoxic MMA^{III} doses. However, none of these studies found a conclusive mechanistic explanation to the cells' acquired resistance to arsenic genotoxic effects. Further, other authors have reported alterations in arsenic-induced ROS levels during the cells' transformation driven by the chronic exposure. As a representative example, Chang et al. (2010) chronically exposed human bronchial epithelial BEAS-2B cells for 24 weeks to subtoxic As^{III} doses until they reached transformation. Then, they reported lower ROS levels in transformed cells than in non-transformed BEAS-2B, suggesting that the overexpression of SOD-2 and catalase antioxidant enzymes was responsible for this event. Although the increased intracellular ROS levels are not always necessarily linked to genotoxicity, DNA damage is a potential outcome induced by ROS production. Thus, that study also hints towards the development of adaptive responses that render the cells more resistant to oxidative stress after transformation.

In this context, the work presented in Chapter 1 of this Thesis complements those studies aiming to explain the ODD and genotoxicity levels variations during the long-term arsenic exposure of the previously presented MEF model cells chronically exposed by Bach et al. (2016). Concordantly with the data obtained by Kojima et al. (2009) and Tokar et al. (2014) we have described that the ODD and genotoxic levels peak at the cells' transformation point, as demonstrated by the comet assay and the MN frequency,

respectively. Then, both ODD and chromosomal damage decreased reaching basal levels similar to those in the early weeks of 2 μM As^{III} exposure. The lack of mechanistic exploration for this event in the literature led us to evaluate the potential role of AS3MT in the progressive increment of DNA damage, and that of MTH1 in its decline.

Regarding the increasingly growing levels of DNA damage, we have focused our efforts in exploring the part played by AS3MT, the key enzyme in the arsenic biotransformation process, closely linked to oxidative stress induction (Hughes et al., 2011). Remarkably, we observed a pattern of AS3MT expression over the weeks of exposure that mimicked the DNA damage behavior; that is, AS3MT expression gradually increased up to the transformation point and then decreased to basal levels. Moreover, its stable inhibition by shRNA significantly reduced the levels of ODD and genotoxicity observed before the transformation point. Our results show that cells overexpress AS3MT to enhance arsenic biotransformation and reduce its cytotoxicity, which in turn, exacerbates arsenic genotoxicity presumably by increasing ROS levels and generating highly reactive intermediate metabolites (Tokar et al., 2014). Thus, a central role of AS3MT in the early stages of arsenic-induced carcinogenesis was demonstrated as it plays an important part in the progressive accumulation of DNA damage and oxidative stress. This role of AS3MT is supported by a recent work showing that AS3MT is overexpressed in an arsenic-exposed cohort, in non-small cell lung cancer (NSCLC) tissues, and also in the human NSCLC cell line (A549). Interestingly, these authors suggest that AS3MT overexpression by arsenic directly influences NSCLC progression by altering the expression of cell cycle genes including *p21*, *CDKs* and several cyclins which enhance cell proliferation, a characteristic feature of early carcinogenesis (Sun et al., 2020).

The decrease in DNA damage levels after the cells' transformation point is an observation that agrees with the arsenic tolerance described by different authors and that has been associated with the acquisition of an apoptotic-resistant phenotype linked to the eventual progression to carcinogenesis (Brambila et al., 2002; Qu et al., 2002; Pi et al., 2005). While antioxidant factors are mainly proposed in the literature as drivers for this adaptation (Flora, 2011), in the work presented in Chapter 1, we aimed to evaluate the potential role of MTH1 in this event, given its essential function preventing DNA damage by sanitizing the oxidized nucleotides from the cells' reservoirs (Markkanen, 2017). *Mth1* expression alterations have previously been described upon short-term exposure to different environmental contaminants such as radon (Nie et al., 2012), particulate matter (Li et al., 2017a), or 1-nitropyrene (Li et al., 2017b). However, to our knowledge, we have been the first to explore its role under long-term exposure settings and in relationship with arsenic-induced carcinogenesis. When monitoring *Mth1*

expression levels throughout the weeks of chronic-arsenic exposure we observed a remarkable overexpression at weeks 40 and 50, while basal levels were detected before the transformation point. Therefore, we proposed that the cells trigger *Mth1* overexpression to reduce the levels of DNA damage induced by the long-term arsenic exposure. This was confirmed by the stable inhibition of *Mth1* expression which led to the rebound of high DNA damage levels.

Importantly, we have also described the essential role of MTH1 for the development of an oncogenic phenotype. In our study, *Mth1* inhibition in arsenic-transformed cells led to a reduction of the aggressiveness of the exposed cells phenotype, evidenced by the cells' decreased ability to grow independently of anchorage, and the reduced migrating and invading potential. Accumulating evidence in the literature shows that *MTH1* overexpression allows tumoral cells to overcome the redox imbalance and high levels of DNA damage inherent to the carcinogenic process and, thus, it is suggested that MTH1 inhibition prevents cancer progression (Gad et al., 2014; Warpman Berglund et al., 2016; Rai & Sobol, 2019). As a representative example, a very recent study by (Moukengue et al., 2020) showed that both osteosarcoma patients and cell lines overexpressed *MTH1*. The chemical inhibition of MTH1 compromised the cells' viability *in vitro*, which correlated with a reduced tumor growth and metastatic potential *in vivo*; therefore, these authors propose the use of the tested inhibitor as a therapeutic option. Likewise, it has been reported that MTH1 inhibition impedes mesothelioma progression *in vivo* (Magkouta et al., 2020), reduces the migrating and invading capacity of gastric cancer cell lines (Zhan et al., 2020), suppresses the rapid proliferation of esophageal squamous carcinoma cells (Wang et al., 2020), compromises the progression of breast cancer (Zhang et al., 2017) and glioblastoma (Tu et al., 2016) cells *in vivo* and *in vitro*. Thus, many studies have focused on the exploration of the effects induced by MTH1 inhibition on multiple cancer models, however, MTH1 relevance for tumor development and aggressiveness had never been defined in the context of arsenic-induced transformation until now. Further, our findings set *Mth1* as a potential biomarker of arsenic carcinogenesis, as arsenic-exposed cells are expected to increase its expression once malignant transformation has occurred.

As indicated before, much of the attention in the arsenic carcinogenesis field has classically been centered in its potential to induce oxidative stress, which still contributes with valuable data on arsenic-induced effects, as shown in this work. Nonetheless, arsenic's adverse impact is not attributable to a single mechanism-of-action but to an array of different effects intertwined with each other that produce enough alterations within the cell to induce its transformation. Therefore, in the recent years, the interest in

evaluating the influence of mechanisms of carcinogenesis, other than those related to oxidative stress and genotoxicity, has grown. Interestingly, accumulating evidence indicates that arsenic-induced genomic deregulation may involve epigenetic modifications, miRNA alterations, and transcription factor dysregulation, which seem crucial for the development of an oncogenic phenotype (Eckstein et al., 2017).

Although the epigenetic changes induced by arsenic exposure are not within the scope of the experimental work presented in this Thesis, it is relevant to point out the recent advances in this regard. On the one hand, arsenic exposure can cause global DNA hypomethylation due to SAM deficiency as a result of the arsenic metabolization process. During arsenic biotransformation, AS3MT transfers a methyl group from SAM to the arsenic species during several rounds of oxidative methylation, thus, reducing the pool of methyl groups available in the cell. Given that DNA methylation is one of the main mechanisms for the cell to control gene expression and maintain genome integrity, the altered methylation status involves changes in the expression pattern of many genes, including those involved in cell differentiation, proliferation, and development (Zhou & Xi, 2018). Besides, arsenic exposure also affects histone post-translational modifications, that have an essential role in chromatin remodeling. Arsenic-mediated alterations on the methylation, acetylation, phosphorylation, and polyadenylation of histones, (e.g. H3K9, H3S10, or H3.1) in different tissues can modify gene expression regulation (Chen et al., 2019), and some are so characteristic that the creation of an arsenic signature panel has been suggested to help in early prognosis (Bhattacharjee & Paul, 2020). Further, arsenic can deregulate the expression of a variety of miRNAs potentially involved in arsenic-induced carcinogenesis. As examples, *in vitro* chronic arsenic exposure leads to the downregulation of the tumor suppressor miR-200 in bladder and skin cell lines, the upregulation of the tumor promoting miR-155 in lung cells and, importantly, the overexpression of the oncogenic miR-21 in skin, lung, and liver cells (Cardoso et al., 2018).

In addition to epigenetic marks, transcription factors (TFs) are other major players in the control of gene expression to maintain cellular homeostasis. Complex signal transduction pathways condition the functionality of TFs which regulate the expression of multiple genes involved in essential cellular processes such as proliferation, differentiation, apoptosis, and many others. Having such a central role in cell status regulation, it is straightforward that TFs also play an essential part in carcinogenesis (Vishnoi et al., 2020). Arsenic exposure is known to alter multiple TFs-related transduction pathways either via direct protein binding or due to the generalized stress status induced which triggers the exposed cells' response (Shen et al., 2013).

Accumulating evidence shows arsenic's potential to induce alterations in the signaling, expression and function of important oxidative stress response TFs like NF-κB, Nrf2, and AP-1. This dysregulation has been proposed as a potential mechanism of arsenic carcinogenesis and, thus, with the work presented in Chapter 2 we aimed to contribute to the existing knowledge on this aspect.

In the literature, it has been reported that the short-term exposure to high doses of arsenic (>10 μM) inhibits NF-κB, triggering a cytotoxic effect; whereas the chronic exposure to subtoxic doses (<10 μM) induces its activation (Druwe & Vaillancourt, 2010) which protects the cells from the oxidative stress and enhances proliferation, promoting tumoral cell progression (Reuter et al., 2010). Likewise, it has been proposed that long-term arsenic exposure leads to the onset of tumorigenesis due to the sustained Nrf2 upregulation. In this respect, the studies carried out by Wu et al. (2019a) and Schmidlin et al. (2020) are noteworthy. Schmidlin and colleagues compared the effects induced by 12 weeks of chronic 0.5 μM As^{III} exposure on Nrf2 knock-out (KO) BEAS-2B cells and their isogenic wild-type (WT) counterparts. Interestingly, they found that WT cells displayed higher proliferation, colony formation, migration, and invasion potentials than those of KO cells, which behave similarly to non-exposed BEAS-2. Therefore, these authors showed that Nrf2 axis contributes to the transformation and tumor invasiveness in a chronic arsenic-induced lung cancer model (Schmidlin et al., 2020). In turn, Wu et al. (2019a) continuously exposed human keratinocytes (HaCaT) to 100 nM As^{III} for 30 weeks until the cells reached a transformed phenotype, characterized by an enhanced anchorage-independent growth ability and high Nrf2 expression levels. When analyzing the effects of silencing Nrf2 they found a significant decrease in the cells' invasion capacity and colony-forming ability; thus, concluding that inhibiting Nrf2 expression during long-term exposure to low doses of arsenite prevents from malignant transformation. Considering these relevant results, it is important to point out that the applicability of chronic exposure approaches is evident in the studies aiming to evaluate the role of arsenic in TFs dysregulation and the functional consequences derived, such as the acquired resistance and the development of an aggressive transformed phenotype.

In contrast with the extensive published research available regarding Nrf2 and NF-κB, few studies have evaluated AP-1 and its signaling axis under arsenic-exposure scenarios, and in relationship with arsenic-induced transformation. AP-1 is an important member of the stress response TFs family involved in the regulation of cell differentiation, survival, proliferation, migration, and transformation (Vesely et al., 2009). Among the most relevant data regarding AP-1 in a context of arsenic exposure, it is noteworthy that

its overexpression has been reported as involved in the arsenic-related apoptotic resistant phenotype of a lung cell line (Aodengqimuge et al., 2014); its DNA binding activity is enhanced by arsenic exposure in bladder cells (Drobná et al., 2003); and this increased activity seems to play an essential part in the MEF cells' transformation after 4 weeks of low-level arsenic exposure (Kim et al., 2016).

AP-1 is a dimeric basic leucine zipper (bZIP) TF that can be formed by different combinations of Fos, Jun, ATF, and MAF family proteins, FRA1 being one of its most common components (Talotta et al., 2020). Thus, for the study presented in Chapter 2, we aimed to describe the role of FRA1 in arsenic carcinogenesis using our chronically exposed MEF model. In line with the works on Nrf2 involvement in arsenic-induced cell transformation mentioned above, we monitored the levels of FRA1, as well as upstream and downstream components of its regulatory axis, at different time-points during 50 weeks of continuous As^{III} exposure. Then, we evaluated the effects produced by FRA1 knock-down on the defining features of the arsenic-induced transformed phenotype.

FRA1 levels are low on normal tissue, but it is frequently overexpressed in tumors. The abnormal expression of FRA1 has been widely explored in multiple cancers including breast, colorectal, lung, cervical, ovarian, and skin cancers, where it is associated with malignant progression and enhanced invasiveness (Jiang et al., 2020). Accordingly, we found that FRA1 is progressively upregulated both at mRNA and protein levels during the weeks of chronic-arsenic exposure, as cells acquire a transformed phenotype. Together with increasing levels of FRA1, we described a correlative upregulation of RAS, ERK and p38 activity but not JNK or c-MET. All these proteins have previously been described as upstream components of FRA1 signaling axis. Also, they are required for FRA1 activation and stabilization via phosphorylation (Jiang et al., 2020; Talotta et al., 2020), and have previously been linked with arsenic-induced effects in different studies. Some authors have shown arsenic's potential to increment ERK, p38, and JNK expression and activity (Dong, 2002; Person et al., 2015; Kim et al., 2016), while RAS is a well-known arsenic target involved in the exposed cells transformation onset and progression (Ngalame et al., 2014; Zhou et al., 2018; Soza-Ried et al., 2019), and c-MET is overexpressed under long-term arsenic trioxide exposure conditions (Kryeziu et al., 2016).

Given that FRA1 has different roles in cancer cell proliferation, survival, EMT, and metastasis (Talotta et al., 2020), its stimulation is a relevant outcome of chronic arsenic exposure. Thus, we aimed to evaluate the impact that it has on the phenotype of exposed cells, and its potential role as a mechanism involved in the arsenic carcinogenesis.

Starting with the transcriptional alterations induced by arsenic-associated FRA1 overexpression, we described the deregulation of different target genes including tumor suppressors, TGF*β* family genes, and EMT-TFs. During the long-term As^{III} exposure, we found a significant downregulation of *Pten*, *Pdcd4*, and *Tmp1*, three relevant tumor suppressors generally highly expressed in non-transformed cells but downregulated during carcinogenesis. This outcome supports the role of FRA1 as an oncogenic driver in arsenic carcinogenesis and agrees with the results in several studies. For instance, Luo et al. (2015) described the decreased expression of *PDCD4* in human bronchial epithelial cells (HBE) which acquired an increased invading and EMT potential after a 5-week exposure to 1 mM As^{III}. Likewise, other authors reported the downregulation of both *PTEN* and *PDCD4* at 15 weeks of 1 mM As^{III} exposure in human embryo lung fibroblasts (HELF) (Ling et al., 2012); and that after a 24-week exposure to 500 nM As^{III}, non-tumoral breast epithelial cells (MCF-10A) acquired a malignant phenotype characterized by the increased colony formation ability, MMP2+9 secretion, invasion potential and *p53* and *PTEN* suppression (Xu et al., 2013). Regarding TGF*β* family genes, we found a progressive upregulation and downregulation of *Tgfβ1* and *Tgfβ2* respectively during the chronic As^{III} exposure, which we propose to be associated with the promotion of the oncogenic phenotype given that TGFβ1 generally acts as a tumor promoter, while TGFβ2 is a tumor suppressor (Levy & Hill, 2006). The role of TGF*β* in arsenic carcinogenesis has not been widely explored in the literature, but it is interesting to point out that it has been proposed that the deregulation of TGF*β* family members leads to altered EMT capacity of arsenic-exposed murine epicardial cells, in the context of arsenic-induced cardiac disorders (Allison et al., 2013). Lastly, we observed an increase in the expression of *Snail, Twist*, *Zeb1,* and *Zeb2* in the transformed cells after 30 weeks of continuous As^{III} exposure which supports the role of FRA1 in the acquisition of the arsenic-induced aggressive phenotype. Accordingly, other studies have demonstrated the alteration of different EMT-TFs upon arsenic exposure, which contribute to the metastatic potential of the transformed cells. As representative examples, the work by Luo et al. (2015) et al. mentioned above showed that the acquisition of a metastatic potential upon chronic arsenic exposure occurs via Twist upregulation; while Jiang et al. (2013b) reported a significant increment in the levels of Snail after chronically exposing human keratinocytes (HaCAT) to 1 µM As^{III} for 5 weeks.

At a functional level, we have demonstrated that arsenic-induced FRA1 stimulation is a key contributor to the malignant transformation. Upon FRA1 stable inhibition, we found a significant decrease in the aggressiveness of the oncogenic phenotype induced by arsenic long-term exposure, evidenced by the marked reduction on the proliferation rate,

the decrease in the anchorage-independent cell growth, and the loss of migrating and invading potentials of knock-down cells when compared to the FRA1-expressing counterparts. This remarkable impact of FRA1 inhibition on the attenuation of the transformed cells' aggressiveness was described in our study for the first time; nonetheless, it agrees with the outcomes derived from the inhibition of important contributors to arsenic-induced tumoral onset and progression such as Nrf2, as previously mentioned (Wu et al., 2019a; Schmidlin et al., 2020), or MTH1 as described by us in the first chapter of this Thesis.

Interestingly, we have also shown that FRA1 knock-down reduced the senescent status of the exposed cells. Senescence is a poorly explored outcome in the context of arsenic exposure except for the reported increase in the proportion of senescent chondrocytes related with arsenic-induced cartilage ageing (Chung et al., 2020). Therefore, further research focused on this aspect of arsenic effects would be compelling given the recent interest raised by the potential role of the senescent-associated secretory phenotype as an important player in tumor growth promotion, relapse, and metastasis (Campisi, 2013; Prieto & Baker, 2019).

Further, we aimed to examine the role of FRA1 on the arsenic-induced generation of CSC from normal differentiated cells, which is recently gaining importance as an oncogenesis driving mechanism and leads to increased tumor aggressiveness and drug resistance (Afify & Seno, 2019; Wang & Yang, 2019). Different authors have previously demonstrated that *in vitro* arsenic chronic exposure leads to cell transformation associated with an increased in stem-like cells in human bronchial epithelial (BEAS-2B) (Bi et al., 2020; Chang et al., 2020) and in human urothelial (HUC1) cell populations (Ooki et al., 2018). These stem-like cells can acquire CSC characteristics such as tumorsphere formation ability, and highly expressed c-Myc, Oct4, Sox2, and Klf4. Accordingly, our study demonstrates that during the long-term arsenic exposure the proportion of cells exhibiting stem-like features increases given the MEFs ability to form progressively bigger tumorspheres. Importantly, FRA1 knockdown led to a significant reduction of the tumorspheres' size in all time-points evaluated, and we found a significant enrichment of FRA1 in the tumorspheres' population in comparison with that in the adherent culture. The mechanism by which malignant stemness is promoted by FRA1 is not explored in our study; however, it is interesting to note that a FRA1-Notch crosstalk has been described (Gu et al., 2016), and some authors have identified Notch as a central player in arsenic-mediated stem cell fate modulation (Anguiano et al., 2020). Thus, taken together, our findings in Chapter 2 not only set arsenic-mediated FRA1 stimulation as an essential part of the arsenic-mediated oncogenesis, but also FRA1 is

elicited here as a necessary component for the emergence and persistence of cancer stem cells during this process.

After the discussion of the first two Chapters of the Thesis, we can highlight that the chronic exposure approach for the purposeful *in vitro* cell transformation is extremely useful as it gives us the chance to dissect various stages of tumor formation, to evaluate molecular changes and their relevance during the process in terms of functional alterations and, ultimately to propose new modes of action and mechanisms of carcinogenesis. In the past years, this approach has led researchers to make remarkable advances in the field of environmental risk assessment and many studies have contributed to expand the existing knowledge on the mechanisms-of-action of very diverse compounds including, of course, arsenic.

Interestingly, many of the most evaluated environmental pollutants that exert a carcinogenic potential, share similar modes of action and functional impacts that eventually lead to malignant transformation. For instance, genotoxicity induction via increased oxidative stress levels and DNA repair inhibition has been widely explored for asbestos (Benedetti et al., 2015), several heavy metals such as cadmium and mercury (Kocadal et al., 2020), and, interestingly, nanoparticles (NPs) of very different nature such as titanium dioxide (TiO_2NPs), cobalt (CoNPs), zinc oxide (ZnONPs), silver (AgNPs) or cerium oxide (CeO_2NPs) nanoparticles (Mortezaee et al., 2019). Also, given that epigenetic changes are gaining attention as a relevant mechanism-of-action of many compounds, there is a growing body of evidence that they play a role in metal adverse effects, for example, global DNA hypomethylation and histone modifications are found in nickel and chromium carcinogenesis (Zhu & Costa, 2020). NPs exposure also leads to epigenetic changes with extensive reports on altered DNA methylation patterns induced by Au, TiO_2, ZnO, and SiO_2NPs, among others (Wong et al., 2017). Regarding miRNAs, central players in gene expression regulation such as miR-222, miR-34, miR-155, and miR-21 are significantly altered under very different exposure scenarios including particulate matter and organic pollutants (Tumolo et al., 2020), NPs, metals, and heavy metals (Balasubramanian et al., 2020). Further, recent reviews show the increasing amount of data that associate these mechanisms of action with the induction of premature senescence (Liang et al., 2020) and the generation CSC-like cells (Wang & Yang, 2019) upon xenobiotics' exposure, including chromium, cadmium, nickel, and organic pollutants. Thus, multiple anthropogenic or natural environmental contaminants present the same mechanisms-of-action as arsenic and lead to similar outcomes.

It is of note that different environmental contaminants can induce alterations closely related to the mechanisms of arsenic carcinogenesis examined in Chapters 1 and 2 of this Thesis. Even if FRA1 and MTH1 role in arsenic carcinogenesis has been described here for the first time, there is existing evidence of their involvement in the malignant transformation induced by other contaminants. On the one hand, regarding FRA1 and its related signaling axis, it is interesting that asbestos regulate AP-1 potentially via ROS production and, eventually, the exposure triggers the expression of the Fos/Jun family members in mesothelioma cells (Benedetti et al., 2015). Also, cadmium has been reported to activate the ERK/MAPKs pathway which is associated with *Fos*/*Jun* gene enrichment in prostate cells' malignant transformation (Dasgupta et al., 2020). Importantly, previous work carried out in our group has shown FRA1 expression deregulation in the transformation process of lung epithelial BEAS-2B cells induced by 6 weeks of co-exposure to CeO_2NPs and cigarette condensate smoke (CSC) (Rubio et al., 2017). Regarding MTH1, its role in NP-induced carcinogenesis was examined by us following a similar approach as the one presented in Chapter 1, which led us to conclude that its overexpression is required for the cells to adapt and undergo transformation after 12 weeks of chronic exposure to Co- and ZnONPs, given that MTH1 knock-down reduced the aggressiveness of the obtained phenotype (Barguilla et al., 2020).

Hence, given the large number of environmental pollutants inducing an impact through similar key mechanisms-of-action or pathways, an important question arises: *is the one-exposure-for-one-effect model the most appropriate for risk assessment?* Under a real-life exposure scenario, single exposures are not common. Pollutants are not isolated in the environment and, thus, they can interact with each other, which may result in a similar impact as that of the independent single exposures, or may induce a joint additive, synergistic or antagonistic effect, depending on the nature of the contaminants. Indeed, a need for a more comprehensive risk assessment has been identified, especially when examining the carcinogenic potential of environmental pollutants. The multistep nature of the carcinogenic process means that both simultaneous and sequential co-exposures have the potential to contribute to the process. Therefore, centering the attention in the carcinogenicity of individual contaminants fails to identify synergies that will most probably arise when evaluating combinations of compounds (Goodson et al., 2015; Bjørklund et al., 2020). In this sense, although the models based on the long-term exposure to subtoxic doses are a useful approximation to the environmental exposure scenario, we believe that a reasonable next step in arsenic risk assessment is to examine the impact of concurrent exposures and, thus, this is the focus of the third part of this Thesis dissertation.

Importantly, arsenic has a well-established co-cytotoxic and co-carcinogenic potential, meaning that it enhances the toxic or mutagenic impact induced by other carcinogens contributing to malignancies. This aspect of arsenic exposure has been long known in regard with ultraviolet (UV) light, other heavy metals, and organic pollutants. Regarding UV light, epidemiological studies have described a positive association between solar UV and non-melanoma skin cancer (SCC) in populations exposed to arsenic (Melkonian et al., 2011); an effect that has also been found *in vivo*, evidenced by the exacerbated development of SCC in mice exposed to both arsenic and UV (Rossman et al., 2004). *In vitro*, keratinocytes (HaCaT) chronically exposed to low-level arsenic for 28 weeks acquire a transformed phenotype characterized by their remarkable resistance to UV-induced genotoxicity; thus, arsenic-induced apoptosis resistance was proposed as a mechanistic explanation for the UV-damaged cells to escape controlled cell death and initiate the carcinogenic process (Chen et al., 2005; Pi et al., 2005). In the case of arsenic and polycyclic hydrocarbons interaction, mice receiving a combined administration of arsenic and benzo[a]pyrene (BaP) showed a more pronounce MN formation that the single-exposed animals (Lewińska et al., 2007). Indeed, it was found that arsenic potentiates the formation of DNA adducts at low doses of BaP and arsenic co-exposure *in vitro* (Evans et al., 2004). Among the available data regarding complex interactions in heavy metal mixtures, the literature has shown that environmentally relevant concentrations of arsenic (2 μM), cadmium (2 μM), and lead (5 μM) mixtures exert a transforming potential as determined by a murine two-stage Balb/c 3T3 cell assay (Rodríguez-Sastre et al., 2014). This transformation is strongly dependent on ROS modulation in the initiation and promotion stages (Martínez-Baeza et al., 2016), when the miR-222 up-regulation also seems a mechanistic explanation as it ultimately impairs DNA repair (Rojas et al., 2019). Also, epidemiological studies have found the association between the arsenic, chromium, lead, manganese, molybdenum, and zinc combined exposure and increased genotoxicity (Annangi et al., 2016), as well as, a higher prostate cancer risk, driven by arsenic and zinc co-exposures (Lim et al., 2019).

At this point, it is interesting to mention that the combined effects of arsenic with other compounds are not always detrimental for human health. Remarkably, this aspect of arsenic exposure has been used to our advantage allowing the development of new therapeutic strategies against cancer. Arsenic trioxide (ATO) was approved by the Food and Drug Administration (FDA) in severe acute promyelocytic leukemia cases in the year 2000, however, it is not as effective in other types of tumors such as hepatocellular carcinoma (Lin et al., 2007) or pancreatic cancer (Kindler et al., 2008). Interestingly, combined therapy with ATO and other antitumoral agents has shown positive results. As

representative examples, ATO combination with ionizing radiation (Kumar et al., 2008), alkylating antineoplastic agents (Lee et al., 2010), and cisplatin (Zheng et al., 2013) has proven to have synergistic antitumoral effects in oral squamous cell carcinoma, bladder, and lung cancer, respectively.

Further, the joint effect of contaminants is not limited to the interaction of the most classical compounds. The ever-increasing number of emergent pollutants released to the environment leads to new interactions that entail different exposure conditions for the subjected populations, potentially incrementing the risk related to unknown outcomes derived from the co-exposures. Indeed, although very few studies have evaluated the combined effects of arsenic and NPs co-exposures, enhanced toxic effects have been described. Rosario et al. reported a moderate decrease in A549 cell survival upon As^{III}/TiO_2NPs, as well as As^{III}/CeO_2NPs at low doses, both after 24 h and 7 days of exposure, compared to the single exposure and the non-exposed controls (Rosário et al., 2020). Arsenic interaction with TiO_2NPs had previously been described by Wang et al. (2017), who found a synergistic genotoxic effect between the two, evidenced by the increased micronucleus formation observed in co-exposed human-hamster hybrid A_L cells. Likewise, Ahamed et al. (2019) described that As^{III}/SiO_2NPs co-exposure led to cell viability reduction, generation of ROS, depletion of antioxidant levels including GSH and SOD, and apoptosis induction in human liver HepG2 cells and in human HT1080 fibroblasts at the short-term.

NPs have gathered much attention in the past 10 years as the most relevant emergent pollutants given their many applications (Alfaro-Moreno et al., 2013). However, although much remains to be unveiled in this regard, the current focus of attention in terms of emergent pollutants is another type of particulate material: MNPLs. MNPLs are small-size plastic particles (< 5 mm) derived from plastic litter degradation and ubiquitously distributed in all environmental compartments, especially affecting aquatic ecosystems (Lehner et al., 2019). Remarkable estimations show that 4.8-12.7 million tons of plastic waste were discarded into the ocean in 2010 and the number is expected to be 10 times higher by 2025 (Jambeck et al., 2015). This accumulation of plastic litter leads to numbers as high as 8.3 billion MNPLs particles in each m^3 of ocean water (Brandon et al., 2020). Thus, the recent acknowledgment of the widespread presence of MNPL has added to the already strong societal reaction against plastic pollution and shifted the general perception of plastic pollution from a problem limited to ecosystems and wildlife to a global environmental health issue. Besides public opinion, the MNPLs' relevance is also evidenced by the growing number of work programs and funding calls aiming to fill in the huge knowledge gaps regarding human exposure to MNPLs and their impact on

health such as the *SC1-BHC-36-2020: Micro- and nano-plastics in our environment: Understanding exposures and impacts on human health* call from the EU, Horizon 2020 program.

As a result of this increasing interest on MNPLs, very recent studies are generating compelling data regarding their potential adverse effects on health using diverse *in vivo* and *in vitro* models. However, multiple limitations have been identified preventing an appropriate risk assessment, including the lack of reliable technologies for MNPLs' detection and quantification in biological matrices, the need for human biomonitoring data and the identification of exposure and effect biomarkers, as well as the insufficient studies examining MNPLs' long-term effects and their potential role as vectors for other environmental contaminants (Rubio et al., 2020a). Thus, we have aimed to cover the latter two aspects in the study presented in Chapter 3, where we explored the combined effects of the arsenic and MNPLs co-exposure at the long-term. This work is equally relevant from the point of view of MNPLs impact assessment and arsenic hazard evaluation, given the previously mentioned need to evaluate concurrent exposures for a more comprehensive risk assessment.

A concerning aspect of MNPLs pollution is that their strong adsorption affinities, due to their high surface-to-volume ratio and high surface hydrophobicity, may result in the so-called *Trojan horse* effects; that is, MNPLs may serve as carriers to enhance the bioaccumulation of other more hazardous contaminants (Liu et al., 2018b; Bradney et al., 2019). Accumulating evidence shows that arsenic adsorption onto MNPLs is a demonstrated event under environmental conditions. As a representative example, Prunier et al. collected multiple plastic samples from the North Atlantic gyre, including microplastics that were collected in a net equipped with a 300 µm pore-size mesh. They demonstrated that, among other trace metals, arsenic contents were significantly higher in the plastic debris samples (0.1 - 0.8 µg/g) than in the new packaging materials (0.05 µg/g) also analyzed (Prunier et al., 2019). Furthermore, Selvam et al. studied trace metal adsorption onto MNPLs in groundwater samples, largely neglected in the literature compared to marine water. Different types of MNPLs were characterized from the collected samples, including polyamide, polyester, polypropylene, and polyethylene particles. Moreover, they showed that the MNPLs presented high adsorption capacities for As, among other metals such as Cd, Cr, or Pb (Selvam et al., 2021). Thus, in Chapter 3 we explored the arsenic and PSNPs (50 nm) interaction, being both widespread water contaminants (Li et al., 2016; Podgorski & Berg, 2020). Dong et al. (2020a) had previously described that the equilibrium time of As^{III} adsorption onto polystyrene microplastics (PSMPs) was 20 h, and the amount of adsorbed As^{III} decreased in

increasingly bigger plastic particles. Accordingly, in our study we found a physical interaction between As^{III} and PSNPs, when the As^{III}/PSNPs association was evaluated via TEM/EDX. This methodological approach let us identify different ways by which both pollutants interact: (1) arsenic is associated to single PSNPs, and (2) arsenic forms aggregates that are ringed by PSNPs, an effect that to our knowledge has not been described before. However, we observed that this interaction did not result in an increased uptake of arsenic by the co-exposed cells, as the intracellular As^{III} levels remained stable with the increasing doses of PSNPs. Thus, our exposure conditions do not entail the role of MNPLs as *Trojan horses* for arsenic, as opposed to the results reported by other authors examining the interaction between arsenic and other NPs. As previously mentioned, different studies demonstrated that the As^{III}/TiO_2NPs and As^{III}/CeO_2NPs co-exposure could efficiently promote the bioavailability of As^{III} in co-exposed cells (Wang et al., 2017; Ahamed et al., 2019).

Interestingly, the lack of enhanced arsenic accumulation is independent from PSNPs internalization under our exposure settings, given that we observed that our model MEF cells uptakes a very significant amount of PSNPs in a dose-dependent manner. This remarkable *in vitro* cell uptake of PSNPs was also reported by other authors in gastric adenocarcinoma (AGS) cells (Forte et al., 2016), human alveolar A549 cells (Xu et al., 2019), human colorectal adenocarcinoma Caco-2 cells (Cortés et al., 2020), and multiple hematopoietic cell lines (Raji-B, TK6, and THP-1) (Rubio et al., 2020b). Importantly, this high internalization rate drives the MNPLs' ability to cross physiological barriers as seen when exposing a differentiated intestinal co-culture model (Caco-2/HT29+RajiB) (Domenech et al., 2020).

Despite the significant MNPLs uptake, the potential adverse effects of this exposure are unclear. While some authors report some degree of pathological effects, namely ROS production and pro-inflammatory responses, many *in vitro* works show that even if these effects arise, mild or no remarkable cytotoxicity is observed. For instance, Schirinzi et al. (2017) reported a lack of toxicity in both cerebral (T98G) and epithelial (HeLa) human cells exposed to polyethylene microplastics (PETMPs) (3-16 μm) or PSMPs (10 μm) for 24 h. Likewise, Magrì et al. (2018) showed that no toxicity emerged in Caco-2 cells exposed to polyethylene nanoplastics (PETNPs); while Wu et al. (2019b) reported that PSNPs (100 nm) and PSMPs (5 μm) produced little cytotoxicity, mild changes in the membrane integrity and a certain disruption of the mitochondrial membrane on the same cell line. Interestingly, ultrastructural changes in mitochondria of Caco-2 cells were also observed in our group, although no significant toxic effects were found after 24 and 48 h of exposure to PSNPs (50 nm) (Cortés et al., 2020).

Notably, all the works mentioned above were performed at short-term. Therefore, we centered our attention on the long-term impact of the (co)exposure. Thus, it is important to point out the relevance of the model used in our study of As^{III}/PSNPs combined effects. As we did in Chapters 1 and 2, in this study we used MEF cells chronically exposed to arsenic (Bach et al., 2016). In this case, we selected transformed cells from the 30th week of 2 µM As^{III} exposure, referred to as arsenic-transformed cells (AsTC). This kind of models based on already transformed cells can prove to be extremely useful for the identification of weak carcinogens or cocarcinogens, as the compounds have to induce a lesser number of cellular events to promote tumor growth during the progression stage than those required for the onset of tumorigenesis and the initiation of the cell transformation process. Hence, AsTC were further exposed for 12 more weeks to As^{III} (2 µM) and PSNPs (25 µg/mL) separately or in combination, which allowed us to identify compelling effects of the (co)exposure described below.

On the one hand, accordingly to what is described by other authors, we found that both the single exposure to As^{III} and to PSNPs trigger genotoxicity and ODD. Arsenic genotoxic effect is well-described and has been previously discussed here due to its central role as a mechanism of carcinogenesis (Flora, 2011); while genotoxicity and ROS production are the most reported outcomes among those studies that find significant adverse effects of the MNPLs exposure. Noteworthy, a study from our group demonstrated that human leukocytic cell lines (RajiB, TK6, and THP-1) presented differential PSNPs internalization capabilities which resulted in diverse outcomes. Monocytic THP-1 cells showed the highest particle internalization, but no adverse effects associated to the exposure. On the contrary, although lymphocytic RajiB and TK6 cells showed lesser PSNPs uptake, mild toxicity and, importantly, significant ROS production and genotoxicity were detected upon exposure (Rubio et al., 2020b). Accordingly, another work from our group performed by Ballesteros et al. (2020) also found different outcomes between several lineages of white peripheral blood cells. In this case, after the *ex vivo* exposure of whole blood samples to the same PSNPs. Remarkably, increased levels of DNA damage were reported in monocytes and polymorphonuclear cells, while no effects were observed in lymphocytes, which also showed limited PSNPS uptake. Besides, other groups have also described increased oxidative stress levels among the potentially adverse effects induced by MNPLs exposure. For instance, Poma et al. found that PSNPs (100 nm) stimulated ROS production and induced genotoxic stress and DNA damage measured as MN frequency following a short-term exposure of human Hs27 fibroblasts (Poma et al., 2019). Other authors showed that a 24 h PSMPs (1.67–2.17 µm) exposure induced certain cytotoxicity, increased ROS levels, triggered inflammatory

responses with increased levels of IL-6 and IL-8 in BEAS-2B cells (Dong et al., 2020b). Also, it has been reported that polypropylene microplastics (PPMPs; 20 μm) induced cytotoxicity at high concentrations and increased intracellular ROS levels in several cell types at the short-term (Hwang et al., 2019). Thus, the result derived from the single exposures are in the line of what other studies have found at the short-term. Nonetheless, here we described for the first time that the chronic As^{III} and PSNPs (co)exposure leads to remarkable higher levels of both total and oxidative DNA damage when compared to single exposed and passage-matched AsTC, which demonstrates the positive interaction between the two pollutants.

Further, we are the first to examine how this positive interaction impacts the development of the oncogenic phenotype. In the literature there is no available data focusing on the potential carcinogenic impact of MNPLs. However, as previously discussed, arsenic exerts a well-characterized cocarcinogenic effect. Interestingly, we found that while the single exposure had no effect upon the phenotype of AsTC, the As^{III}/PSNP concurrent exposure did aggravate the arsenic-indued oncogenic phenotype. This effect was evidenced by the morphological changes towards a more spindle-like cell, the increased capacity of cells to grow independently of anchorage, as well as the enhanced migration and invasion potential of co-exposed AsTC. Thus, our data reveal a potential additive and cocarcinogenic effect of arsenic and MNPLs, as it was previously described for arsenic and UV light (Rossman et al., 2004), or arsenic and heavy metal combinations (Rodríguez-Sastre et al., 2014). All this brings out the need to further explore both the long-term effects of relevant pollutants such as MNPLs and to consider complex mixtures when assessing the safety of a compound.

Overall, from our studies we can conclude that arsenic has a capability to induce an impact at many different levels which entails the involvement of multiple components such as AS3MT, MTH1, or FRA1; signaling pathways including FRA1 signaling axis; and functional effects like genotoxicity, epigenetic alterations, or senescence and stemness status deregulation. Nonetheless, it is of utmost importance to not miss that this already complex scenario can be magnified if we broaden the focus of study to complex mixtures that would be more representative of a real-life exposure situation. Thus, as the information available on the effects of a certain contaminant grows, it is interesting to analyze the perspective from which this impact is evaluated and to identify knowledge gaps, such as concurrent exposure effects, which would contribute to a more comprehensive risk assessment model.

5. CONCLUSIONS

5. CONCLUSIONS

In accordance with the objectives raised in the frame of this Thesis and the discussion of the obtained results, we conclude that:

1. Variations in the DNA damage levels during the chronic arsenic exposure are closely linked with the development of an oncogenic phenotype. *Chapter 1*

    a. A time-dependent accumulation of ODD and chromosomal damage takes place during the arsenic-associated tumorigenesis up to the transformation point.

    b. AS3MT is involved in the progressively higher levels of DNA damage during transformation.

    c. MTH1 induction drives DNA damage resistance and the development of the tumor aggressive phenotype in arsenic-transformed cells.

2. FRA1 signaling axis is involved in the development of an *in vitro* transformed phenotype upon chronic arsenic exposure. *Chapter 2*

    a. FRA1 is progressively overexpressed during the acquisition of the oncogenic phenotype.

    b. ERK, p38, and RAS are pinpointed as upstream potential candidates involved in arsenic-induced FRA1 activation, which in turn potentially leads to tumor suppressor, TGFβ and EMT-TFs gene expression deregulation.

    c. Arsenic-associated FRA1 stimulation is necessary for the chronically exposed cells to develop an aggressive tumoral phenotype, senescence resistance and a stem-like status.

3. Additive effects emerge when evaluating the effects of arsenic and nanoplastic co-exposure. Thus, considering interactions in complex mixtures is of utmost importance when evaluating the contaminants' associated risk.

    a. Arsenic and PSNPs physically interact, although this interaction does not increment arsenics' bioavailability.

    b. Long-term PSNPs exposure, as well as arsenic and PSNPs co-exposure, induce oxidative DNA damage.

    c. Arsenic and PSNPs combined exposure exacerbates the aggressiveness of cells' oncogenic phenotype.

6. REFERENCES

6. REFERENCES

Abdul, K. S., Jayasinghe, S. S., Chandana, E. P. S., Jayasumana, C., & De Silva, P. M. C. S. (2015). Arsenic and human health effects: A review. *Environmental Toxicology and Pharmacology, 40*(3), 828–846.

Achanzar, W. E., Brambila, E. M., Diwan, B. A., Webber, M. M., & Waalkes, M. P. (2002). Inorganic arsenite-induced malignant transformation of human prostate epithelial cells. *Journal of the National Cancer Institute, 94*(24), 1888–1891.

Afify, S. M., & Seno, M. (2019). Conversion of stem cells to cancer stem cells: Undercurrent of cancer initiation. *Cancers, 11*(3), 1–19.

Ahamed, M., Akhtar, M. J., & Alhadlaq, H. A. (2019). Co-exposure to SiO2 nanoparticles and arsenic induced augmentation of oxidative stress and mitochondria-dependent apoptosis in human cells. *International Journal of Environmental Research and Public Health, 16*(17), 3199.

Alfaro-Moreno, E., Nawrot, T. S., Nemmar, A., Rosas, I., & Schwarze, P. (2013). Particulate matter and nanoparticles toxicology. BioMed Research International, 2013: 642974.

Allison, P., Huang, T., Broka, D., Parker, P., Barnett, J. V., & Camenisch, T. D. (2013). Disruption of Canonical TGFβ-signaling in Murine Coronary Progenitor Cells by Low Level Arsenic. *Bone, 272*(1), 147–153.

Anguiano, T., Sahu, A., Qian, B., Tang, W. Y., Ambrosio, F., & Barchowsky, A. (2020). Arsenic directs stem cell fate by imparting notch signaling into the extracellular matrix niche. *Toxicological Sciences, 177*(2), 494–505.

Annangi, B., Bonassi, S., Marcos, R., & Hernández, A. (2016). Biomonitoring of humans exposed to arsenic, chromium, nickel, vanadium, and complex mixtures of metals by using the micronucleus test in lymphocytes*. Mutation Research - Reviews in Mutation Research, 770*, 140–161.

Annys, E., Billington, R., Clayton, R., Bremm, K. D., Graziano, M., McKelvie, J., Ragan, I., Schwarz, M., Van der Laan, J. W., Wood, C., Öberg, M., Wester, P., & Woodward, K. N. (2014). Advancing the 3Rs in regulatory toxicology - Carcinogenicity testing: Scope for harmonisation and advancing the 3Rs in regulated sectors of the european union. *Regulatory Toxicology and Pharmacology, 69*(2), 234–242.

Aodengqimuge, Liu, S., Mai, S., Li, X., Li, Y., Hu, M., Yuan, S., & Song, L. (2014). AP-1 activation attenuates the arsenite-induced apoptotic response in human bronchial epithelial cells by up-regulating HO-1 expression. *Biotechnology Letters, 36*(10), 1927–1936.

Arslan, B., Djamgoz, M. B. A., & Akün, E. (2017). Arsenic: A Review on Exposure Pathways, Accumulation, Mobility and Transmission into the Human Food Chain. *Rev Environ Contam Toxicol, 243*, 27–51.

Bach, J., Peremartí, J., Annangi, B., Marcos, R., & Hernández, A. (2016). Oxidative DNA damage enhances the carcinogenic potential of in vitro chronic arsenic exposures. *Archives of Toxicology, 90*(8), 1893–1905.

Bakiri, L., MacHo-Maschler, S., Custic, I., Niemiec, J., Guió-Carrión, A., Hasenfuss, S. C., Eger, A., Müller, M., Beug, H., & Wagner, E. F. (2015). Fra-1/AP-1 induces EMT in mammary epithelial cells by modulating Zeb1/2 and TGFβ expression. *Cell Death and Differentiation, 22*(2), 336–350.

Balasubramanian, S., Gunasekaran, K., Sasidharan, S., Jeyamanickavel Mathan, V., & Perumal, E. (2020). MicroRNAs and Xenobiotic Toxicity: An Overview. *Toxicology Reports, 7*(February), 583–595.

Ballesteros, S., Domenech, J., Barguilla, I., Cortés, C., Marcos, R., & Hernández, A. (2020). Genotoxic and immunomodulatory effects in human white blood cells after ex vivo exposure to polystyrene nanoplastics . *Environmental Science: Nano, 7,* 3431-3446

Barguilla, I., Barszczewska, G., Annangi, B., Domenech, J., Velázquez, A., Marcos, R., & Hernández, A. (2020). MTH1 is involved in the toxic and carcinogenic long-term effects induced by zinc oxide and cobalt nanoparticles. *Archives of Toxicology, 94*(6), 1973–1984.

Basu, A., Mahata, J., Roy, A. K., Sarkar, J. N., Poddar, G., Nandy, A. K., Sarkar, P. K., Dutta, P. K., Banerjee, A., Das, M., Ray, K., Roychaudhury, S., Natarajan, A. T., Nilsson, R., & Giri, A. K. (2002). Enhanced frequency of micronuclei in individuals exposed to arsenic through drinking water in West Bengal, India. *Mutation Research - Genetic Toxicology and Environmental Mutagenesis, 516*(1–2), 29–40.

Bejjani, F., Evanno, E., Zibara, K., Piechaczyk, M., & Jariel-Encontre, I. (2019). The AP-1 transcriptional complex: Local switch or remote command? *Biochimica et Biophysica Acta - Reviews on Cancer, 1872*(1), 11–23.

Benbrahim-Tallaa, L., & Waalkes, M. P. (2008). Inorganic arsenic and human prostate cancer. *Environmental Health Perspectives, 116*(2), 158–164.

Benedetti, S., Nuvoli, B., Catalani, S., & Galati, R. (2015). Reactive oxygen species a double-edged sword for mesothelioma*. Oncotarget, 6*(19), 16848–16865.

Bhattacharjee, P., & Paul, S. (2020). Understanding the mechanistic insight of arsenic exposure and decoding the histone cipher. *Toxicology, 430*(November 2019), 152340.

Bi, Z., Zhang, Q., Fu, Y., Wadgaonkar, P., Zhang, W., Almutairy, B., Xu, L., Rice, M., Qiu, Y., Thakur, C., & Dr, F. C. (2020). Nrf2 and HIF1α converge to arsenic-induced metabolic reprogramming and the formation of the cancer stem-like cells. *Theranostics, 10*(9), 4134–4149.

Bjørklund, G., Tippairote, T., Rahaman, M. S., & Aaseth, J. (2020). Developmental toxicity of arsenic: a drift from the classical dose–response relationship. *Archives of Toxicology, 94*(1), 67–75.

Bouwmeester, H., Hollman, P. C. H., & Peters, R. J. B. (2015). Potential Health Impact of Environmentally Released Micro- and Nanoplastics in the Human Food Production Chain: Experiences from Nanotoxicology. *Environmental Science and Technology, 49*(15), 8932–8947.

Bradney, L., Wijesekara, H., Palansooriya, K. N., Obadamudalige, N., Bolan, N. S., Ok, Y. S., Rinklebe, J., Kim, K. H., & Kirkham, M. B. (2019). Particulate plastics as a vector for toxic trace-element uptake by aquatic and terrestrial organisms and human health risk. *Environment International, 131*(July), 104937.

Brambila, E. M., Achanzar, W. E., Qu, W., Webber, M. M., & Waalkes, M. P. (2002). Chronic arsenic-exposed human prostate epithelial cells exhibit stable arsenic tolerance: mechanistic implications of altered cellular glutathione and glutathione S-transferase. *Toxicology and Applied Pharmacology, 183*(2), 99–107.

Brandon, J. A., Freibott, A., & Sala, L. M. (2020). Patterns of suspended and salp-ingested microplastic debris in the North Pacific investigated with epifluorescence microscopy. *Limnology and Oceanography Letters, 5*(1), 46–53.

Bredfeldt, T. G., Jagadish, B., Eblin, K. E., Mash, E. A., & Gandolfi, A. J. (2006). Monomethylarsonous acid induces transformation of human bladder cells. *Toxicology and Applied Pharmacology, 216*(1), 69–79.

Breheny, D., Oke, O., & Faux, S. P. (2011). The use of in vitro systems to assess cancer mechanisms and the carcinogenic potential of chemicals. *ATLA Alternatives to Laboratory Animals, 39*(3), 233–255.

Bussard, K. M., Mutkus, L., Stumpf, K., Gomez-Manzano, C., & Marini, F. C. (2016). Tumor-associated stromal cells as key contributors to the tumor microenvironment. *Breast Cancer Research, 18*(1), 1–11.

Campanale, C., Massarelli, C., Savino, I., Locaputo, V., & Uricchio, V. F. (2020). A detailed review study on potential effects of microplastics and additives of concern on human health. *International Journal of Environmental Research and Public Health, 17*(4), 1212.

Campisi, J. (2013). Aging, Cellular Senescence, and Cancer. *Annu Rev Physiol, 75*, 685–705.

Cardoso, A. P. F., Al-Eryani, L., & Christopher States, J. (2018). Arsenic-Induced Carcinogenesis: The Impact of miRNA Dysregulation. *Toxicological Sciences, 165*(2), 284–290.

Chang, Q., Pan, J., Wang, X., Zhang, Z., Chen, F., & Shi, X. (2010). Reduced reactive oxygen species-generating capacity contributes to the enhanced cell growth of arsenic-transformed epithelial cells. *Cancer Research, 70*(12), 5127–5135.

Chang, Q., Bi, Z., Fu, Y., Rice, M. K. A., Zhang, Q., Wadgaonkar, P., Almutairy, B., Zhang, W., Lu, Y., Xu, L., Thuka, C., & Chen, F. (2020). Characterization of Arsenic-Induced Cancer Stem-Like Cells. In Stem Cell Transcriptional Networks: Methods and Protocols, Methods in Molecular Biology (Vol. 2117).

Chen, P. H., Lan, C. C. E., Chiou, M. H., Hsieh, M. C., & Chen, G. S. (2005). Effects of arsenic and UVB on normal human cultured keratinocytes: Impact on apoptosis and implication on photocarcinogenesis. *Chemical Research in Toxicology, 18*(2), 139–144.

Chen, Q., Yin, D., Jia, Y., Schiwy, S., Legradi, J., Yang, S., & Hollert, H. (2017). Enhanced uptake of BPA in the presence of nanoplastics can lead to neurotoxic effects in adult zebrafish. *Science of the Total Environment, 609*, 1312–1321.

Chen, Q. Y., DesMarais, T., & Costa, M. (2019). Metals and Mechanisms of Carcinogenesis. *Annu Rev Pharmacol Toxicol, 59*, 537–554.

Chung, Y. P., Chen, Y. W., Weng, T. I., Yang, R. Sen, & Liu, S. H. (2020). Arsenic induces human chondrocyte senescence and accelerates rat articular cartilage aging. *Archives of Toxicology, 94*(1), 89–101.

Corsini, E., Asti, L., Viviani, B., Marinovich, M., & Galli, C. L. (1999). Sodium arsenate induces overproduction of interleukin-1α in murine keratinocytes: Role of mitochondria. *Journal of Investigative Dermatology, 113*(5), 760–765.

Cortés, C., Domenech, J., Salazar, M., Pastor, S., Marcos, R., & Hernández, A. (2020). Nanoplastics as a potential environmental health factor: Effects of polystyrene nanoparticles on human intestinal epithelial Caco-2 cells. *Environmental Science: Nano, 7*(1), 272–285.

Cui, X., Wakai, T., Shirai, Y., Hatakeyama, K., & Hirano, S. (2006). Chronic oral exposure to inorganic arsenate interferes with methylation status of p16INK4a and RASSF1A and induces lung cancer in A/J mice. *Toxicological Sciences, 91*(2), 372–381.

Darwiche, N. (2020). Epigenetic mechanisms and the hallmarks of cancer: an intimate affair. *American Journal of Cancer Research, 10*(7), 1954–1978.

Dasgupta, P., Kulkarni, P., Bhat, N. S., Majid, S., Shiina, M., Shahryari, V., Yamamura, S., Tanaka, Y., Gupta, R. K., Dahiya, R., & Hashimoto, Y. (2020). Activation of the Erk/MAPK signaling pathway is a driver for cadmium induced prostate cancer. *Toxicology and Applied Pharmacology, 401*(June), 115102.

de la Rosa, R., Steinmaus, C., Akers, N. K., Conde, L., Ferreccio, C., Kalman, D., Zhang, K. R., Skibola, C. F., Smith, A. H., Zhang, L., & Smith, M. T. (2017). Associations between arsenic (+3 oxidation state) methyltransferase (AS3MT) and N-6 adenine-specific DNA methyltransferase 1 (N6AMT1) polymorphisms, arsenic metabolism, and cancer risk in a chilean population. *Environmental and Molecular Mutagenesis, 58*(6), 411–422.

Dhillon, A. S., & Tulchinsky, E. (2015). FRA-1 as a driver of tumour heterogeneity: A nexus between oncogenes and embryonic signalling pathways in cancer. *Oncogene, 34*(34), 4421–4428.

Domenech, J., Hernández, A., Rubio, L., Marcos, R., & Cortés, C. (2020). Interactions of polystyrene nanoplastics with in vitro models of the human intestinal barrier. *Archives of Toxicology, 94*(9), 2997–3012.

Dong, Z. (2002). The molecular mechanisms of arsenic-induced cell transformation and apoptosis. *Environmental Health Perspectives, 110*(suppl 5), 757–759.

Dong, Y., Gao, M., Song, Z., & Qiu, W. (2019). Adsorption mechanism of As(III) on polytetrafluoroethylene particles of different size. *Environmental Pollution, 254*, 112950.

Dong, Y., Gao, M., Song, Z., & Qiu, W. (2020a). As(III) adsorption onto different-sized polystyrene microplastic particles and its mechanism. *Chemosphere, 239*, 124792.

Dong, C. Di, Chen, C. W., Chen, Y. C., Chen, H. H., Lee, J. S., & Lin, C. H. (2020b). Polystyrene microplastic particles: In vitro pulmonary toxicity assessment. Journal of Hazardous *Materials, 385*(May 2019), 121575.

Drobná, Z., Jaspers, I., Thomas, D. J., & Stýblo, M. (2003). Differential activation of AP-1 in human bladder epithelial cells by inorganic and methylated arsenicals. *The FASEB Journal : Official Publication of the Federation of American Societies for Experimental Biology, 17*(1), 67–69.

Druwe, I. L., & Vaillancourt, R. R. (2010). Influence of arsenate and arsenite on signal transduction pathways: an update*. Archives of Toxicology, 84*(8), 585–596.

Eckstein, M., Eleazer, R., Rea, M., & Fondufe-Mittendorf, Y. (2017). Epigenomic reprogramming in inorganic arsenic-mediated gene expression patterns during carcinogenesis. *Reviews on Environmental Health, 32*(1–2), 93–103.

Egeblad, M., & Werb, Z. (2002). New functions for the matrix metalloproteinases in cancer progression. *Nature Reviews Cancer, 2*(3), 161–174.

Evans, C. D., LaDow, K., Schumann, B. L., Savage, R. E., Caruso, J., Vonderheide, A., Succop, P., & Talaska, G. (2004). Effect of arsenic on benzo[a]pyrene DNA adduct levels in mouse skin and lung. *Carcinogenesis, 25*(4), 493–497.

Fawell, J. (2012). Chemicals in the water environment. Where do the real and future threats lie? *Ann Ist Super Sanità, 48*(4), 347–353.

Ferreccio, C., Smith, A. H., Durán, V., Barlaro, T., Benítez, H., Valdés, R., Aguirre, J. J., Moore, L. E., Acevedo, J., Vásquez, M. I., Pérez, L., Yuan, Y., Liaw, J., Cantor, K. P., & Steinmaus, C. (2013). Case-control study of arsenic in drinking water and kidney cancer in uniquely exposed Northern Chile. *American Journal of Epidemiology, 178*(5), 813–818.

Flora, S. J. S. (2011). Arsenic-induced oxidative stress and its reversibility. *Free Radical Biology and Medicine, 51*(2), 257–281.

Forte, M., Iachetta, G., Tussellino, M., Carotenuto, R., Prisco, M., De Falco, M., Laforgia, V., & Valiante, S. (2016). Polystyrene nanoparticles internalization in human gastric adenocarcinoma cells. *Toxicology in Vitro, 31*, 126–136.

Freire, C., Amaya, E., Gil, F., Fernández, M. F., Murcia, M., Llop, S., Andiarena, A., Aurrekoetxea, J., Bustamante, M., Guxens, M., Ezama, E., Fernández-Tardón, G., & Olea, N. (2018). Prenatal co-exposure to neurotoxic metals and neurodevelopment in preschool children: The Environment and Childhood (INMA) Project. *Science of the Total Environment, 621*(November 2017), 340–351.

Gad, H., Koolmeister, T., Jemth, A. S., Eshtad, S., Jacques, S. A., Ström, C. E., Svensson, L. M., Schultz, N., Lundbäck, T., Einarsdottir, B. O., Saleh, A., Göktürk, C., Baranczewski, P., Svensson, R., Berntsson, R. P. A., Gustafsson, R., Strömberg, K., Sanjiv, K., Jacques-Cordonnier, M. C., … Helleday, T. (2014). MTH1 inhibition eradicates cancer by preventing sanitation of the dNTP pool. *Nature, 508*(7495), 215–221.

Ganapathy, S., Liu, J., Xiong, R., Yu, T., Makriyannis, A., & Chen, C. (2019). Chronic low dose arsenic exposure preferentially perturbs mitotic phase of the cell cycle. *Genes and Cancer, 10*(1–2), 39–51.

Geissen, V., Mol, H., Klumpp, E., Umlauf, G., Nadal, M., van der Ploeg, M., van de Zee, S. E. A. T. M., & Ritsema, C. J. (2015). Emerging pollutants in the environment: A challenge for water resource management. *International Soil and Water Conservation Research, 3*(1), 57–65.

Goodson, W. H., Lowe, L., Carpenter, D. O., Gilbertson, M., Ali, A. M., de Cerain Salsamendi, A. L., Lasfar, A., Carnero, A., Azqueta, A., Amedei, A., Charles, A. K., Collins, A. R., Ward, A., Salzberg, A. C., Colacci, A., Olsen, A. K., Berg, A., Barclay, B. J., Zhou, B. P., … Hu, Z. (2015). Assessing the carcinogenic potential of low-dose exposures to chemical mixtures in the environment: The challenge ahead. *Carcinogenesis, 36*, S254–S296.

Grau-Perez, M., Navas-Acien, A., Galan-Chilet, I., Briongos-Figuero, L. S., Morchon-Simon, D., Bermudez, J. D., Crainiceanu, C. M., de Marco, G., Rentero-Garrido, P., Garcia-Barrera, T., Gomez-Ariza, J. L., Casasnovas, J. A., Martin-Escudero, J. C., Redon, J., Chaves, F. J., & Tellez-Plaza, M. (2018). Arsenic exposure, diabetes-related genes and diabetes prevalence in a general population from Spain. *Environmental Pollution, 235*, 948–955.

Gu, X., Lu, C., He, D., Lu, Y., Jin, J., Liu, D., & Ma, X. (2016). Notch3 negatively regulates chemoresistance in breast cancers. *Tumor Biology, 37*(12), 15825–15833.

Han, F. X., Su, Y., Monts, D. L., Plodinec, M. J., Banin, A., & Triplett, G. E. (2003). Assessment of global industrial-age anthropogenic arsenic contamination. *Naturwissenschaften, 90*(9), 395–401.

Hanahan, D., & Weinberg, R. A. (2011). Hallmarks of cancer: The next generation. *Cell, 144*(5), 646–674.

Heeg, S., Doebele, M., von Werder, A., & Opitz, O. G. (2006). In Vitro Transformation Models. *Cell Cycle, 5*(6), 630–634.

Hernández, A., & Marcos, R. (2008). Genetic variations associated with interindividual sensitivity in the response to arsenic exposure. *Pharmacogenomics, 9*(8), 1113–1132.

Hernández, A., Paiva, L., Creus, A., Quinteros, D., & Marcos, R. (2014). Micronucleus frequency in copper-mine workers exposed to arsenic is modulated by the AS3MT Met287Thr polymorphism. *Mutation Research - Genetic Toxicology and Environmental Mutagenesis, 759*, 51–55.

Hong, Y. S., Song, K. H., & Chung, J. Y. (2014). Health effects of chronic arsenic exposure. *Journal of Preventive Medicine and Public Health, 47*(5), 245–252.

Hong, Y. S., Ye, B. J., Kim, Y. M., Kim, B. G., Kang, G. H., Kim, J. J., Song, K. H., Kim, Y. H., & Seo, J. W. (2017). Investigation of health effects according to the exposure of low concentration arsenic contaminated ground water. *International Journal of Environmental Research and Public Health, 14*(12), 1461.

Huang, Y. K., Huang, Y. L., Hsueh, Y. M., Yang, M. H., Wu, M. M., Chen, S. Y., Hsu, L. I., & Chen, C. J. (2008). Arsenic exposure, urinary arsenic speciation, and the incidence of urothelial carcinoma: A twelve-year follow-up study. *Cancer Causes and Control, 19*(8), 829–839.

Huang, C. Y., Su, C. T., Chung, C. J., Pu, Y. S., Chu, J. S., Yang, H. Y., Wu, C. C., & Hsueh, Y. M. (2012). Urinary total arsenic and 8-hydroxydeoxyguanosine are associated with renal cell carcinoma in an area without obvious arsenic exposure. *Toxicology and Applied Pharmacology, 262*(3), 349–354.

Hughes, M. F., Beck, B. D., Chen, Y., Lewis, A. S., & Thomas, D. J. (2011). Arsenic exposure and toxicology: A historical perspective. *Toxicological Sciences, 123*(2), 305–332.

Hwang, J., Choi, D., Han, S., Choi, J., & Hong, J. (2019). An assessment of the toxicity of polypropylene microplastics in human derived cells. *Science of the Total Environment, 684*, 657–669.

IARC, International Agency for Research on Cancer. (2012). Arsenic, metals fibres and dusts. Monographs on the evaluation of carcinogenic risk to humans. *Int. Agency. Res. Cancer*, *100*, 407–443.

Iwama, K., Nakajo, S., Aiuchi, T., & Nakaya, K. (2001). Apoptosis induced by arsenic trioxide in leukemia U937 cells is dependent on activation of p38, inactivation of ERK and the Ca2+-dependent production of superoxide. *International Journal of Cancer, 92*(4), 518–526.

Jambeck, J. R., Geyer, R., Wilcox, C., Siegler, T. R., Perryman, M., Andrady, A., Narayan, R., & Law, K. L. (2015). Plastic waste inputs from land into the ocean. *Science, 347*(6223), 768–771.

Jiang, X., Chen, C., Zhao, W., & Zhang, Z. (2013a). Sodium arsenite and arsenic trioxide differently affect the oxidative stress, genotoxicity and apoptosis in A549 cells: An implication for the paradoxical mechanism. *Environmental Toxicology and Pharmacology, 36*(3), 891–902.

Jiang, R., Li, Y., Xu, Y., Zhou, Y., Pang, Y., Shen, L., Zhao, Y., Zhang, J., Zhou, J., Wang, X., & Liu, Q. (2013b). EMT and CSC-like properties mediated by the IKKβ/IκBα/RelA signal pathway via the transcriptional regulator, Snail, are involved in the arsenite-induced neoplastic transformation of human keratinocytes. *Archives of Toxicology, 87*(6), 991–1000.

Jiang, X., Xie, H., Dou, Y., Yuan, J., Zeng, D., & Xiao, S. (2020). Expression and function of FRA1 protein in tumors. *Molecular Biology Reports, 47*(1), 737–752.

Jomova, K., Jenisova, Z., Feszterova, M., Baros, S., Liska, J., Hudecova, D., Rhodes, C. J., & Valko, M. (2011). Arsenic: Toxicity, oxidative stress and human disease. *Journal of Applied Toxicology, 31*(2), 95–107.

Jones, F. T. (2007). A broad view of arsenic. *Poultry Science, 86*(1), 2–14.

Khairul, I., Wang, Q. Q., Jiang, Y. H., Wang, C., & Naranmandura, H. (2017). Metabolism, toxicity and anticancer activities of arsenic compounds. *Oncotarget, 8*(14), 23905–23926.

Kim, H. G., Shi, C., Bode, A. M., & Dong, Z. (2016). p38α MAPK is required for arsenic-induced cell transformation. *Molecular Carcinogenesis, 55*(5), 910–917.

Kim, T. H., Seo, J. W., Hong, Y. S., & Song, K. H. (2017). Case–control study of chronic low-level exposure of inorganic arsenic species and non-melanoma skin cancer. *Journal of Dermatology, 44*(12), 1374–1379.

Kindler, H. L., Aklilu, M., Nattam, S., & Vokes, E. E. (2008). Arsenic trioxide in patients with adenocarcinoma of the pancreas refractory to gemcitabine: A phase II trial of the University of Chicago phase II consortium. *American Journal of Clinical Oncology: Cancer Clinical Trials, 31*(6), 553–556.

Kinoshita, A., Wanibuchi, H., Morimura, K., Wei, M., Nakae, D., Arai, T., Minowa, O., Noda, T., Nishimura, S., & Fukushima, S. (2007). Carcinogenicity of dimethylarsinic acid in Ogg1-deficient mice. *Cancer Science, 98*(6), 803–814.

Kocadal, K., Alkas, F. B., Battal, D., & Saygi, S. (2020). Cellular pathologies and genotoxic effects arising secondary to heavy metal exposure: A review. *Human and Experimental Toxicology, 39*(1), 3–13.

Kojima, C., Ramirez, D. C., Tokar, E. J., Himeno, S., Drobná, Z., Stýblo, M., Mason, R. P., & Waalkes, M. P. (2009). Requirement of arsenic biomethylation for oxidative DNA damage. *Journal of the National Cancer Institute, 101*(24), 1670–1681.

Kramer, N., Walzl, A., Unger, C., Rosner, M., Krupitza, G., Hengstschläger, M., & Dolznig, H. (2013). In vitro cell migration and invasion assays. *Mutation Research - Reviews in Mutation Research, 752*(1), 10–24.

Kryeziu, K., Pirker, C., Englinger, B., van Schoonhoven, S., Spitzwieser, M., Mohr, T., Körner, W., Weinmüllner, R., Tav, K., Grillari, J., Cichna-Markl, M., Berger, W., & Heffeter, P. (2016). Chronic arsenic trioxide exposure leads to enhanced aggressiveness via Met oncogene addiction in cancer cells. *Oncotarget, 7*(19), 27379-93.

Kumar, P., Gao, Q., Ning, Y., Wang, Z., Krebsbach, P. H., & Polverini, P. J. (2008). Arsenic trioxide enhances the therapeutic efficacy of radiation treatment of oral squamous carcinoma while protecting bone. *Molecular Cancer Therapeutics, 7*(7), 2060–2069.

Kuo, Y. C., Lo, Y. S., & Guo, H. R. (2017). Lung Cancer Associated with Arsenic Ingestion: Cell-type Specificity and Dose Response. *Epidemiology, 28*(October), S106–S112.

Lee, P. C., Kakadiya, R., Su, T. L., & Lee, T. C. (2010). Combination of bifunctional alkylating agent and arsenic trioxide synergistically suppresses the growth of drug-resistant tumor cells. *Neoplasia, 12*(5), 376–387.

Lee, C. H., Yu, C. C., Wang, B. Y., & Chang, W. W. (2016). Tumorsphere as an effective in vitro platform for screening anticancer stem cell drugs. *Oncotarget, 7*(2), 1215–1226.

Lehner, R., Weder, C., Petri-Fink, A., & Rothen-Rutishauser, B. (2019). Emergence of Nanoplastic in the Environment and Possible Impact on Human Health. *Environmental Science and Technology, 53*(4):1748-1765.

Levy, L., & Hill, C. S. (2006). Alterations in components of the TGF-β superfamily signaling pathways in human cancer. *Cytokine and Growth Factor Reviews, 17*(1–2), 41–58.

Lewińska, D., Arkusz, J., Stańczyk, M., Palus, J., Dziubałtowska, E., & Stepnik, M. (2007). Comparison of the effects of arsenic and cadmium on benzo(a)pyrene-induced micronuclei in mouse bone-marrow. *Mutation Research - Genetic Toxicology and Environmental Mutagenesis, 632*(1–2), 37–43.

Li, Y., Ling, M., Xu, Y., Wang, S., Li, Z., Zhou, J., Wang, X., & Liu, Q. (2010). The repressive effect of NF-κB on p53 by mot-2 is involved in human keratinocyte transformation induced by low levels of arsenite. *Toxicological Sciences, 116*(1), 174–182.

Li, W. C., Tse, H. F., & Fok, L. (2016). Plastic waste in the marine environment: A review of sources, occurrence and effects. *Science of the Total Environment, 566–567*, 333–349.

Li, R., Zhao, L., Zhang, L., Chen, M., Shi, J., Dong, C., & Cai, Z. (2017a). Effects of ambient PM2.5 and 9-nitroanthracene on DNA damage and repair, oxidative stress and metabolic enzymes in the lungs of rats. *Toxicology Research, 6*(5), 654–663.

Li, R., Zhao, L., Zhang, L., Chen, M., Dong, C., & Cai, Z. (2017b). DNA damage and repair, oxidative stress and metabolism biomarker responses in lungs of rats exposed to ambient atmospheric 1-nitropyrene. *Environmental Toxicology and Pharmacology, 54*(March), 14–20.

Liang, Y., Liang, N., Yin, L., & Xiao, F. (2020). Cellular and molecular mechanisms of xenobiotics-induced premature senescence. *Toxicology Research, 9*(5), 669–675.

Lim, J. T., Tan, Y. Q., Valeri, L., Lee, J., Geok, P. P., Chia, S. E., Ong, C. N., & Seow, W. J. (2019). Association between serum heavy metals and prostate cancer risk – A multiple metal analysis. *Environment International, 132*(July), 105109.

Lin, C. C., Hsu, C., Hsu, C. H., Hsu, W. L., Cheng, A. L., & Yang, C. H. (2007). Arsenic trioxide in patients with hepatocellular carcinoma: A phase II trial. *Investigational New Drugs, 25*(1), 77–84.

Lin, H. J., Sung, T. I., Chen, C. Y., & Guo, H. R. (2013). Arsenic levels in drinking water and mortality of liver cancer in Taiwan. *Journal of Hazardous Materials, 262*, 1132–1138.

Lin, Y. C., Chen, W. J., Huang, C. Y., Shiue, H. S., Su, C. T., Ao, P. L., Pu, Y. S., & Hsueh, Y. M. (2018). Polymorphisms of arsenic (13 Oxidation State) methyltransferase and arsenic methylation capacity affect the risk of bladder cancer. *Toxicological Sciences, 164*(1), 328–338.

Ling, M., Li, Y., Xu, Y., Pang, Y., Shen, L., Jiang, R., Zhao, Y., Yang, X., Zhang, J., Zhou, J., Wang, X., & Liu, Q. (2012). Regulation of miRNA-21 by reactive oxygen species-activated ERK/NF-κB in arsenite-induced cell transformation. *Free Radical Biology and Medicine, 52*(9), 1508–1518.

Liu, H., Lu, S., Zhang, B., Xia, W., Liu, W., Peng, Y., Zhang, H., Wu, K., Xu, S., & Li, Y. (2018). Maternal arsenic exposure and birth outcomes: A birth cohort study in Wuhan, China. *Environmental Pollution, 236*, 817–823.

Liu, Jie, Benbrahim-Tallaa, L., Qian, X., Yu, L., Xie, Y., Boos, J., Qu, W., & Waalkes, M. P. (2006). Further studies on aberrant gene expression associated with arsenic-induced malignant transformation in rat liver TRL1215 cells. *Toxicology and Applied Pharmacology, 216*(3), 407–415.

Liu, Jin, Ma, Y., Zhu, D., Xia, T., Qi, Y., Yao, Y., Guo, X., Ji, R., & Chen, W. (2018). Polystyrene Nanoplastics-Enhanced Contaminant Transport: Role of Irreversible Adsorption in Glassy Polymeric Domain. *Environmental Science and Technology, 52*(5), 2677–2685.

Liu, S. X., Athar, M., Lippai, I., Waldren, C., & Hei, T. K. (2001). Induction of oxyradicals by arsenic: Implication for mechanism of genotoxicity*. Proceedings of the National Academy of Sciences of the United States of America, 98*(4), 1643–1648.

Longás H. (2014). Una nueva diana contra el cáncer. EL PAÍS.

López de Andrés, J., Griñán-Lisón, C., Jiménez, G., & Marchal, J. A. (2020). Cancer stem cell secretome in the tumor microenvironment: a key point for an effective personalized cancer treatment. *Journal of Hematology and Oncology, 13*(1), 1–22.

Luo, F., Ji, J., Liu, Y., Xu, Y., Zheng, G., Jing, J., Wang, B., Xu, W., Shi, L., Lu, X., & Liu, Q. (2015). MicroRNA-21, up-regulated by arsenite, directs the epithelial-mesenchymal transition and enhances the invasive potential of transformed human bronchial epithelial cells by targeting PDCD4. *Toxicology Letters, 232*(1), 301–309.

Lynn, S., Gurr, J. R., Lai, H. T., & Jan, K. Y. (2000). NADH oxidase activation is involved in arsenite-induced oxidative DNA damage in human vascular smooth muscle cells. *Circulation Research, 86*(5), 514–519.

Magkouta, S. F., Pappas, A. G., Vaitsi, P. C., Agioutantis, P. C., Pateras, I. S., Moschos, C. A., Iliopoulou, M. P., Kosti, C. N., Loutrari, H. V., Gorgoulis, V. G., & Kalomenidis, I. T. (2020). MTH1 favors mesothelioma progression and mediates paracrine rescue of bystander endothelium from oxidative damage. *JCI Insight, 5*(12), 1–16.

Magrì, D., Sánchez-Moreno, P., Caputo, G., Gatto, F., Veronesi, M., Bardi, G., Catelani, T., Guarnieri, D., Athanassiou, A., Pompa, P. P., & Fragouli, D. (2018). Laser ablation as a versatile tool to mimic polyethylene terephthalate nanoplastic pollutants: Characterization and toxicology assessment. *ACS Nano, 12*(8), 7690–7700.

Mahata, J., Basu, A., Ghoshal, S., Sarkar, J. N., Roy, A. K., Poddar, G., Nandy, A. K., Banerjee, A., Ray, K., Natarajan, A. T., Nilsson, R., & Giri, A. K. (2003). Chromosomal aberrations and sister chromatid exchanges in individuals exposed to arsenic through drinking water in West Bengal, India. *Mutation Research - Genetic Toxicology and Environmental Mutagenesis, 534*(1–2), 133–143.

Malakar, A., & Snow, D. D. (2020). Nanoparticles as sources of inorganic water pollutants. In *Inorganic Pollutants in Water*. Elsevier, 337-370.

Mandal, P. (2017). Molecular insight of arsenic-induced carcinogenesis and its prevention. *Naunyn-Schmiedeberg's Archives of Pharmacology, 390*(5), 443–455.

Markkanen, E. (2017). Not breathing is not an option: How to deal with oxidative DNA damage. *DNA Repair, 59*(September), 82–105.

Martínez-Baeza, E., Rojas, E., & Valverde, M. (2016). Metal mixture (As-Cd-Pb)-induced cell transformation is modulated by OLA1. *Mutagenesis, 31*(4), 463–473.

Martínez, V., Creus, A., Venegas, W., Arroyo, A., Beck, J. P., Gebel, T. W., Surrallés, J., & Marcos, R. (2004). Evaluation of micronucleus induction in a Chilean population environmentally exposed to arsenic. *Mutation Research - Genetic Toxicology and Environmental Mutagenesis, 564*(1), 65–74.

Martinez, V. D., Thu, K. L., Vucic, E. A., Hubaux, R., Adonis, M., Gil, L., Macaulay, C., Lam, S., & Lam, W. L. (2013). Whole-genome sequencing analysis identifies a distinctive mutational spectrum in an arsenic-related lung tumor. *Journal of Thoracic Oncology, 8*(11), 1451–1455.

Massos, A., & Turner, A. (2017). Cadmium, lead and bromine in beached microplastics. *Environmental Pollution, 227*, 139–145.

Masuda, H. (2018). Arsenic cycling in the Earth's crust and hydrosphere: interaction between naturally occurring arsenic and human activities. *Progress in Earth and Planetary Science, 5,* 68*.*

Melkonian, S., Argos, M., Pierce, B. L., Chen, Y., Islam, T., Ahmed, A., Syed, E. H., Parvez, F., Graziano, J., Rathouz, P. J., & Ahsan, H. (2011). A prospective study of the synergistic effects of arsenic exposure and smoking, sun exposure, fertilizer use, and pesticide use on risk of premalignant skin lesions in bangladeshi men. *American Journal of Epidemiology, 173*(2), 183–191.

Merrick, A. B., Phadke, D. P., Bostrom, M. A., Shah, R. R., Wright, G. M., Wang, X., Gordon, O., Pelch, K. E., Auerbach, S. S., Paules, R. S., DeVito, M. J., Waalkes, M. P., & Tokar, E. J. (2019). Arsenite malignantly transforms human prostate epithelial cells in vitro by gene amplification of mutated KRAS. *PLoS ONE, 14*(4), 1–23.

Mori, S., Chang, J. T., Andrechek, E. R., Matsumura, N., Baba, T., Yao, G., Kim, J. W., Gatza, M., Murphy, S., & Nevins, J. R. (2009). An Anchorage-Independent Cell Growth Signature Identifies Tumors with Metastatic Potential. *Oncogene, 28*(31), 2796–2805.

Mortezaee, K., Najafi, M., Samadian, H., Barabadi, H., Azarnezhad, A., & Ahmadi, A. (2019). Redox interactions and genotoxicity of metal-based nanoparticles: A comprehensive review. *Chemico-Biological Interactions, 312*(August), 108814.

Moukengue, B., Brown, H. K., Charrier, C., Battaglia, S., Baud'huin, M., Quillard, T., Pham, T. M., Pateras, I. S., Gorgoulis, V. G., Helleday, T., Heymann, D., Berglund, U. W., Ory, B., & Lamoureux, F. (2020). TH1579, MTH1 inhibitor, delays tumour growth and inhibits metastases development in osteosarcoma model. *EBioMedicine*, *53*, 102704.

Nakabeppu, Y., Ohta, E., & Abolhassani, N. (2017). MTH1 as a nucleotide pool sanitizing enzyme: Friend or foe? *Free Radical Biology and Medicine, 107*(October 2016), 151–158.

Naujokas, M. F., Anderson, B., Ahsan, H., Vasken Aposhian, H., Graziano, J. H., Thompson, C., & Suk, W. A. (2013). The broad scope of health effects from chronic arsenic exposure: Update on a worldwide public health problem. *Environmental Health Perspectives, 121*(3), 295–302.

Ngalame, N. N. O., Tokar, E. J., Person, R. J., & Waalkes, M. P. (2014). Silencing KRAS overexpression in arsenic-transformed prostate epithelial and stem cells partially mitigates malignant phenotype. *Toxicological Sciences, 142*(2), 489–496.

Nie, J. H., Chen, Z. H., Liu, X., Wu, Y. W., Li, J. X., Cao, Y., Hei, T. K., & Tong, J. (2012). Oxidative damage in various tissues of rats exposed to radon. *Journal of Toxicology and Environmental Health - Part A: Current Issues, 75*(12), 694–699.

OECD, Organisation for Economic Co-operation and Development. (2013). In Vitro Carcinogenicity: Bhas 42 Cell Transformation Assay. OECD Guidelines, HRI draft, 1–21.

Ooki, A., Begum, A., Marchionni, L., Vandenbussche, C. J., Mao, S., Kates, M., & Hoque, M. O. (2018). Arsenic Promotes the COX2/PGE2-SOX2 Axis to Increase the Malignant Stemness Properties of Urothelial Cells. *International Journal of Cancer*, 143(1), 113–126.

Oya-Ohta, Y., Kaise, T., & Ochi, T. (1996). Induction of chromosomal aberrations in cultured human fibroblasts by inorganic and organic arsenic compounds and the different roles of glutathione in such induction. *Mutation Research - Fundamental and Molecular Mechanisms of Mutagenesis, 357*(1–2), 123–129.

Palma-Lara, I., Martínez-Castillo, M., Quintana-Pérez, J. C., Arellano-Mendoza, M. G., Tamay-Cach, F., Valenzuela-Limón, O. L., García-Montalvo, E. A., & Hernández-Zavala, A. (2020). Arsenic exposure: A public health problem leading to several cancers. *Regulatory Toxicology and Pharmacology, 110*(November 2019), 104539.

Person, R. J., Ngalame, N. N. O., Makia, N. L., Bell, M. W., Waalkes, M. P., & Tokar, E. J. (2015). Chronic inorganic arsenic exposure in vitro induces a cancer cell phenotype in human peripheral lung epithelial cells. *Toxicology and Applied Pharmacology, 286*(1), 36–43.

Pi, J., He, Y., Bortner, C., Huang, J., Liu, J., Zhou, T., Qu, W., North, S. L., Kasprzak, K. S., Diwan, B. A., Chignell, C. F., & Waalkes, M. P. (2005). Low level, long-term inorganic arsenite exposure causes generalized resistance to apoptosis in cultured human keratinocytes: Potential role in skin co-carcinogenesis. *International Journal of Cancer, 116*(1), 20–26.

Pi, J., Diwan, B. A., Sun, Y., Liu, J., Qu, W., He, Y., Styblo, M., & Waalkes, M. P. (2008). Arsenic-induced malignant transformation of human keratinocytes: Involvement of Nrf2. *Free Radical Biology and Medicine*, 45(5), 651–658.

Pichler, G., Maria Grau-Perez, M., Tellez-Plaza, M., Umans, J., Bes, L., Cole, S., Goessler, W., Francesconi, K., Newman, J., Redon, J., Devereux, R., & Navas-Acien, A. (2019). Association of Arsenic Exposure With Cardiac Geometry and Left Ventricular Function in Young Adults. *Circulation: Cardiovascular Imaging, 12*(5), e009018 .

Pietras, K., & Östman, A. (2010). Hallmarks of cancer: Interactions with the tumor stroma. *Experimental Cell Research, 316*(8), 1324–1331.

Podgorski, J., & Berg, M. (2020). Global threat of arsenic in groundwater. *Science, 368*(6493), 845–850.

Poma, A., Vecchiotti, G., Colafarina, S., Zarivi, O., Aloisi, M., Arrizza, L., Chichiriccò, G., & Di Carlo, P. (2019). In vitro genotoxicity of polystyrene nanoparticles on the human fibroblast hs27 cell line. *Nanomaterials, 9*(9), 1–13.

Powers, M., Sanchez, T. R., Grau-Perez, M., Yeh, F., Francesconi, K. A., Goessler, W., George, C. M., Heaney, C., Best, L. G., Umans, J. G., Brown, R. H., & Navas-Acien, A. (2019). Low-moderate arsenic exposure and respiratory in American Indian communities in the Strong Heart Study. *Environmental Health: A Global Access Science Source, 18*(1), 1–12.

Prieto, L. I., & Baker, D. J. (2019). Cellular senescence and the immune system in cancer. *Gerontology, 65*(5), 505–512.

Prunier, J., Maurice, L., Perez, E., Gigault, J., Pierson Wickmann, A. C., Davranche, M., & Halle, A. ter. (2019). Trace metals in polyethylene debris from the North Atlantic subtropical gyre. *Environmental Pollution, 245*, 371–379.

Qu, W., Bortner, C. D., Sakurai, T., Hobson, M. J., & Waalkes, M. P. (2002). Acquisition of apoptotic resistance in arsenic-induced malignant transformation: role of the JNK signal transduction pathway. *Carcinogenesis, 23*(1), 151–159.

Rai, P., & Sobol, R. W. (2019). Mechanisms of MTH1 inhibition-induced DNA strand breaks: The slippery slope from the oxidized nucleotide pool to genotoxic damage. *DNA Repair, 77*, 18–26.

Ravenscroft, P., Brammer, H., & Richards, K. (2009). Arsenic Pollution. In *Arsenic Pollution: A Global Synthesis*. Wiley-Blackwell. A John Wiley and Sons Ltd.

Reuter, S., Gupta, S. C., Chaturvedi, M. M., & Aggarwal, B. B. (2010). Oxidative stress, inflammation, and cancer: How are they linked? *Free Radical Biology and Medicine, 49*(11), 1603–1616.

Rochman, C. M., Hoh, E., Kurobe, T., & Teh, S. J. (2013). Ingested plastic transfers hazardous chemicals to fish and induces hepatic stress. *Scientific Reports, 3*, 1–7.

Rodríguez-Sastre, M. A., Rojas, E., & Valverde, M. (2014). Assessing the impact of As-Cd-Pb metal mixture on cell transformation by two-stage Balb/c 3T3 cell assay. *Mutagenesis, 29*(4), 251–257.

Rojas, E., Martínez-Pacheco, M., Rodríguez-Sastre, M. A., & Valverde, M. (2019). As-Cd-Pb mixture induces cellular transformation via post-transcriptional regulation of RAD51C by miR-222. *Cellular Physiology and Biochemistry, 53*(6), 910–920.

Rosário, F., Bessa, M. J., Brandão, F., Costa, C., Lopes, C. B., Estrada, A. C., Tavares, D. S., Teixeira, J. P., & Reis, A. T. (2020). Unravelling the potential cytotoxic effects of metal oxide nanoparticles and metal(loid) mixtures on A549 human cell line. *Nanomaterials, 10*(3), 447.

Rossman, T. G., Uddin, A. N., & Burns, F. J. (2004). Evidence that arsenite acts as a cocarcinogen in skin cancer. *Toxicology and Applied Pharmacology, 198*(3), 394–404.

Roy, N. K., Murphy, A., & Costa, M. (2020). Arsenic methyltransferase and methylation of inorganic arsenic. *Biomolecules, 10*(9), 1–13.

Rubio, L., Bach, J., Marcos, R., & Hernández, A. (2017). Synergistic role of nanoceria on the ability of tobacco smoke to induce carcinogenic hallmarks in lung epithelial cells. *Nanomedicine, 12*(23), 2623–2635.

Rubio, L., Marcos, R., & Hernández, A. (2018). Nanoceria acts as antioxidant in tumoral and transformed cells. *Chemico-Biological Interactions, 291*(November 2017), 7–15.

Rubio, L., Marcos, R., & Hernández, A. (2020a). Potential adverse health effects of ingested micro- and nanoplastics on humans. Lessons learned from in vivo and in vitro mammalian models. *Journal of Toxicology and Environmental Health - Part B: Critical Reviews, 23*(2), 51–68.

Rubio, L., Barguilla, I., Domenech, J., Marcos, R., & Hernández, A. (2020b). Biological effects, including oxidative stress and genotoxic damage, of polystyrene nanoparticles in different human hematopoietic cell lines. *Journal of Hazardous Materials, 398*, 122900.

Sage, A. P., Minatel, B. C., Ng, K. W., Stewart, G. L., Dummer, T. J. B., Lam, W. L., & Martinez, V. D. (2017). Oncogenomic disruptions in arsenic-induced carcinogenesis. *Oncotarget, 8*(15), 25736–25755.

Sahai, E., Astsaturov, I., Cukierman, E., DeNardo, D. G., Egeblad, M., Evans, R. M., Fearon, D., Greten, F. R., Hingorani, S. R., Hunter, T., Hynes, R. O., Jain, R. K., Janowitz, T., Jorgensen, C., Kimmelman, A. C., Kolonin, M. G., Maki, R. G., Powers, R. S., Puré, E., … Werb, Z. (2020). A framework for advancing our understanding of cancer-associated fibroblasts. *Nature Reviews Cancer, 20*(3), 174–186.

Samaranayake, G. J., Huynh, M., & Rai, P. (2017). MTH1 as a chemotherapeutic target: The elephant in the room. *Cancers, 9*(5), 1–15.

Sampayo-Reyes, A., Hernández, A., El-Yamani, N., López-Campos, C., Mayet-Machado, E., Rincón-Castañeda, C. B., Limones-Aguilar, M. de L., López-Campos, J. E., de León, M. B., González-Hernández, S., Hinojosa-Garza, D., & Marcos, R. (2010). Arsenic induces DNA damage in environmentally exposed Mexican children and adults. Influence of GSTO1 and AS3MT polymorphisms. *Toxicological Sciences : An Official Journal of the Society of Toxicology, 117*(1), 63–71.

Sanders, A. P., Henn, B. C., & Wright, R. O. (2015). Perinatal and Childhood Exposure to Cadmium, Manganese, and Metal Mixtures and Effects on Cognition and Behavior: A Review of Recent Literature Compliance with Ethics Guidelines Human and Animal Rights and Informed Consent HHS Public Access. *Curr Environ Health Rep, 2*(3), 284–294.

Schirinzi, G. F., Pérez-Pomeda, I., Sanchís, J., Rossini, C., Farré, M., & Barceló, D. (2017). Cytotoxic effects of commonly used nanomaterials and microplastics on cerebral and epithelial human cells. *Environmental Research, 159*(June), 579–587.

Schmidlin, C. J., Zeng, T., Liu, P., Wei, Y., Dodson, M., Chapman, E., & Zhang, D. D. (2020). Chronic arsenic exposure enhances metastatic potential via NRF2-mediated upregulation of SOX9. *Toxicology and Applied Pharmacology, 402*(June), 115138.

Selvam, S., Jesuraja, K., Venkatramanan, S., Roy, P. D., & Jeyanthi Kumari, V. (2021). Hazardous microplastic characteristics and its role as a vector of heavy metal in groundwater and surface water of coastal south India. *Journal of Hazardous Materials, 402*(May 2020), 123786.

Shearer, M. J. J., Wold, E. A., Umbaugh, C. S., Lichti, C. F., Nilsson, C. L., & Figueiredo, M. L. (2016). Inorganic arsenic-related changes in the stromal tumor microenvironment in a prostate cancer cell-conditioned media. *Environmental Health Perspectives, 124*(7), 1009–1015.

Shen, S., Li, X. F., Cullen, W. R., Weinfeld, M., & Le, X. C. (2013). Arsenic binding to proteins. *Chemical Reviews, 113*(10), 7769–7792.

Sherr, C. J. (1996). Cancer cell cycles. *Science, 274*(5293), 1672–1674.

Signes-Pastor, A. J., Vioque, J., Navarrete-muñoz, E. M., Carey, M., García-villarino, M., Fernández-somoano, A., Tardón, A., Santa-, L., Irizar, A., Casas, M., Guxens, M., & Llop, S. (2019). Inorganic arsenic exposure and neuropsychological development of children of 4-5 years of age living in Spain. *Environmental Research, 174*, 135–142.

Smedley, P. L., & Kinniburgh, D. G. (2002). A review of the source, behaviour and distribution of arsenic in natural waters. *Applied Geochemistry, 17*, 517–568.

Smith, A. H., Lingas, E. O., & Rahman, M. (2000). Contamination of Drinking Water by Arsenic in Bangladesh: A Public Health Emergency. *Bulletin of the World Health Organization, 78*(August 2016), 1093.

Soza-Ried, C., Bustamante, E., Caglevic, C., Rolfo, C., Sirera, R., & Marsiglia, H. (2019). Oncogenic role of arsenic exposure in lung cancer: A forgotten risk factor. *Critical Reviews in Oncology/Hematology, June 2018*, 1–6.

Spratlen, M. J., Grau-Perez, M., Umans, J. G., Yracheta, J., Best, L. G., Francesconi, K., Goessler, W., Balakrishnan, P., Cole, S. A., Gamble, M. V, Howard, B. V, & Navas-Acien, A. (2018). Arsenic, one carbon metabolism and diabetes-related outcomes in the Strong Heart Family Study. *Environment International, 121*(Pt 1), 728–740.

Steinberg, P., Reifferscheid, G., & Buchinger, S. (2017). In Vitro–In Vivo Carcinogenicity. In Adv Biochem Eng Biotechnol (Vol. 157).

Stueckle, T. A., Lu, Y., Davis, M. E., Wang, L., Jiang, B.-H., Holaskova, I., Schafer, R., Barnett, J. B., & Rojanasakul, Y. (2012). Chronic occupational exposure to arsenic induces carcinogenic gene signaling networks and neoplastic transformation in human lung epithelial cells. *Toxicology and Applied Pharmacology, 61*(2), 204–216.

Sun, M., Tan, J., Wang, M., Wen, W., & He, Y. (2020). Inorganic arsenic-mediated upregulation of AS3MT promotes proliferation of nonsmall cell lung cancer cells by regulating cell cycle genes. *Environmental Toxicology, August*, 1–9.

Taddei, M. L., Giannoni, E., Fiaschi, T., & Chiarugi, P. (2012). Anoikis: An emerging hallmark in health and diseases. *Journal of Pathology, 226*(2), 380–393.

Talotta, F., Casalino, L., & Verde, P. (2020). The nuclear oncoprotein Fra-1: a transcription factor knocking on therapeutic applications' door. *Oncogene, 39*(23), 4491–4506.

Tanabe, A., & Sahara, H. (2020). The metabolic heterogeneity and flexibility of cancer stem cells. *Cancers, 12*(10), 1–22.

Tokar, E. J., Benbrahim-Tallaa, L., Ward, J. M., Lunn, R., Sams, R. L., & Waalkes, M. P. (2010a). Cancer in experimental animals exposed to arsenic and arsenic compounds. *Critical Reviews in Toxicology, 40*(10), 912–927.

Tokar, E. J., Diwan, B. A., & Waalkes, M. P. (2010b). Arsenic exposure transforms human epithelial stem/progenitor cells into a cancer stem-like phenotype. *Environmental Health Perspectives, 118*(1), 108–115.

Tokar, E. J., Qu, W., Liu, J., Liu, W., Webber, M. M., Phang, J. M., & Waalkes, M. P. (2010c). Arsenic-specific stem cell selection during malignant transformation. *Journal of the National Cancer Institute, 102*(9), 638–649.

Tokar, E. J., Person, R. J., Sun, Y., Perantoni, A. O., & Waalkes, M. P. (2013). Chronic exposure of renal stem cells to inorganic arsenic induces a cancer phenotype. *Chemical Research in Toxicology, 26*(1), 96–105.

Tokar, E. J., Kojima, C., & Waalkes, M. P. (2014). Methylarsonous acid causes oxidative DNA damage in cells independent of the ability to biomethylate inorganic arsenic. *Archives of Toxicology, 88*(2), 249–261.

Treas, J., Tyagi, T., & Singh, K. P. (2013). Chronic exposure to arsenic, estrogen, and their combination causes increased growth and transformation in human prostate epithelial cells potentially by hypermethylation-mediated silencing of MLH1. *Prostate, 73*(15), 1660–1672.

Tu, Y., Wang, Z., Wang, X., Yang, H., Zhang, P., Johnson, M., Liu, N., Liu, H., Jin, W., Zhang, Y., & Cui, D. (2016). Birth of MTH1 as a therapeutic target for glioblastoma: MTH1 is indispensable for gliomatumorigenesis. *American Journal of Translational Research, 8*(6), 2803–2811.

Tumolo, M. R., Panico, A., De Donno, A., Mincarone, P., Leo, C. G., Guarino, R., Bagordo, F., Serio, F., Idolo, A., Grassi, T., & Sabina, S. (2020). The expression of microRNAs and exposure to environmental contaminants related to human health: a review. *International Journal of Environmental Health Research, May*, 1–23.

Vesely, P. W., Staber, P. B., Hoefler, G., & Kenner, L. (2009). Translational regulation mechanisms of AP-1 proteins. *Mutation Research - Reviews in Mutation Research, 682*(1), 7–12.

Vishnoi, K., Viswakarma, N., Rana, A., & Rana, B. (2020). Transcription Factors in Cancer Development and Therapy. *Cancers, 12*, 2296.

Wang, X., Zhang, J., Xu, W., Huang, Q., Liu, L., Tian, M., Xia, Y., Zhang, W., & Shen, H. (2016). Low-level environmental arsenic exposure correlates with unexplained male infertility risk. *Science of the Total Environment, 571*, 307–313.

Wang, X., Liu, Y., Wang, J., Nie, Y., Chen, S., Hei, T. K., Deng, Z., Wu, L., Zhao, G., & Xu, A. (2017). Amplification of arsenic genotoxicity by TiO2 nanoparticles in mammalian cells: new insights from physicochemical interactions and mitochondria. *Nanotoxicology, 11*(8), 978–995.

Wang, Z., & Yang, C. (2019). Metal carcinogen exposure induces cancer stem cell-like property through epigenetic reprograming: A novel mechanism of metal carcinogenesis. *Seminars in Cancer Biology, December 2018*, 0–1.

Wang, J. J., Liu, T. H., Li, J., Li, D. N., Tian, X. Y., Ouyang, Q. G., & Cai, J. P. (2020). The high expression of MTH1 and NUDT5 predict a poor survival and are associated with malignancy of esophageal squamous cell carcinoma. *PeerJ, 2020*(5), 1–22.

Warpman Berglund, U., Sanjiv, K., Gad, H., Kalderén, C., Koolmeister, T., Pham, T., Gokturk, C., Jafari, R., Maddalo, G., Seashore-Ludlow, B., Chernobrovkin, A., Manoilov, A., Pateras, I. S., Rasti, A., Jemth, A. S., Almlöf, I., Loseva, O., Visnes, T., Einarsdottir, B. O., … Helleday, T. (2016). Validation and development of MTH1 inhibitors for treatment of cancer. *Annals of Oncology, 27*(12), 2275–2283.

Wen, G., Calaf, G. M., Partridge, M. A., Echiburú-Chau, C., Zhao, Y., Huang, S., Chai, Y., Li, B., Hu, B., & Hei, T. K. (2008). Neoplastic transformation of human small airway epithelial cells induced by arsenic. *Molecular Medicine, 14*(1–2), 2–10.

WHO, World Health Organization. (2019). Preventing Disease through Healthy Environment. Exposure to Arsenic: A Major Public Health Concern. Preventing Disease through Healthy Environment, 1–5.

Wong, B. S. E., Hu, Q., & Baeg, G. H. (2017). Epigenetic modulations in nanoparticle-mediated toxicity. *Food and Chemical Toxicology, 109*, 746–752.

Wu, X., Sun, R., Wang, H., Yang, B., Wang, F., Xu, H., Chen, S., Zhao, R., Pi, J., & Xu, Y. (2019a). Enhanced p62-NRF2 Feedback Loop due to Impaired Autophagic Flux Contributes to Arsenic-Induced Malignant Transformation of Human Keratinocytes. Oxidative Medicine and Cellular Longevity, *2019*, 1038932.

Wu, B., Wu, X., Liu, S., Wang, Z., & Chen, L. (2019b). Size-dependent effects of polystyrene microplastics on cytotoxicity and efflux pump inhibition in human Caco-2 cells. *Chemosphere, 221*, 333–341.

Xu, Y., Zhao, Y., Xu, W., Luo, F., Wang, B., Li, Y., Pang, Y., & Liu, Q. (2013). Involvement of HIF-2α-mediated inflammation in arsenite-induced transformation of human bronchial epithelial cells. *Toxicology and Applied Pharmacology, 272*, 542–550.

Xu, Y., Tokar, E. J., & Waalkes, M. P. (2014). Arsenic-induced cancer cell phenotype in human breast epithelia is estrogen receptor-independent but involves aromatase activation. *Archives of Toxicology, 88*(2), 263–274.

Xu, M., Halimu, G., Zhang, Q., Song, Y., Fu, X., Li, Y., Li, Y., & Zhang, H. (2019). Internalization and toxicity: A preliminary study of effects of nanoplastic particles on human lung epithelial cell. *Science of the Total Environment, 694,* 133794.

Yang, J., & Weinberg, R. A. (2008). Epithelial-Mesenchymal Transition: At the Crossroads of Development and Tumor Metastasis. *Developmental Cell, 14*(6), 818–829.

Yih, L. H., & Lee, T. C. (1999). Effects of exposure protocols on induction of kinetochore-plus and -minus micronuclei by arsenite in diploid human fibroblasts. *Mutation Research - Genetic Toxicology and Environmental Mutagenesis, 440*(1), 75–82.

Yong, C. Q. Y., Valiyaveetill, S., & Tang, B. L. (2020). Toxicity of microplastics and nanoplastics in Mammalian systems. *International Journal of Environmental Research and Public Health, 17*(5), 1509.

Yu, F., Yang, C., Zhu, Z., Bai, X., & Ma, J. (2019). Adsorption behavior of organic pollutants and metals on micro/nanoplastics in the aquatic environment*. Science of the Total Environment, 694*, 133643.

Zhan, D., Zhang, X., Li, J., Ding, X., Cui, Y. X., & Jia, J. (2020). MTH1 Inhibitor TH287 Suppresses Gastric Cancer Development through the Regulation of PI3K/AKT Signaling. *Cancer Biotherapy and Radiopharmaceuticals, 35*(3), 223–232.

Zhang, Z., Pratheeshkumar, P., Son, Y.-O., Kim, D., & Shi, X. (2015). Role of reactive oxygen species in arsenic-induced transformation of human lung bronchial epithelial (BEAS-2B) cells. *Biochem Biophys Res Commun, 456*(2), 643–648.

Zhang, X., Song, W., Zhou, Y., Mao, F., Lin, Y., Guan, J., & Sun, Q. (2017). Expression and function of MutT homolog 1 in distinct subtypes of breast cancer. *Oncology Letters, 13*(4), 2161–2168.

Zhang, C., Kibriya, M. G., Jasmine, F., Roy, S., Gao, J., Sabarinathan, M., Shinkle, J., Delgado, D., Ahmed, A., Islam, T., Eunus, M., Islam, M. T., Hasan, R., Graziano, J. H., Ahsan, H., & Pierce, B. L. (2018). A study of telomere length, arsenic exposure, and arsenic toxicity in a Bangladeshi cohort. *Environmental Research, 164*, 346–355.

Zhao, C. Q., Young, M. R., Diwan, B. A., Coogan, T. P., & Waalkes, M. P. (1997). Association of arsenic-induced malignant transformation with DNA hypomethylation and aberrant gene expression. *Proceedings of the National Academy of Sciences of the United States of America, 94*(20), 10907–10912.

Zhao, F. J., McGrath, S. P., & Meharg, A. A. (2010). Arsenic as a food chain contaminant: Mechanisms of plant uptake and metabolism and mitigation strategies. *Annual Review of Plant Biology, 61*, 535–559.

Zheng, C. Y., Lam, S. kwan, Li, Y. Y., Fong, B. M. W., Mak, J. C.W., & Ho, J. C. man. (2013). Combination of arsenic trioxide and chemotherapy in small cell lung cancer. *Lung Cancer, 82*(2), 222–230.

Zhou, Q., & Xi, S. (2018). A review on arsenic carcinogenesis: Epidemiology, metabolism, genotoxicity and epigenetic changes. *Regulatory Toxicology and Pharmacology, 99*(September), 78–88.

Zhou, Q., Jin, P., Liu, J., Wang, F., & Xi, S. (2018). HER2 and Src co-regulate proliferation, migration and transformation by downstream signaling pathways in arsenite-treated human uroepithelial cells. *Metallomics, 10*(8), 1141–1159.

Zhu, Y., & Costa, M. (2020). Metals and molecular carcinogenesis. *Carcinogenesis, 41*(9), 1161–1172.